UNPUBLISHED PRELIMINARY DATA

West Virginia University

NsG - 533

GPO PRICE $ ______

OTS PRICE(S) $ ______

Hard copy (HC) $4.00

Microfiche (MF) $0.75

STRAIN RATE SENSITIVITY OF CERTAIN BIOLOGICAL MATERIALS

Final Rpt.

by

Dr. James H. McElhaney

Dr. Edward F. Byars

STRAIN RATE SENSITIVITY OF

CERTAIN BIOLOGICAL MATERIALS

by

Dr. J. H. McElhaney

Dr. E. F. Byars

Final Report

for

National Aeronautics and Space Administration

West Virginia University
Research Grant NsG 533

Department of
Theoretical and Applied Mechanics

West Virginia University
Morgantown, West Virginia
1965

22653

ABSTRACT

Strain Rate Sensitivity of Certain Biological Materials

The object of this research was to provide basic information concerning the mechanical response of bone and muscle tissue to impacts of varying velocity and to develop suitable instrumentation and experimental techniques that would allow a continuing investigation of strain rate sensitivity in general.

A high velocity air gun type testing machine was developed capable of performing constant velocity tests to strain rates of 4,000/sec. Adjustable stops are provided that allow predetermined strains to be applied to miniature specimens. High frequency response instrumentation utilizing a piezoelectric load cell and capacitance displacement transducer was used. Load and displacement histories of fresh bovine femur bone, embalmed human femur bone, bovine tissue, nylon and aluminum were measured over a wide range of strain rates.

Results are presented in the form of stress-strain diagrams at selected strain rates. Curves of various properties, as affected by rate of loading, are also provided. A critical velocity was noted for both types of bone in the neighborhood corresponding to a strain rate of 1/sec. A stress, strain, strain rate surface representation of the data is suggested and similarities between the dynamic response of bone, nylon and aluminum noted. The intersection of this surface with planes parallel to the stress-strain coordinate plane were found to be exponentials.

H. Allen

TABLE OF CONTENTS

LIST OF TABLES

LIST OF FIGURES

I. PURPOSE

The purpose of this research is to provide basic information hitherto unavialable concerning the mechanical response of bone and muscle tissue to impacts of varying velocity and to develop suitable instrumentation and experimental techniques that will allow a continuing study of the strain rate sensitivity of materials in general. The long range goal of such a program is the classification of materials according to the rheological models which characterize their response to a broad spectrum of strain rates. It is hoped that this information will be of value to designers of ejection seats, acceleration couches, and other equipment whose purpose is to protect the human body from shock and impact.

While there is little known about the dynamic behavior of the mechanical subcomponents of the human system, a number of investigations have been made into the overall behavior of live subjects exposed to shock and vibration. A combination of the results of these tests with information as to the dynamic behavior of the individual materials involved may lead to a workable mathematical model from which predictions of the bounds of safe load-time applications may be made.

II. INTRODUCTION AND SCOPE

With the advent of high speed aircraft, rockets, and space vehicles, designers have become increasingly aware of the frailty of the human elements of the system. Since in most cases failure of the human component leads to destruction of the whole system, or vice-versa, it is important to provide protection for this vital part. Thus, we have seen the evolution of various isolating and load distributing devices ranging from seat belts and padded sunvisors to ejection seats, crash helmets, and acceleration couches. While there is a large amount of information available regarding the response of inanimate material to vibration and impact, there is an equal dearth of knowledge pertaining to the mechanical properties of biological materials. Therefore, the design of such support equipment is often based on intuition because of the lack of information about the mechanical response of the human body.

It has long been known that the vast majority of solid materials possess mechanical properties that are functions of the strain rate. However, it is only recently that instrumentation and experimental equipment have been developed that enable accurate measurement of this phenomena at high rates. In this connection, rate sensitivity is defined as the degree to which mechanical properties are affected by the strain rate at which they are measured. A great deal of work remains to be done before groups of materials may be classified and this behavior characterized at specific rates of loading over a broad time scale.

There exists a large body of literature describing work aimed at devising experimental techniques to provide data on the mechanical properties of metals under rapid loading. However, most investigators have not provided information of a sufficiently fundamental nature to give an understanding of basic concepts concerning the behavior of materials under dynamic conditions. Furthermore, at the higher rates of loading, it becomes increasingly difficult to isolate the mechanical properties of interest and the cross sensitivity and frequency response of the measuring transducers becomes of paramount importance. Since the simultaneous recording of the transient stress and strain at a given point of the specimen has not yet been satisfactorily accomplished, information concerning the material behavior must be deduced from auxilliary measurements which at best provide only average values of the stress and strain.

Still, information of this kind is important; for, although primitive in origin, it serves to explain gross properties and points the way for further studies of a more fundamental nature. Also, it should be recalled that structural failures of the human system (in fact, most mechanical systems) are seldom static in nature, but rather they occur rapildy and are frequently due to impacts of varying velocity. Analysis of these failures and their prevention must be built on a knowledge of the dynamic properties of the materials involved.

It should be emphasized that a five foot drop results in an impact velocity of more than 200 in/sec. Thus, under even mild service conditions, the rate at which materials are strained is quite high.

Engineering applications of information regarding such material behavior are numerous. As an example, consider the growing interest in the strain-rate effects in metals as an aid to rational design of aircraft and rocket air-frames against impacts imposed by blasts and gust loads, which produce high stresses for short intervals. In high-speed aircraft, gust loads with duration as little as 0.01 seconds have been reported.[56*] It also appears possible that the phenomenon of fatigue in metals may be related to strain-rate effects. The implications of this theory pose some interesting experimental design complications.[56]

Another engineering application of the knowledge of the effect of strain rate on the properties of materials has been the selection, through dynamic test methods, of materials for shock-cushioning, isolation and energy adsorbtion. Large differences in the static and dynamic stress-strain characteristics have been demonstrated for many of these materials.[51,52]

---

*Refers to items in the Bibliography at the end of this paper.

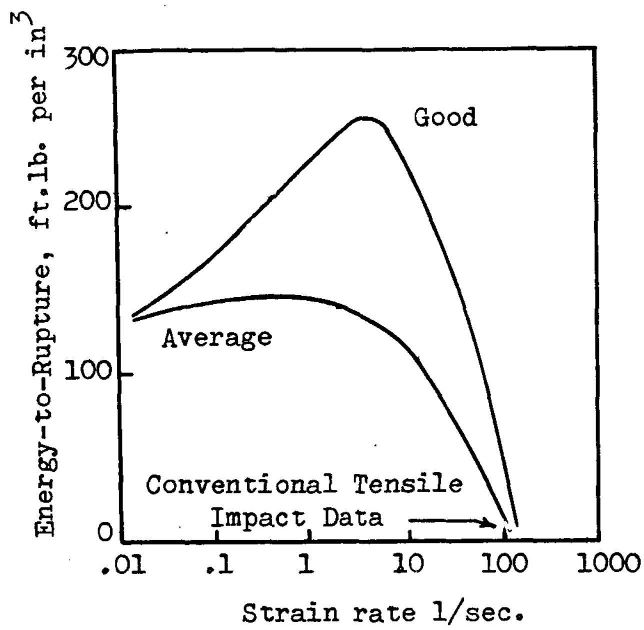

Fig. 1. Energy to rupture vs. strain rate for high impact polystyrene sheet materials used as liners for refrigerator doors.

(From Reference 51)

Figure 1 shows data for two plastic sheeting materials used in refrigerator door inner liners which were found to perform differently in service (Strain rates of about 10 - 100/sec.). No differences between materials could be detected by static tension tests or by tensile impact and Izod impact tests. However, energy to rupture tests at intermediate strain rates (the actual service conditions) were significantly higher for the sheet known to be superior than for the sheet known to be inferior in service.

In the following pages, a series of experiments will be described whose aim was to investigate the effect of varying strain rates on the gross physical properties of bone and muscle tissue. The strain rates considered will include the range from 0.001/sec. (the region of so-called static tests) to 1,500/sec. This last value was chosen because, while higher rates may be obtained with the "air gun" loading system used in the experiments, it is felt that this represents an upper limit for the instrumentation. A test at this rate requires instrumentation with overall rise times of 10^{-5} sec. or less and the capability of true fidelity at frequencies in excess of 40,000 cycles per second. There is some question whether the fastest transducer systems available satisfy these requirements. Thus, while some experimentors supply data on material properties measured above this rate, such information must be used judiciously with due regard for the limitations of existing measuring systems.

With these considerations in mind, equipment was designed to apply compressive loads on small samples at varying rates and instrumentation developed to measure the load-time history and the displacement-time history of the specimens during the test.

Experiments were performed on samples of bovine femur, embalmed human femur, fresh bovine muscle tissue, nylon and aluminum. The data from these tests is presented as stress-strain curves at various strain rates and plots of various properties versus the strain rate at which they were measured. Further condensation of the results is accomplished by the construction of summary equations and a surface representation of the stress, strain, strainrate relationships.

It should be emphasized that this effort represents only a small beginning in the study of strain rate phenomena. Plans have already been made for a continuation and expansion of this work with special emphasis on the design and calibration of high frequency response instrumentation and the development of a theory that will predict the response of materials based on a now non-existent classification. What is required is a basic theoretical approach to the problem. Then very few experiments will serve to verify the theory. Malvern[37] presents a remarkably successful attempt of this type for a material with a particular constitutive equation containing the strain rate explicitly. Careful preparation of such a test program should result in a minimum of actual tests with a maximum of correct interpretation. The great danger of a program of this sort is to become absorbed with the data collection possibilities without planning to make the data succeptible to intelligent interpretation.

III. PREVIOUS EXPERIMENTAL STUDIES

A. Introduction

The study of stress rate phenomena has long been of interest to the scientific community. Ever since 1872, when J. Hopkinson[26] first described his impact experiments on iron wires, the engineer and metallurgist have attempted to explore and explain such effects. Their efforts have largely centered on the effect of the rate of straining on the properties of materials as defined by the stress strain diagram. While many investigations have been concerned with one or two properties, it would seem that this was due to expediency rather than choice and the ultimate evolving goal of such studies is the production of stress-strain curves under a wide variety of dynamic conditions. It is tacitly assumed that, concurrent with the development of experiments providing such data, there will occur the required theory to generalize sufficiently so that this information is of use to engineers confronted with impact problems.

In the study of the dynamic properties of materials, both the loading of the specimens and the measurement and recording of loads and deformations have presented various difficulties. Chief among these has been the great variety of behavior that materials exhibit. This in many cases requires different tests and measuring techniques for different materials and often for different regimes of loading.

This considerably complicates the task of cataloging and comparing such responses.

In the past, the study of strain rate phenomena has encompassed wide ranges in specimen shapes from the 30 ft. long wires that were tested by Hopkinson[26] to the 0.05 inch thick discs investigated by Kolsky[31,32]. Ranges of strain rates considered (creep studies not included) extend from the 0.001 in/in/sec. for tests conducted on standard screw machines to 17,000 in/in/sec. for the explosive impact tester used by Austin and Steidel.[2]

Although it is of historical interest to know the origins of work and the original thinking in a subject, it is important to observe that by far the major part of the research in dynamic properties of materials has occurred in the last two decades. Thus, for example, while Goldsmith[20] lists 442 papers in his bibliography, many of these describe experiments that are obsolete or in error in the light of modern measurement techniques. The purpose of this survey will, therefore, be the description of the experimental methods that typify the "state of the art," used in the study of the dynamic properties of materials. Furthermore, the discussion will be limited to those methods capable of "high" strain rates since the methods for making slower tests are well known.

There have been essentially seven different approaches through which experimentors have attacked the design of testing machines capable of generating high strain rates.

1) Hydraulic driven rams
(useful in the range 0.001 - 10 in/sec.)

2) Gas driven rams
(useful in the range 0.001 - 100 in/sec.)

3) Flywheel devices
(useful in the range 10 - 1,000 in/sec.)

4) Dropped or gas driven weights
(useful in the range 50 - 5,000 in/sec.)

5) Explosive operated devices
(useful in the region 1,000 - 15,000 in/sec.)

6) Strain energy devices
(useful in the range 100 - 1,000 in/sec.)

7) Hopkinson pressure bar devices
(useful in the range 1,000 - 10,000 in/sec.)

Note that pendulum impact testing machines such as the Izod and Charpy are useful in the limited range 100 - 150 in/sec. and generally indicate only the total energy during the test.

Of these, the first two are inherently incapable of attaining high velocities and will not be discussed further except to point out that the new designs incorporating a double-acting piston with feedback offer the opportunity to make some very finely controlled studies of material behavior in the lower strain rate ranges.

B) <u>Flywheel Devices</u>

A typical example of the use of rotating or flywheel devices is that used by Manjoine and Nadai.[38,39] They were among the first to attempt the determination of the effects of strain rate on the properties of metals at elevated temperatures. In addition, they were also among the first to measure directly and record simultaneously both load and deformation.

The apparatus which they used is shown schematically in Figure 9. The loading device is similar to the high-velocity tension impact machine developed by Mann[40]. Duwez, Wood, and Clark[15] also used this type of loading machine. It consists essentially of a heavy flywheel which is driven by a DC motor with two hammers attached to the flywheel. When the flywheel is rotating at the desired velocity, a solenoid activates the hammers to engage the lower end of the specimen. Strain rates up to 1,000 in/in/sec. were obtained. The authors indicate that above this rate severe oscillations occurred and the data was not reliable.

There are two basic difficulties with this method. First, as the authors point out, it is very difficult to design movable hammers and supports rigid enough to provide the high natural frequency required to prevent oscillations. Second, it is difficult to insure a proper alignment of the hammers and the test specimen. Thus, there are doubts as to whether or not plane impact is attained.

C) Explosive Devices

Shepler[49] at Massachusetts Institute of Technology has given an extensive account of work done on an explosive impact tester developed by DeForest and his associates. Shepler used this tester to obtain strain rates claimed to be as high as 25,000/sec. for steel, aluminum and copper. Calculations of strain rate were based on the assumption that the elongation followed the same trend in time as the diameter of the specimen. Specifically, the strain rate was calculated by dividing

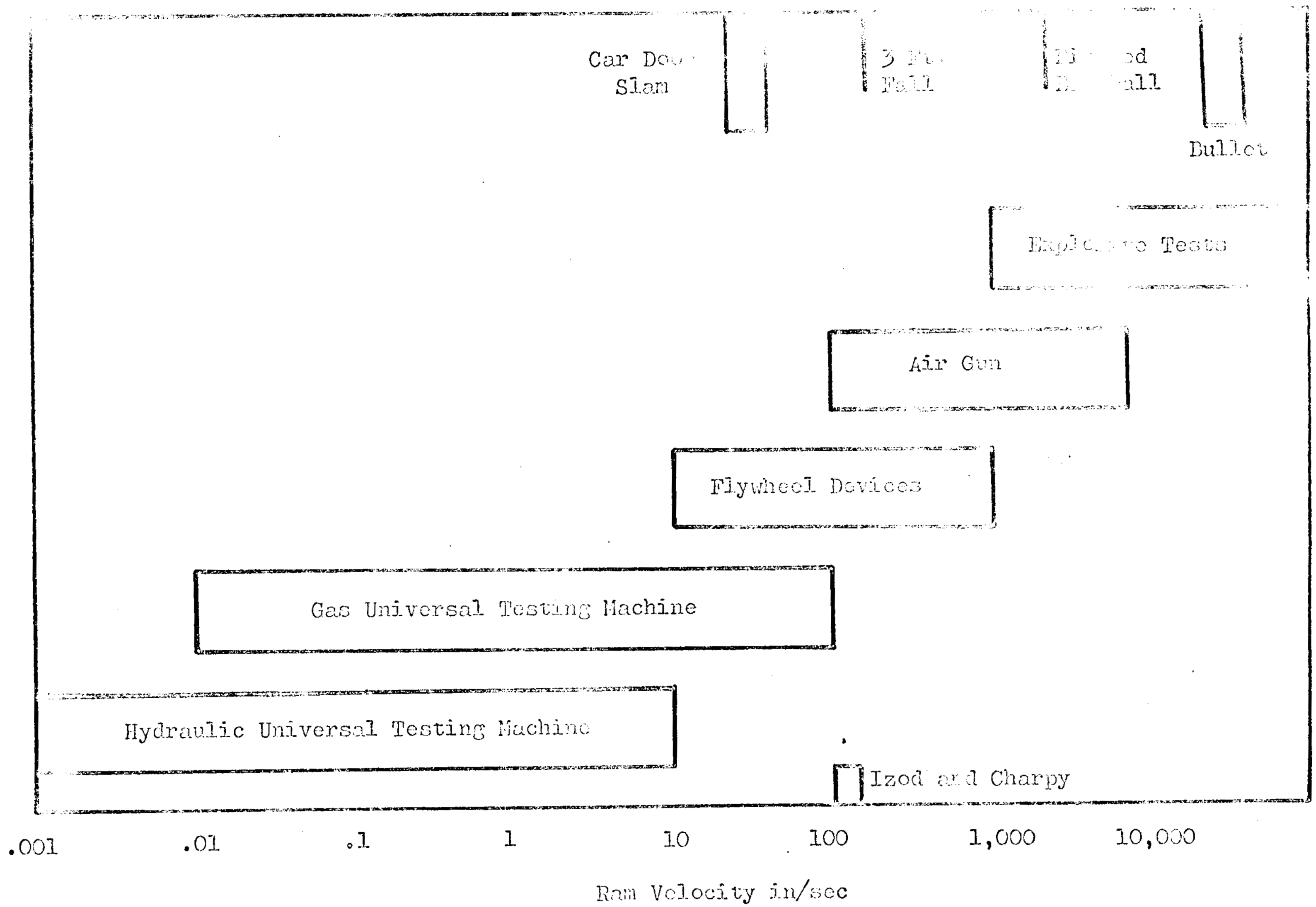

Fig. 2. Velocity Ranges Encountered in Service

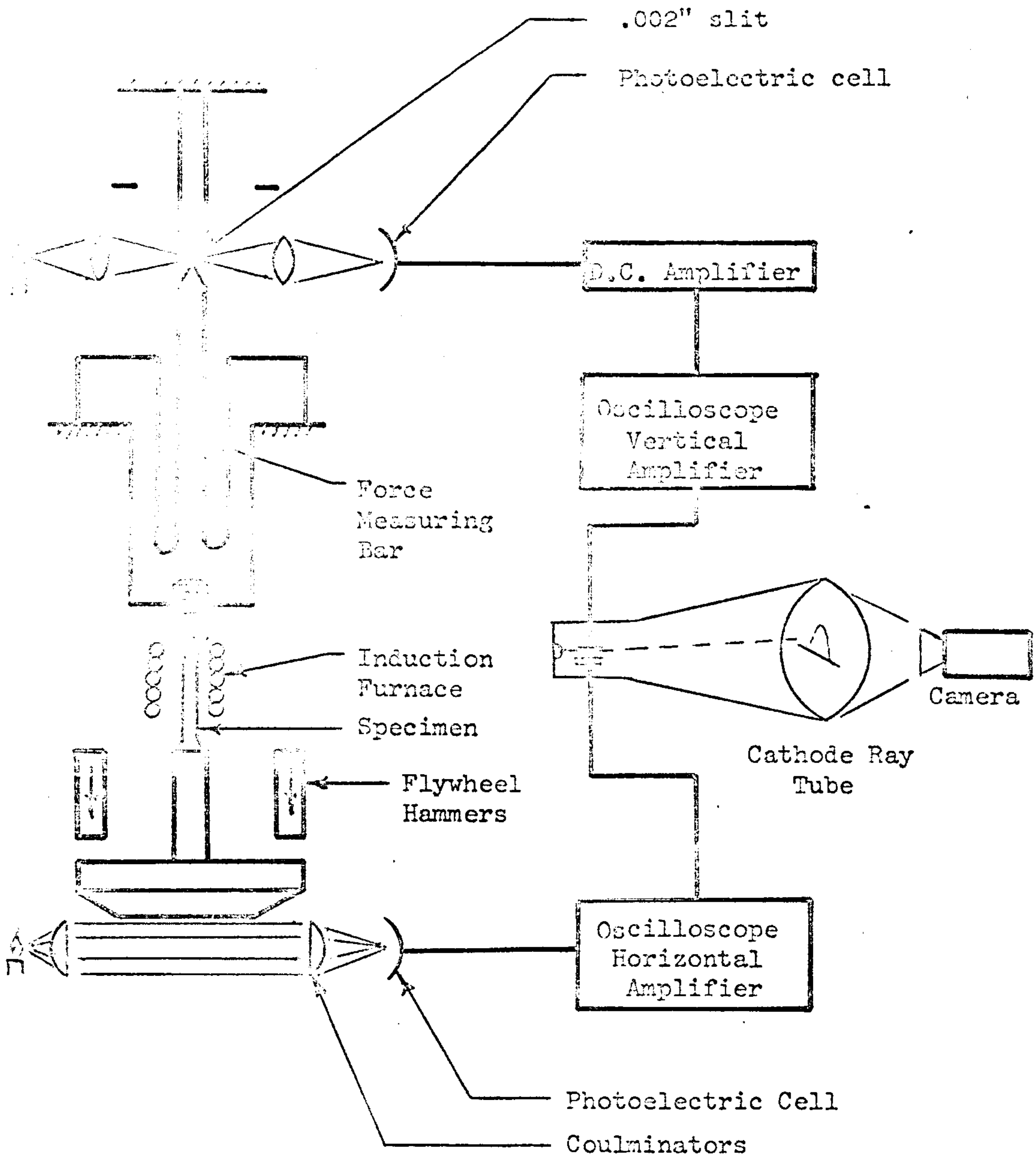

Fig. 3. Schematic-Manjoine-Nadai High Speed Tension Machine

(From reference 39.)

the logarithmic strain from yield to fracture by the time from yield to fracture and multiplying by the ratio of fracture velocity to the average velocity from yield to fracture.

The impact tester consists of four main parts: a fixed frame or base, a steel weighbar mounting for strain gages (or similar load cell) to provide load measurement, a cylinder block and a piston. The specimen is attached to the base through the load cell at one end and the piston at the other. The explosive then activates the piston to load the specimen. A similar device was used by Austin and Steidel[2] in 1959 with considerable improvements in instrumentation techniques.

While this testing machine applies the load slowly with an increasing rate, it is not capable of attaining constant rate tests. Thus, the load and strain rates are functions of the specimen material properties and the explosive pressure rise characteristics. This makes a correlation of the data obtained from this tester, with such desirable parameters as the strain rate or load rate, rather difficult.

D) Hopkinson Pressure Bar

The Hopkinson Pressure Bar, developed by Hopkinson,[26] has been used by a number of investigators. Kolsky[30], Davies[10], and Malvern[36,37] have used this device with some success. Kolsky was able to deduce stress-strain curves for copper, lead, rubber, and Perspex (polymethyl-methacrylate) when stresses were applied for times of the order of 20 microseconds.

Hopkinson's apparatus was originally devised as a means of studying the pulses generated by impact. It consists of a cylindrical steel

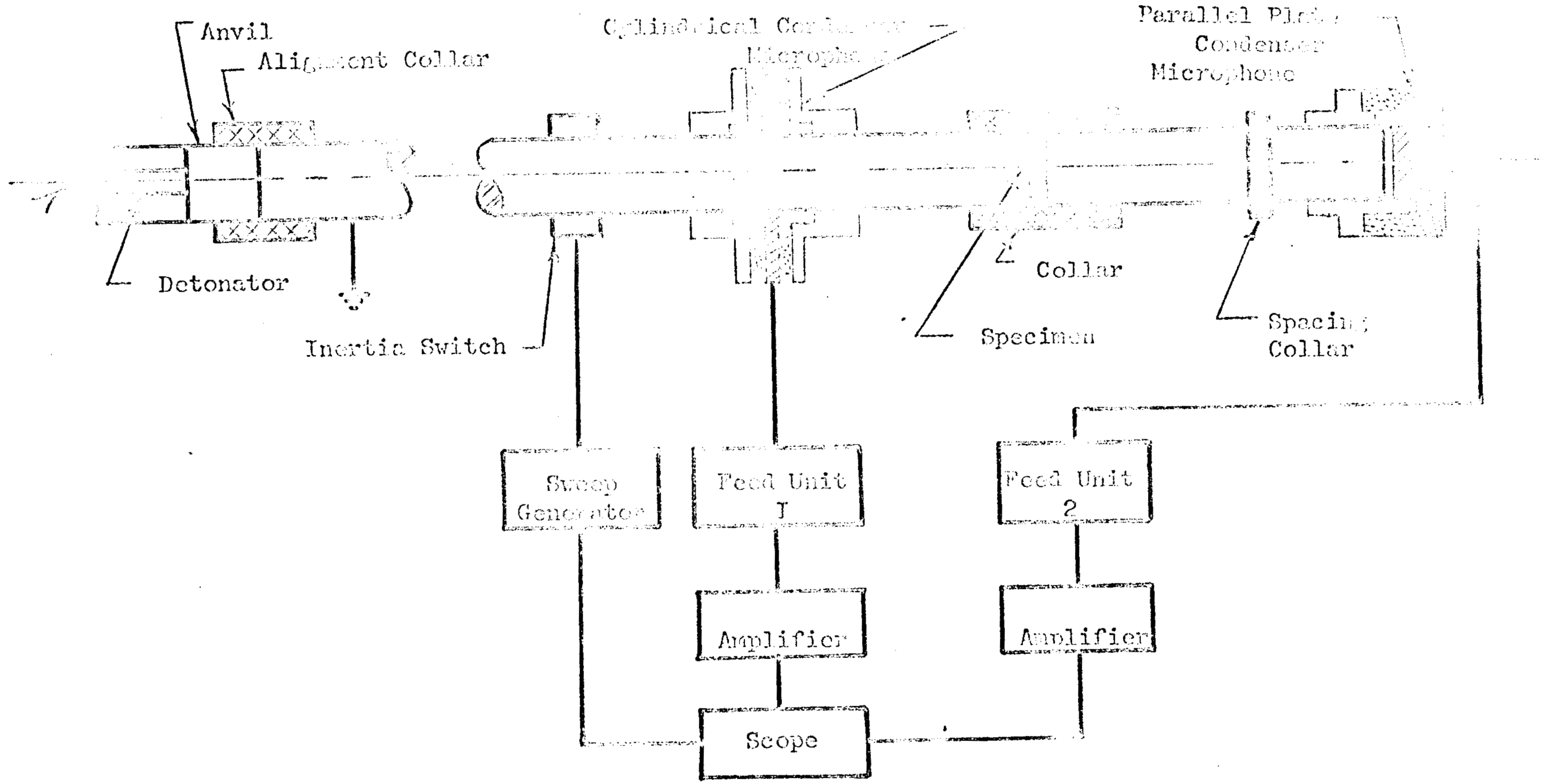

Fig. 4. The Hopkinson Pressure Bar as Modified by Davies and Kolsky.

(From Reference 30).

rod suspended as a ballistic pendulum. The impulse to be measured was applied to one end of the bar. To the other end was attached a "time piece" in the form of a relatively short cylinder of the same diameter and material. The end surfaces of the bar and time piece were ground flat to provide a close fit. When a little grease was applied to the ground surfaces, the time piece could be "wrung" to the bar. As a compression wave traveled down the bar, it was reflected as a tension wave at the free end of the time piece. When this reflected wave produced tension at the interface, the time piece flew off. Since the momentum trapped in the time piece was equal to a section of the pulse of twice the length of the piece, successive experiments with pieces of different lengths gave the nature of the pulse.

Malvern, Davies, Kolsky, and others have modified this apparatus to measure the dynamic properties of materials other than wave phenomena. A thin specimen is sandwiched between pressure bars and the stress pulse loads the specimen. Since the wave front of the stress pulse is quite steep, high rates of loading are attained.

While this method offers a simple way of obtaining very high load rates, there are several disadvantages. The stress-strain history of the specimen can only be obtained using indirect methods which involve assumptions as to the dynamic values of the modulus of elasticity and Poisson's ratio. Also, there is no direct control of the load or strain rate, although this may be varied within narrow limits by varying the specimen size. However, as Kolsky pointed out, too thin a specimen makes accurate determinations of the strains difficult and

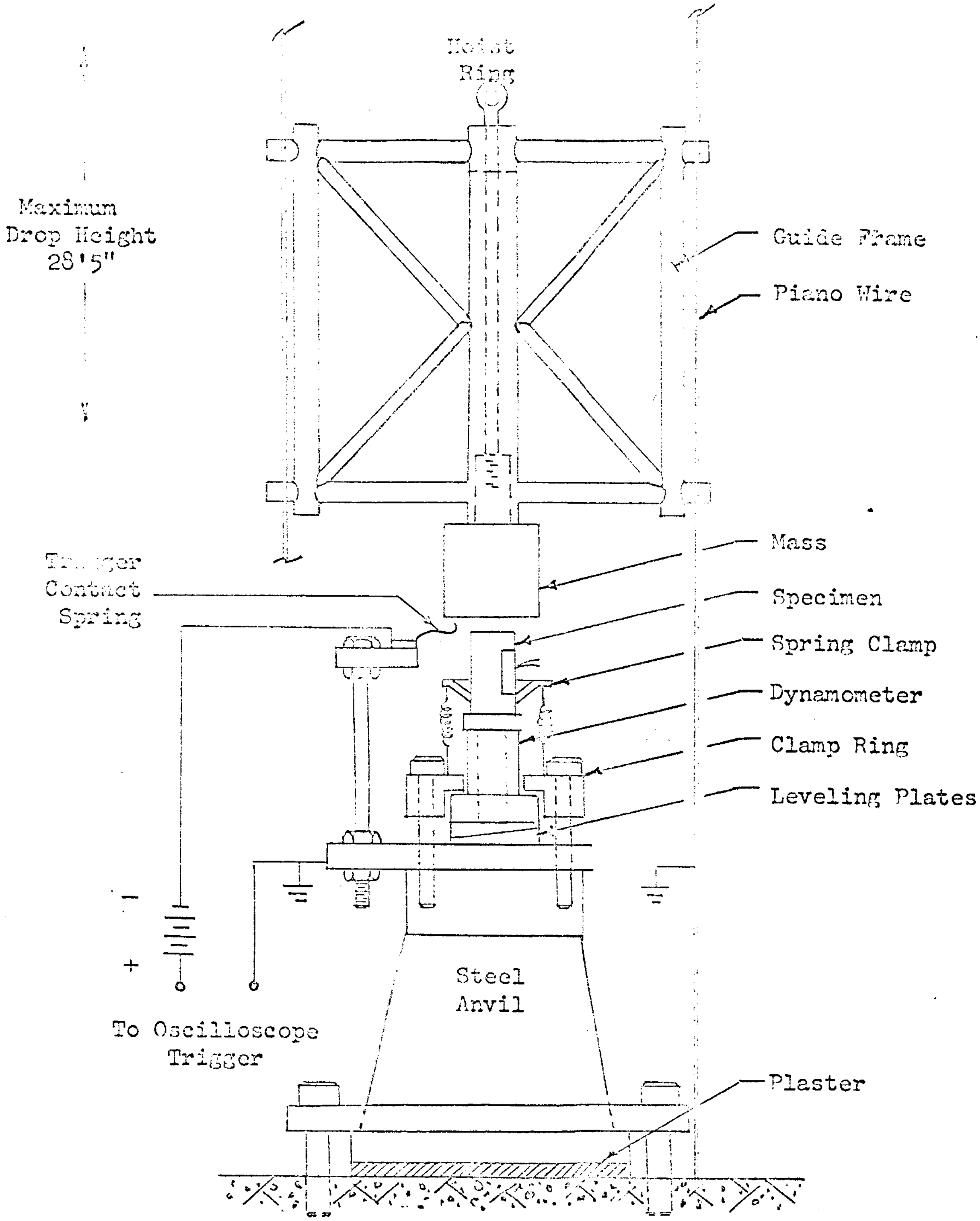

Fig. 5. Schematic of the Dropped Weight Device of Turbow.

(From Reference 56).

specimens that are too thick disallow the assumption that the stresses on the two faces are equal.

E) Dropped and Gas Driven Weights

Dropped or gas drived weights have been used by several investigators in dynamic property studies. Notable among these are Turbow[56] and Habib[22]. Habib used an energy method for indirect measurements of the stress-strain properties. The energy required to produce a given plastic deformation was determined by assuming it equal to the change in kinetic energy of the piston directly before and after impact. The plastic deformation of the specimen was measured and, together with the energy measurement, gave a point on an energy-displacement curve. Despite the obvious disadvantages of this method, Habib's work is quite remarkable for the consistency of the experimental results. In both Habib's and Turbow's tests, the piston was caused to come to rest by the specimen itself. Thus, the velocity varied considerably and could only be assumed constant in the early stages of impact.

The gas driven weight or air gun offers an advantage over the dropped weight in both the velocity range and the guidance system. It is generally quite difficult to provide for plane impact with the dropped weight machine and for very high velocity tests, the dropping heights become excessive.

F) Strain Energy Devices

Recently a device utilizing the strain energy of two beams has been marketed by Optron, Inc., of Santa Barbara, California. This machine is promising in that the loads can be applied gradually, avoiding, to a certain extent, the impact problems of some of the other previously mentioned apparatus. However, the specimen size and properties influence, to some extent, the strain rate. Also, the velocity is neither constant nor uniaxial. This offers complications in both correlation and grip design.

G) Load Indicating Transducers

Very few force measuring systems offer the frequency response required in these experiments. Three types have been used with varying degrees of success.

a) Photoelectric Indicators

b) Strain Gage Load Cells

c) Piezoelectric Load Cells

Of these, the photoelectric types are limited by the response characteristics of the cell material and by the inertia of the movable member, (Figure 3). Most investigations[6,7,16,28,35,56] have used strain gage load cells. There are, of course, numerous problems associated with such load cells operating at high frequency. Frequency response is gained at the expense of sensitivity and signal noise characteristics become important. Also, the frequency response characteristics of the strain gage elements is virtually uncharted territory[43].

Also, these cells generally are undamped and thus problems of overshoot and large spurious oscillations are often encountered. Consider, for example, the natural frequency of a one-inch cube of steel; it is approximately 100,000 c.p.s. Since there is essentially no damping present, a load cell, if constructed from this block, would be usable to about 30,000 c.p.s. Transient inputs would have to be limited to harmonic components of less than this figure for good fidelity. Of course, such a load cell would be very insensitive; and the resolution, limited by the noise level, would be poor.

It is the author's opinion that load cell design and calibration is the most important single aspect of further progress in the study of dynamic material properties.

Piezoelectric load cells with electronic devices that permit static calibration offer much promise in this respect. They have very good resolution, high sensitivity, and can be constructed with very high natural frequencies. Their internal damping is also much higher than metallic load cells. Unfortunately, few investigations[29] have used them. However, it is expected that the future will see broader application.

H) <u>Strain or Displacement Indicating Transducer</u>

A large number of schemes have been described in the literature to provide direct or indirect measurements of strain. Generally, it can be said that the indirect methods involve assumptions about the very properties of materials that are being measured. Thus, without adequate dynamic calibration, these methods are suspect.

Of the direct methods, high speed photography of grids or diffraction patterns appears to be the only way at present of measuring strain fields. Strain gages have been used successfully[6,7,16,28,35,56] by a number of investigators to measure the average strains over the area of the gage. Disadvantages are the high cost and the inability to measure strains larger than about 15 percent. Note that the strain measuring problem does not require as high a frequency response solution as the load measuring one in the constant strain rate test.

A capacitance device was used by Kolsky and Davies in Hopkinson Bar studies to provide an indirect measurement of strain (Figure 4). However, a correction for radial kinetic energy was required. There are no known references using capacitance for direct measurements of average strain.

Photoelectric instruments similar to that used by Manjoine and Nadai have also been used, (Figure 3). These generally have lower resolution and frequency response and require large massive bases to reduce oscillations and extraneous motions.

IV. DESIGN OF THE EXPERIMENT

A) General Considerations

The essential requirements of the equipment necessary to perform the experiment as previously described are:

1) A means of applying deformations to the specimen at varying velocities. The rate must be kept reasonably constant, and the direction of the velocity must be properly oriented.

2) A means of accurately measuring the load as the specimen is deformed.

3) A means of simultaneously measuring the deformation on a time base so that strains and strain rates may be determined.

B) Specimen Size

The specimen size and properties, to a large extent, determine the testing machine and instrumentation parameters. Because of the brittleness of bone and difficulty of gripping muscle tissue, it was decided to test in the compressive mode. This is consistent with the usual load direction when the human system is subjected to impact loading. Also, for this reason, the bone was loaded in the direction of the fibers. Since it is very difficult to obtain bone specimens thicker than 0.175 inches, a specimen size 0.175 x 0.175 x 0.250 inches long was chosen for the bone specimens. Specimens of nylon and aluminum were made in this size so as to allow comparison. The bovine tissue specimens were 0.850 inches dia. x 0.370 inches high, which permitted testing with essentially the same equipment and procedures as used with the bone.

There are two distinct advantages in using specimens with a small gage length. First, the shorter the specimen, the smaller the transit time for stress waves. This means that more reflections will occur and uniform stress is then more closely realized. Second, since the strain rate is approximately the velocity of the piston divided by the length, short specimens enable high strain rates to be obtained with lower striking velocities.

C) Testing Machine

An air operated testing machine (air gun) was constructed especially for this work. The machine consists of a reservoir to store the air, a ground and honed cylinder with a carefully fitted piston, a quick-release mechanism and a platform supported on butyl rubber to hold the specimen and catch the piston. The machine may be operated over a velocity range of 75 to 3,000 in/sec. with a six pound piston. While theoretically the velocity of the piston cannot be constant without some feedback system, it may be made very nearly so by providing that the strain energy adsorbed by the specimen is much less than the total kinetic energy of the piston. The design and specimen size are such that this ratio is always more than ten to one.

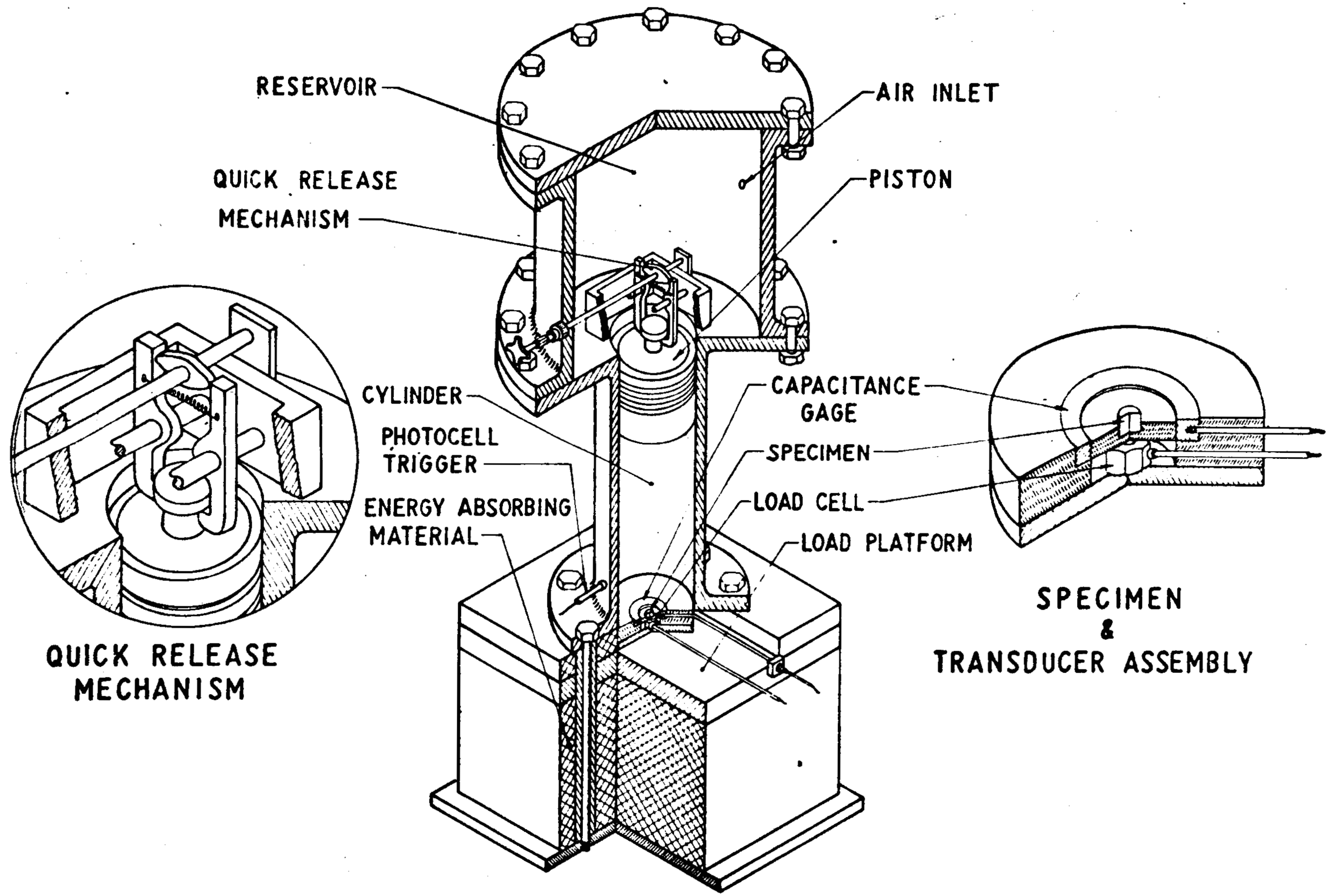

VARIABLE STRAIN-RATE TESTING MACHINE

Fig. 6

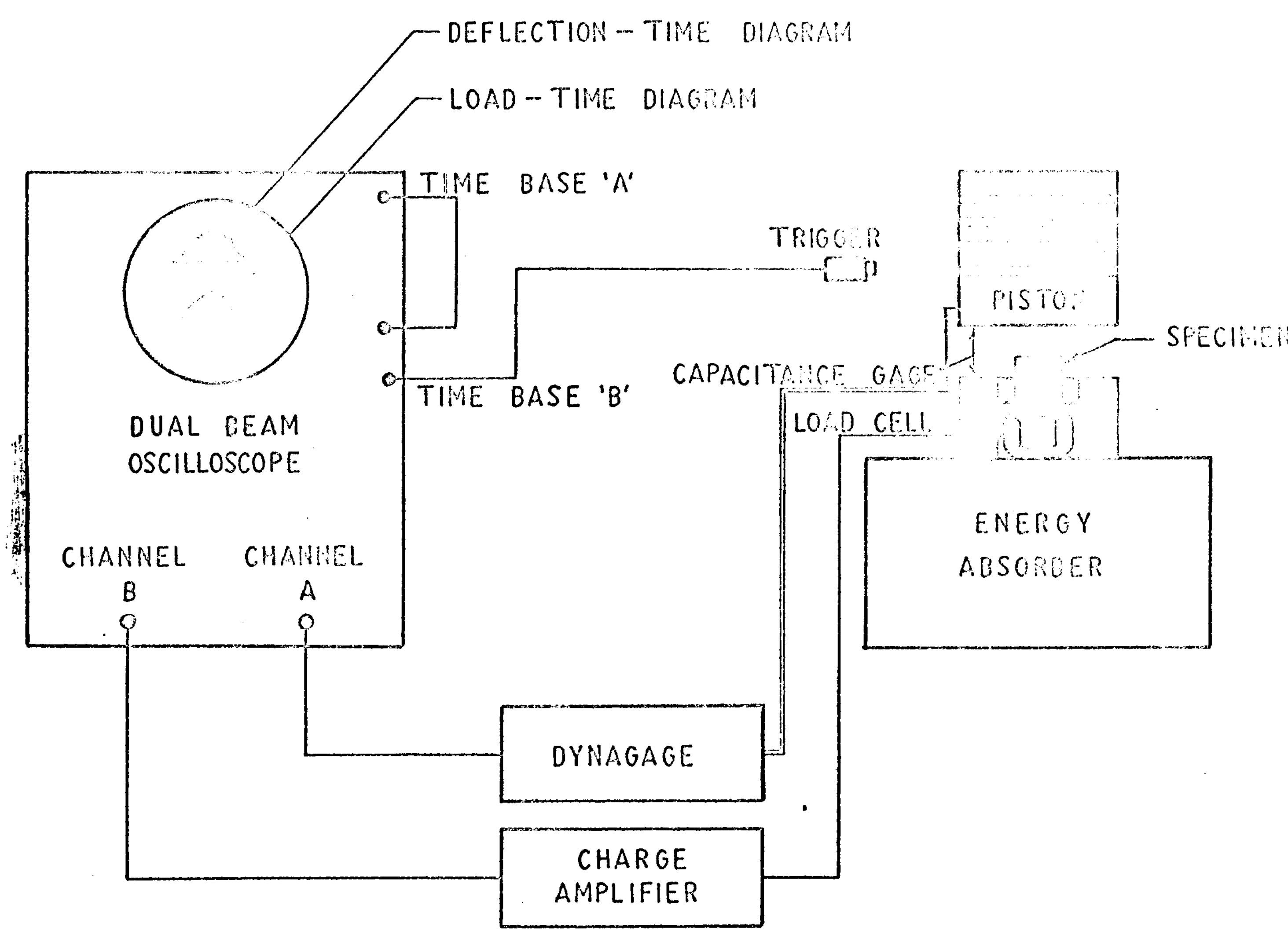

BLOCK DIAGRAM FOR STRAIN-RATE TEST

Fig. 7

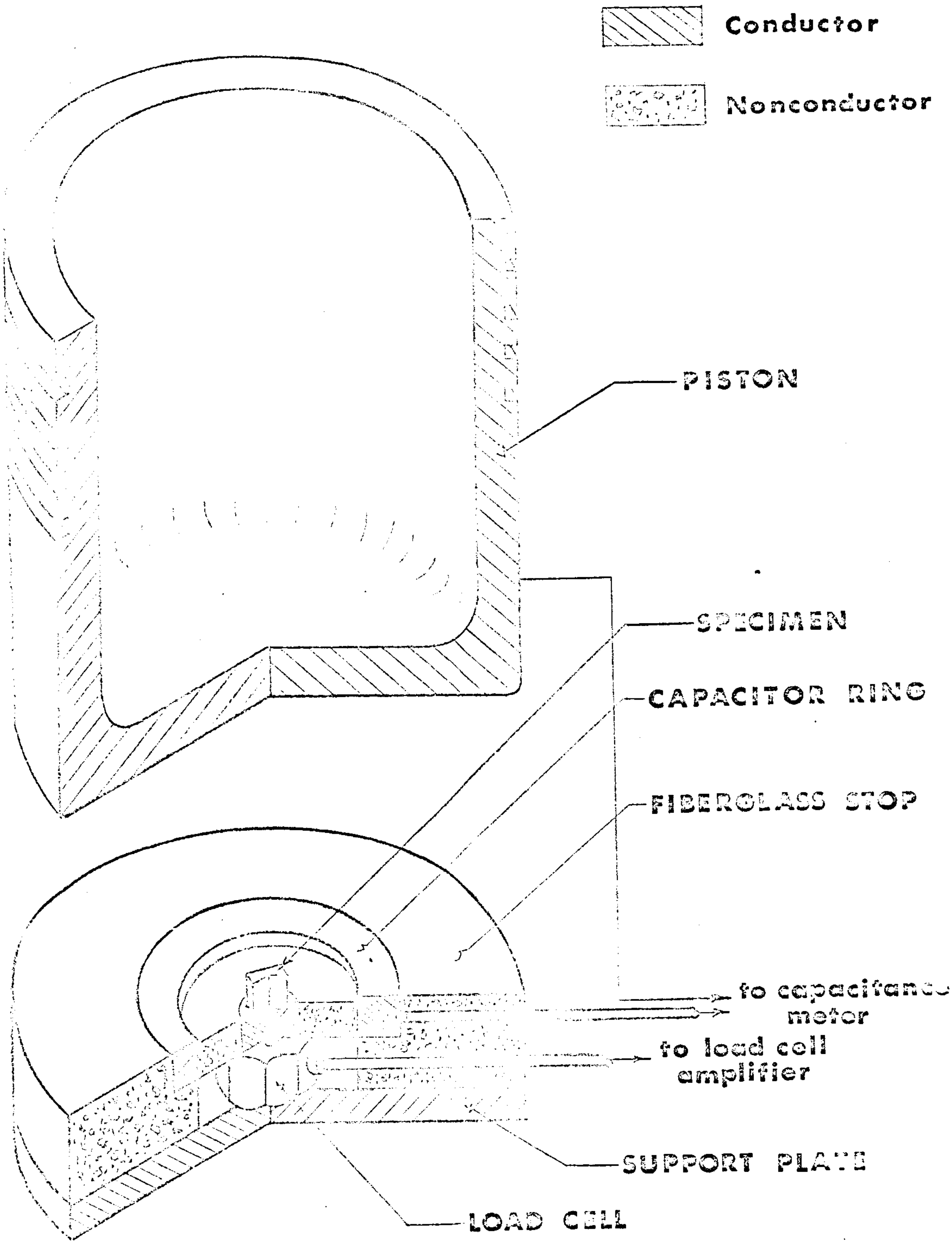

Fig. 7a CAPACITANCE METER

Thus, the piston velocity changes by less than 3 percent during loading. These figures apply to the lowest rate. With all other rates the velocity of the piston during the compression test becomes more and more constant until, at the highest rate, the velocity changes by less than 0.1 percent. Such a small change is hardly detectable.

The amount of specimen compression is controlled by shimming the load platform; and for the bone, nylon and aluminum was set at 0.065 inches. For the tissue specimens, this was increased to 0.110 inches. After compressing the specimen the set amount, the piston strikes a fiberglas stop; and the entire load platform is moved downward, compressing the butyl rubber blocks until the kinetic energy is absorbed. Butyl rubber has a very large hysteresis loss and provides sufficient damping so that almost no bouncing occurs. This is important because the load and displacement transducers are mounted on the load platform and could be damaged by repeated shocks. During the initial testing of the "air gun", the reservoir was filled with oil and with the quick release mechanism engaging the piston a pressure of 500 psi was applied (actual maximum operating pressure is 300 psi) for a period of six hours with no leakage. Only one difficulty in the operation of this machine was encountered; that is, a tendency for the piston to stick in the bottom part of the cylinder after firing. A lever system is then required to free the piston before the aspirator can pull it up to be engaged by the release mechanism. This difficulty is attributed to the poor finish on the cylinder interior which was not manufactured to the specified tolerances.

A Tinius-Olsen Electromatic Testing machine was used for the lower rates and the static tests. Although advertised as a constant rate machine, a speed variation of over 10 percent was noted in the tests of nylon and aluminum. The strain rate-time curve follows the load rate-time curve. This is due to the torque characteristics of the device, (Figure 21). The reported rates are, therefore, average values of those occurring during the test. Since the load rate for bone is essentially constant, the strain rate was also essentially constant in these tests.

D) Load Measurement

The load-time history of the specimen was obtained by mounting a piezoelectric quartz load cell directly under the specimen as the primary transducing element. This load cell was manufactured by Kistler Instrument Corporation (Model 910). The manufacturer's specifications were:

Maximum Load	5,000 pounds
Resolution	0.01 pounds
Charge Sensitivity	20 PC b/lb.
Linearity	1 percent
Deflection of Full Load	less than 0.001 inches
Natural Frequency	100 KC
Signal Rise Time	1 microsecond

Actual measurements indicated the natural frequency of the load measuring system including the associated amplifiers to be approximately

83KC and the rise time to be between 3 and 4 microseconds. Naturally, these figures depend on the method of mounting.

The intermediate modifier to which the transducer was coupled was a Kistler Charge Amplifier Model No. 566. This rather new solid state device allows static calibration of piezoelectric transducers and has a flat frequency response from DC to 150,000 c.p.s. and a linearity error of less than 0.1 percent.

E) Displacement Measurement

The displacement was measured with a specially designed capacitance transducer. This transducer consisted of an aluminum ring of 1.75 square inches area. The specimen was mounted in the center of this ring and the change in capacitance between the ring and the piston bottom was related to the displacement of the piston. This capacitor was connected to an inductor to form a tuned radio frequency circuit. This circuit was coupled by means of a low impedance cable to the oscillator-detector circuit of a Dynagage Amplifier, Model DG 605, supplied by Photocon Research Corporation. The Dynagage consists of a radio frequency oscillator coupled to a diode detector circuit. The small changes in capacity due to motion of the piston head produce relatively large changes in the diode detector impedance. Therefore, over a limited range, the output of the detector is proportional to the change in capacitance. The rectified output of the detector is coupled through a single stage cathode follower and transsistor filter network to provide a carrier free low impedance output.

The tuning range of this instrument is 610 kcps to 850 kcps. The frequency response curve as supplied by the manufacturer was essentially flat to 15,000 cps but could be used with a corresponding loss of fidelity to 30,000 cps. The square wave rise time was specified as less than 15 microseconds.

Electrode capacities between 2 and 30μμf are necessary for tuning the Dynagage. The minimum movement that can be measured is limited to the threshold noise level of the equipment. This is dictated to a large extent by the initial air gap. Good linearity of output vs. change of air gap exists for approximately 20 percent of the initial gap. The ring and air gap used here could easily resolve 50 micro-inches.

F) Lateral Strain Measurement

Lateral strains were measured by resistance foil strain gages. High elongation gages, Type 1 x 1 M075, manufactured by Budd Instruments Company were used. These were cemented with GA-5 cement, a high elongation heat curing epoxy. Because of obvious difficulties in installing such gages on wet bone, this measurement was made on thoroughly dried bone, nylon, and aluminum. The grid of the strain gages covered approximately one fourth of the lateral surface area. Two gages were used, on opposing sides of the specimen with this output connected in series. Thus, an electrical averaging occurred and flexure strains due to non-uniform loading and response of the specimen tended to cancel.

Two separate signal modifying systems were used in these measurements. For the low rates up to 1/sec., a Datronic Model 800 carrier wave amplifier was used. This instrument has a frequency response that is flat to 400 cps and, therefore, could not be used at the higher rates. At the higher rate, a Type Q Tektronic carrier wave amplifier was used. This system is usable at frequencies up to 6 KC and has a rise time of 60 microseconds.

G) Data Recording

In the initial phases of this work, a Tektronic No. 531 oscilloscope with a Type M preamplifier was used for data display. The Type M preamplifier provides for four separate input signals by means of an electronic switching device that alternately switches from input to input at a rate of 100 KC divided by the number of channels in use. At the higher strain rates, this switching frequency proved inadequate and, as a Tektronic No. 555 dual beam oscilloscope became available, it was then used. This provided two-channel recording at frequencies far in excess of the capability of the primary measuring transducers. However, since only two-channel recording was possible at the higher rates, the Poisson ratio studies at these rates were made without recording the load-time history of the specimen. This could have been recorded on a separate oscilloscope; but, since this data was not considered necessary for the Poisson's ratio studies, it was not recorded.

The actual data recording was done photographically using a technique known as "single shot oscillophotography." Basically, this consists of using a lockout device that allows the oscilloscope to sweep only once. The camera lens is left open, and the sweep is initiated by an appropriate triggering device. The photographic film then records the data that follows for a period of time dependent on the sweep speed of the oscilloscope. This method is quite valuable in the study of fast transient phenomena but represents several technical difficulties. First, the effective writing rate of the oscilloscope, camera lens, film combination must be determined and has both maximum and minimum values that cannot be exceeded. Thus, in this work over such a broad range of strain rates, three different films were required:

1. Polaroid Type 55 P/N ASA 25 for rates up to 1/sec.

2. Polaroid Type 47 ASA 3,000 for rates up to 1,000/sec.

3. Polaroid Special Purpose Type 51 ASA 10,000 for rates up to 8,000/sec.

Sweep triggering is especially critical in single shot oscillophotography. In these experiments, several schemes were attempted to generate an accurate triggering signal. The Type 531 oscilloscope was internally modified so that a variable time delay could be imposed between the triggering signal and the advent of the single sweep. This allowed precise synchronization of the initiation of the sweep with the start of the compression tests. With test times on the order of 10 microseconds, the importance of sweep synchronization cannot be overemphasized. The Type 555 oscilloscope came equipped with this feature so that no modification was necessary. At the low rates, a simple contact switch served as the triggering device. At rates much above 10/sec, however, switch breakage occurred and another method was required. A magnetic proximity pick-up was tried, but the output waveform and the oscilloscope triggering stability characteristics introduced an uncontrollable variation in timing which made operation difficult. A photoelectric trigger was then tried and, while subject to the same difficulties as the magnetic pick-up, operated in a more reliable fashion. Finally, when the Type 555 oscilloscope became available, it provided a fine vernier adjustment for the triggering stability which allowed triggering on the incoming load cell wave form. This proved the best method and was used subsequently.

With this system, photographs displaying two wave forms representing the load-time history and the displacement-time history of the specimen were obtained. For the Poisson's ratio studies, the lateral strain-time was substituted for the load-time history. It is possible to record the load-displacement diagram directly with this equipment. This diagram, by definition, is tantamount to the engineering stress-strain curve. All that would be required to do this would be to connect the load signal to the horizontal input of the oscilloscope. A similar scheme could be done with the two strain signals in the Poisson's ratio tests. The secant modulus of this curve would then give Poisson's ratio. These methods would not yield velocity measurements and were not used for this reason.

H) Summary

The salient features of this equipment are:

a) An air gun that provides for precise alignment and control of the piston velocity.

b) A piston kinetic energy to specimen strain energy ratio that is always larger than 10 to 1 so that the velocity of the piston during the test is reasonably constant.

c) Provision to measure the load with accuracy and high fidelity.

d) Provision to measure the velocity and displacement of the piston, thus allowing computation of the average strain and average strain rate.

e) Recording of the load-displacement history of the specimen.

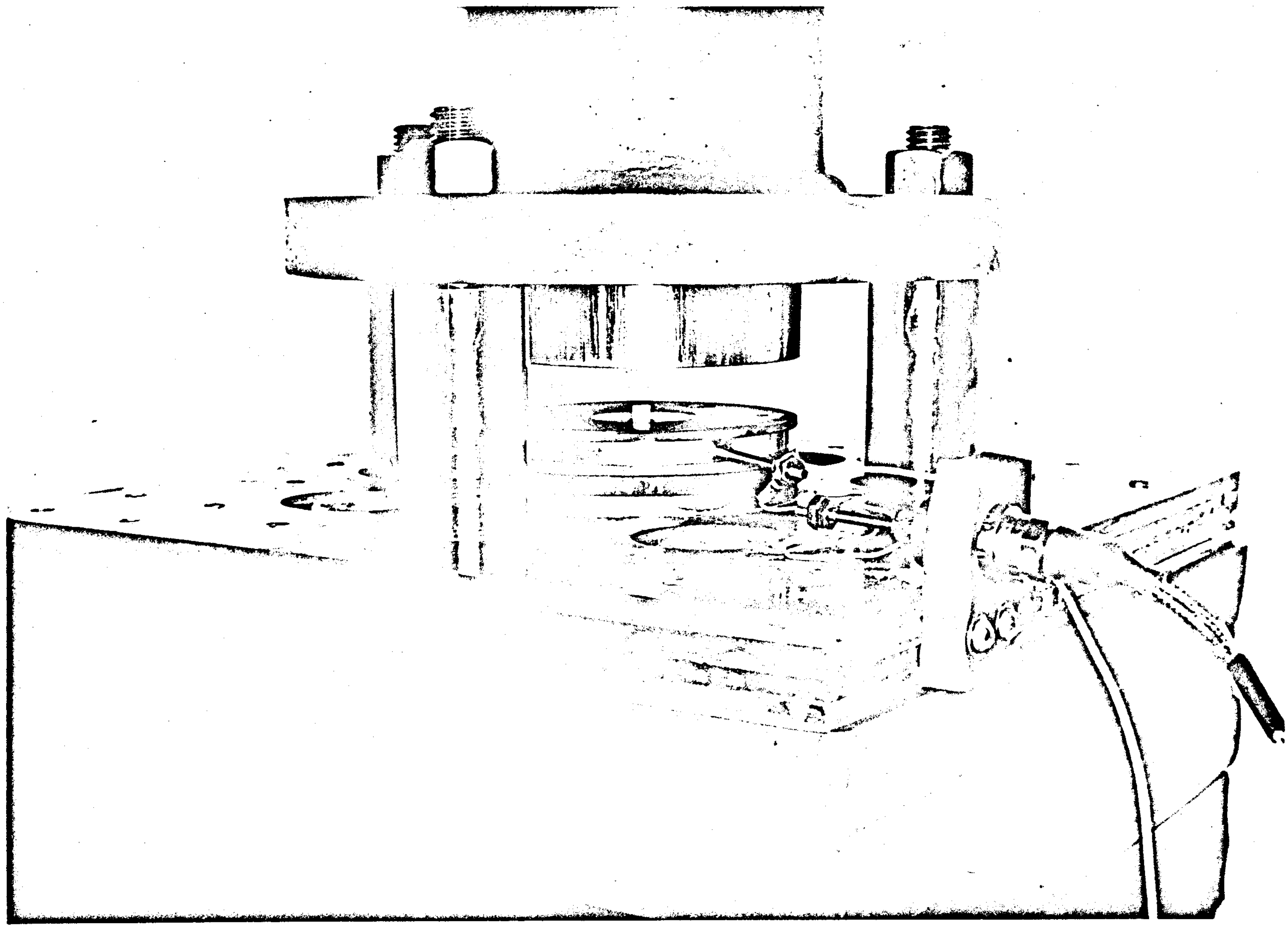

Fig. 8 LOAD PLATFORM

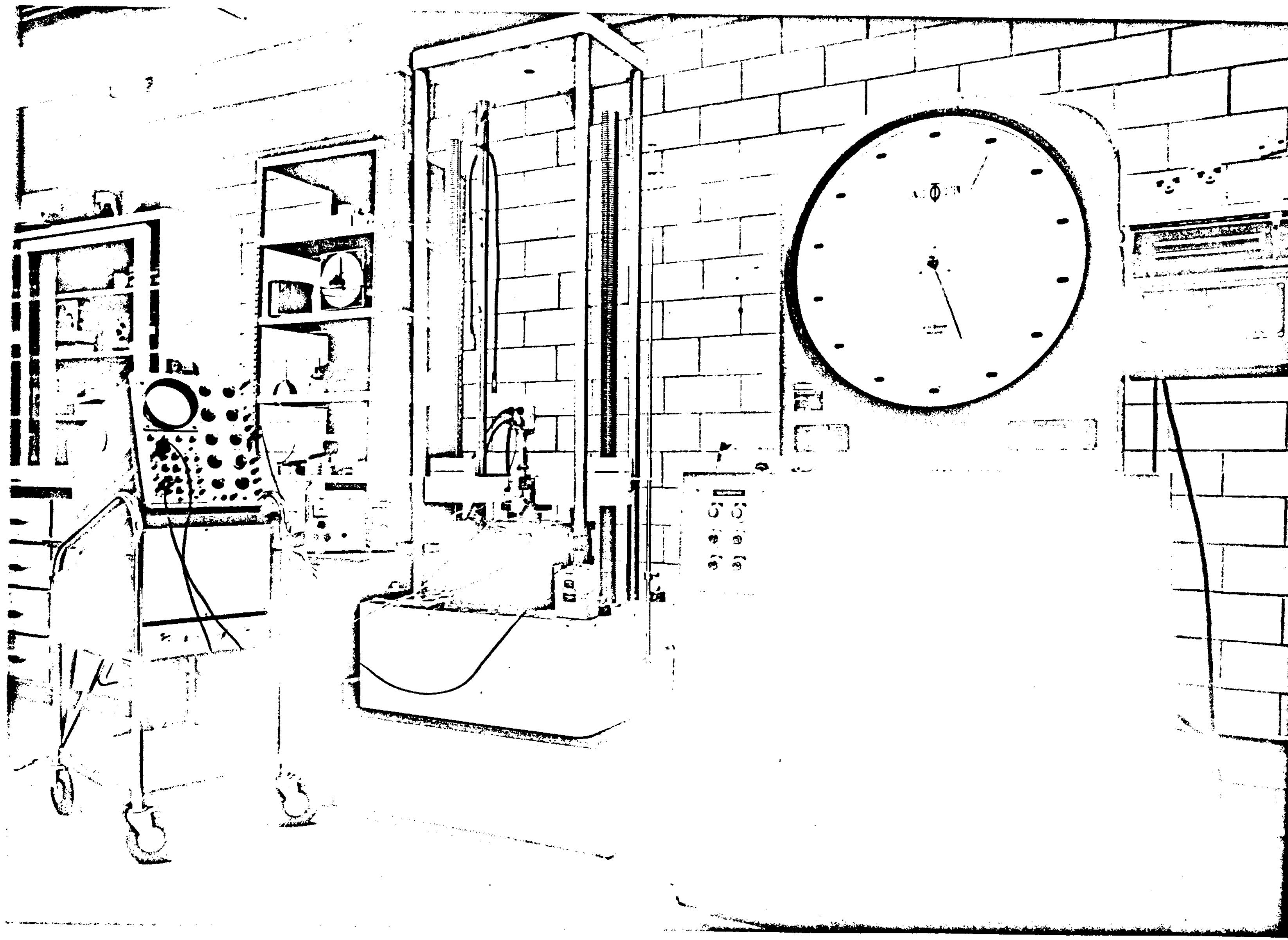

Fig. 9 LOW STRAIN RATE TEST

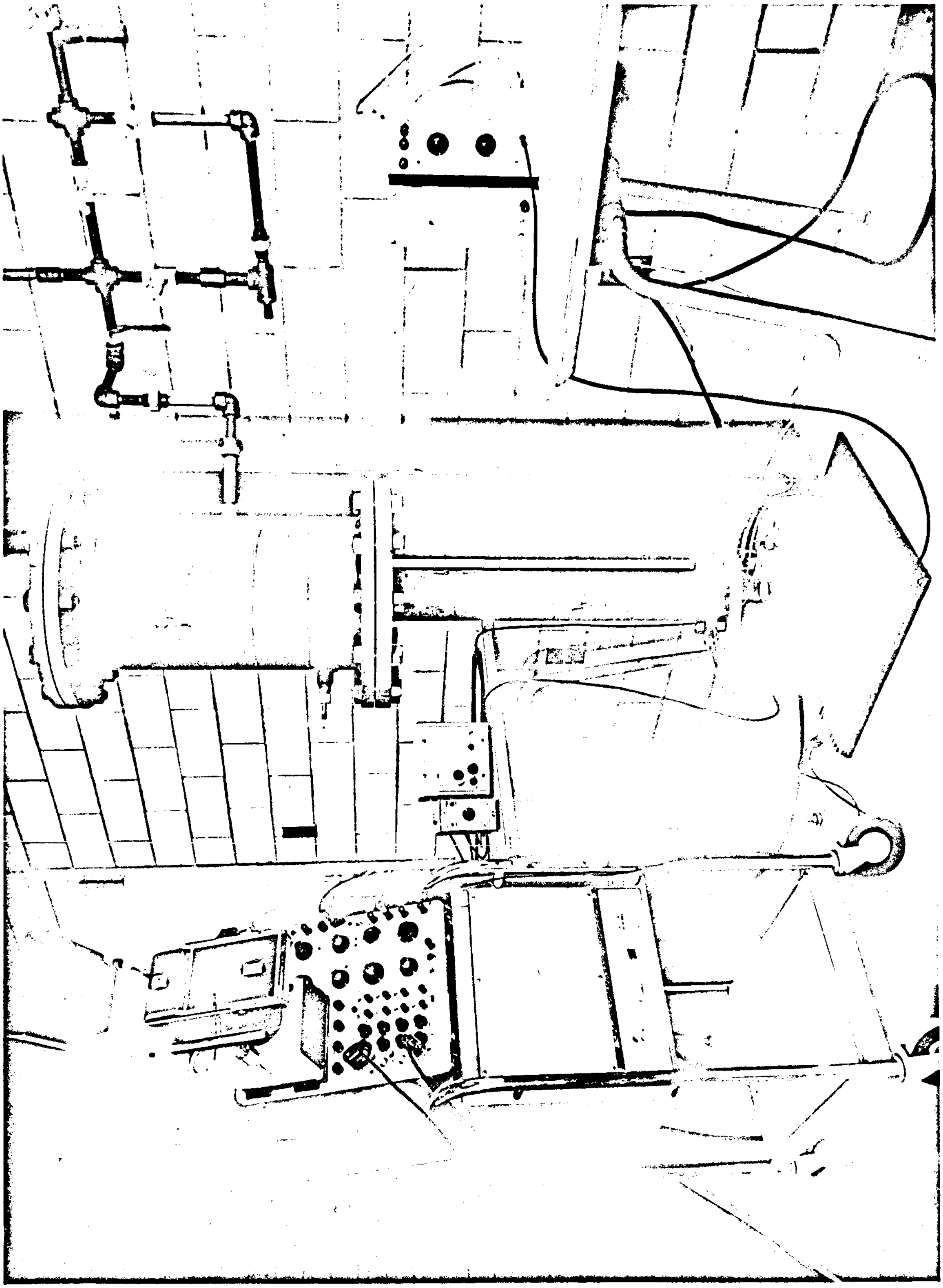

Fig.10 HIGH STRAIN RATE TEST

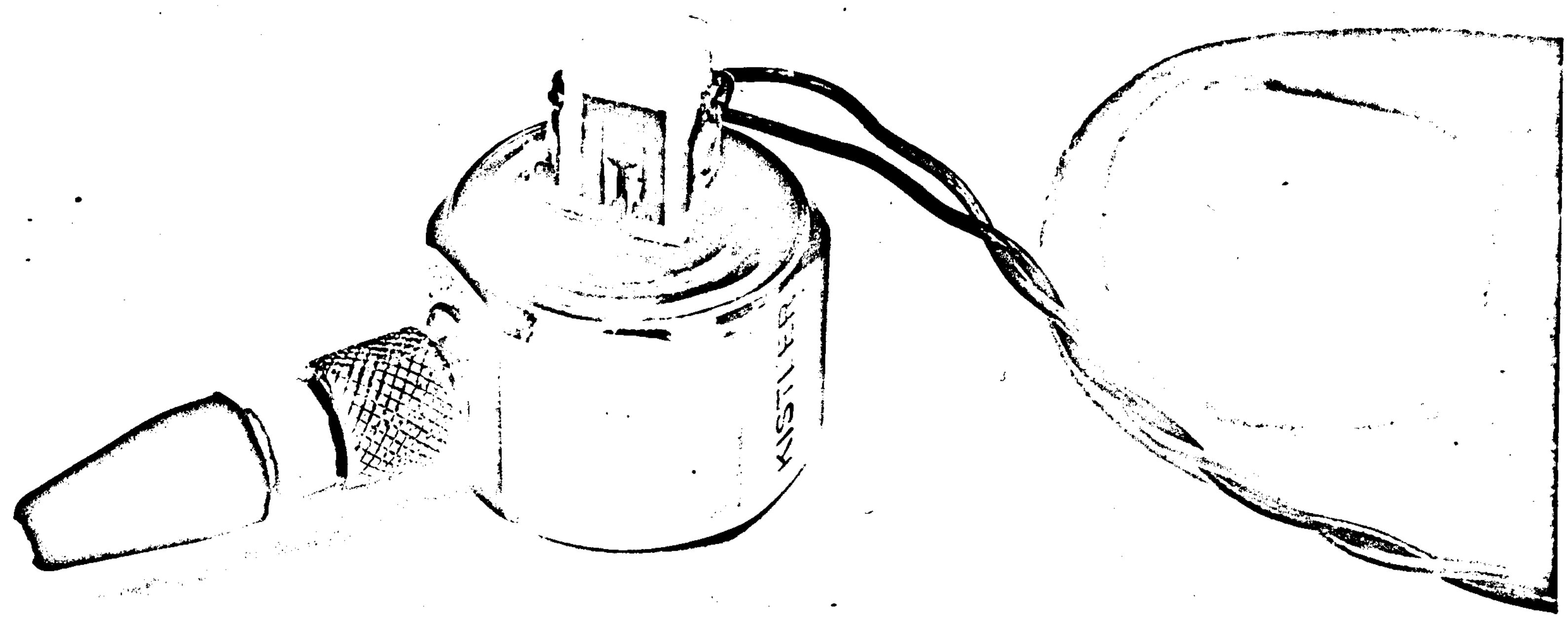

Fig. 11 BONE SPECIMEN, STRAIN GAGES AND LOAD CELL

V. CALIBRATION

A) Introduction

Dynamic calibration of force and motion measuring systems is extremely important; but, unfortunately, it is generally quite difficult. As a consequence, the dynamic calibration of such instrumentation is frequently accomplished through a static calibration and consideration of the natural frequency of the device. Analogies may then be made with the frequency response of a linear harmonic oscillator to a sinusoidal input. A harmonic analysis of the input waveform then indicates to some extent the fidelity of the system in question, and the accuracy of a static calibration may be estimated. The chief source of error in this approach is the disparity between the theoretical behavior of a linear harmonic oscillator and the actual behavior of real systems. Unfortunately, the only accurate method of assessing this error is through a comparison of the true dynamic response of the actual system and the estimated theoretical response based on the abovementioned scheme.

B) Load Cell

The load cell, as mounted in the support platform, had a measured natural frequency of 83 KC and a rise time between 3 and 4 microseconds. This was determined by ringing the cell and observing the ensuing waveforms. Static calibration of such quartz load cells is the accepted procedure and recommended by the manufacturer. The static calibration of the cell used in these experiments was made by loading in a Tinius Olsen Electromatic Testing machine with the cell mounted in the support platform in exactly the same way as during the experiments. The output was displayed on the oscilloscope and calibration curves perpared, (Figure 12). Thus, an overall system calibration was made from a known force input. The testing machine had previously been calibrated at several discrete points with dead weights and errors were all less than 2 percent. An investigation of the effect of load eccentricity on the output of the load cell was made and indicated that, within broad limits, the effect was negligible. Since adequate centering was provided in the support frame design, this was not pursued further.

C) Capacitance Displacement Meter

A special fixture was constructed for use in the calibration of the capacitance displacement meter, (Figure 14). This consisted of a differential screw that allowed precise movement of the piston. A dial indicator with an estimated accuracy of ± 0.0005 inches was used to measure this movement. The output of the capacitance meter was measured through the Dynagage and the oscilloscope in the same manner as during the actual experiment. This gave a simple system calibration. It should be pointed out that the initial zero or tuned point on the Dynagage has a significant effect on the calibration. This requires that the specimens all have the same height. Furthermore, since the sensing ring of the capacitance meter surrounds the specimen, the electrical properties of the gap are influenced by the specimen. Calibration should, therefore, occur with the specimen in place. However, calibration tests with and without a specimen indicated no detectable difference in the case of the bone, aluminum, and nylon. This is attributed to the large gap volume compared to the small specimen volume. In the case of the larger muscle tissue specimens, however, considerable difference occurred and calibration had to be made with a specimen in place.

D) Strain Gages

No calibration of the strain gages was made. The manufacturer's gage factor was used for strain computation and no correction was made for cross-sensitivity.

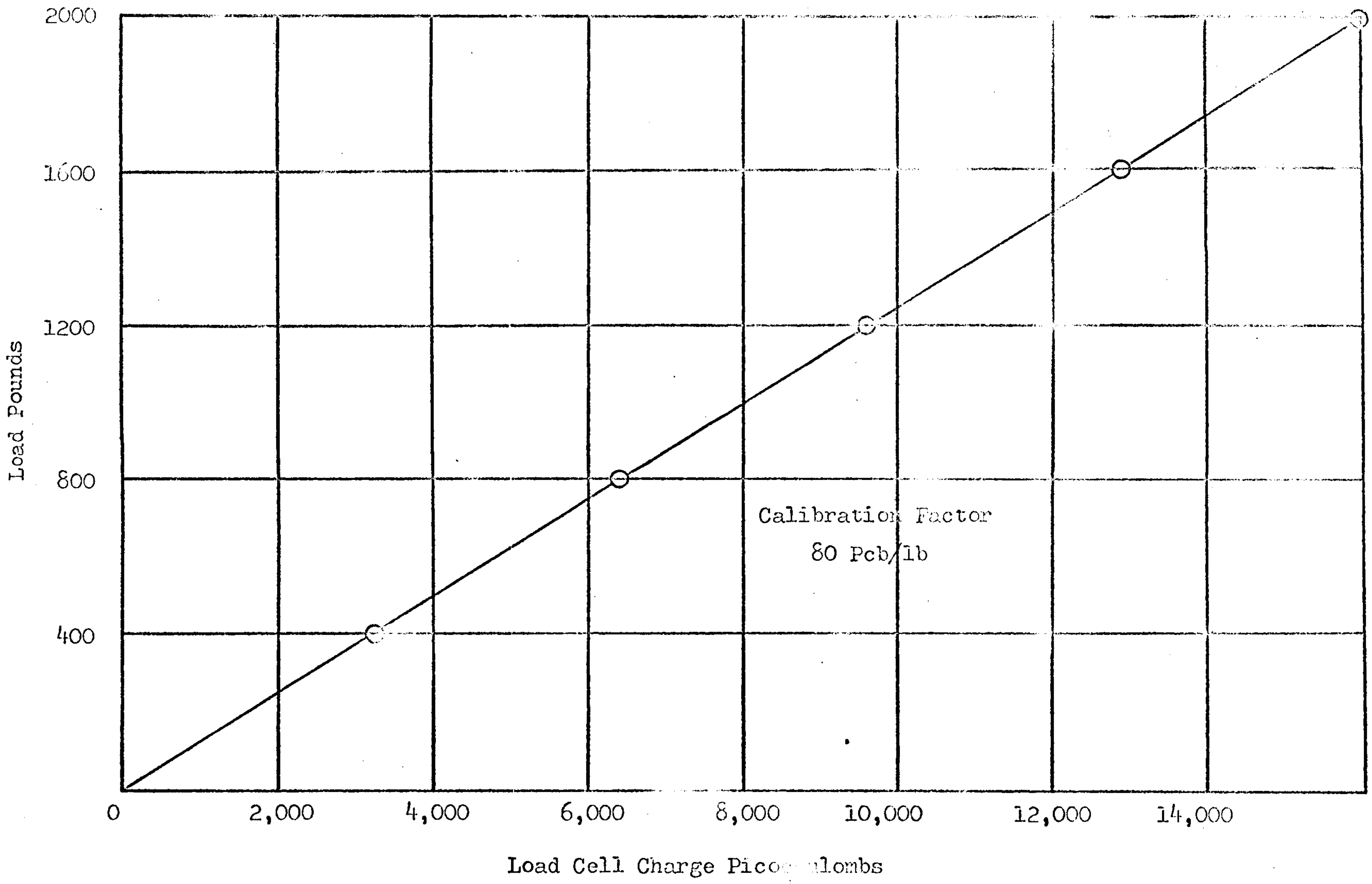

Fig. 12. Calibration Curve Kistler 910 Load Cell

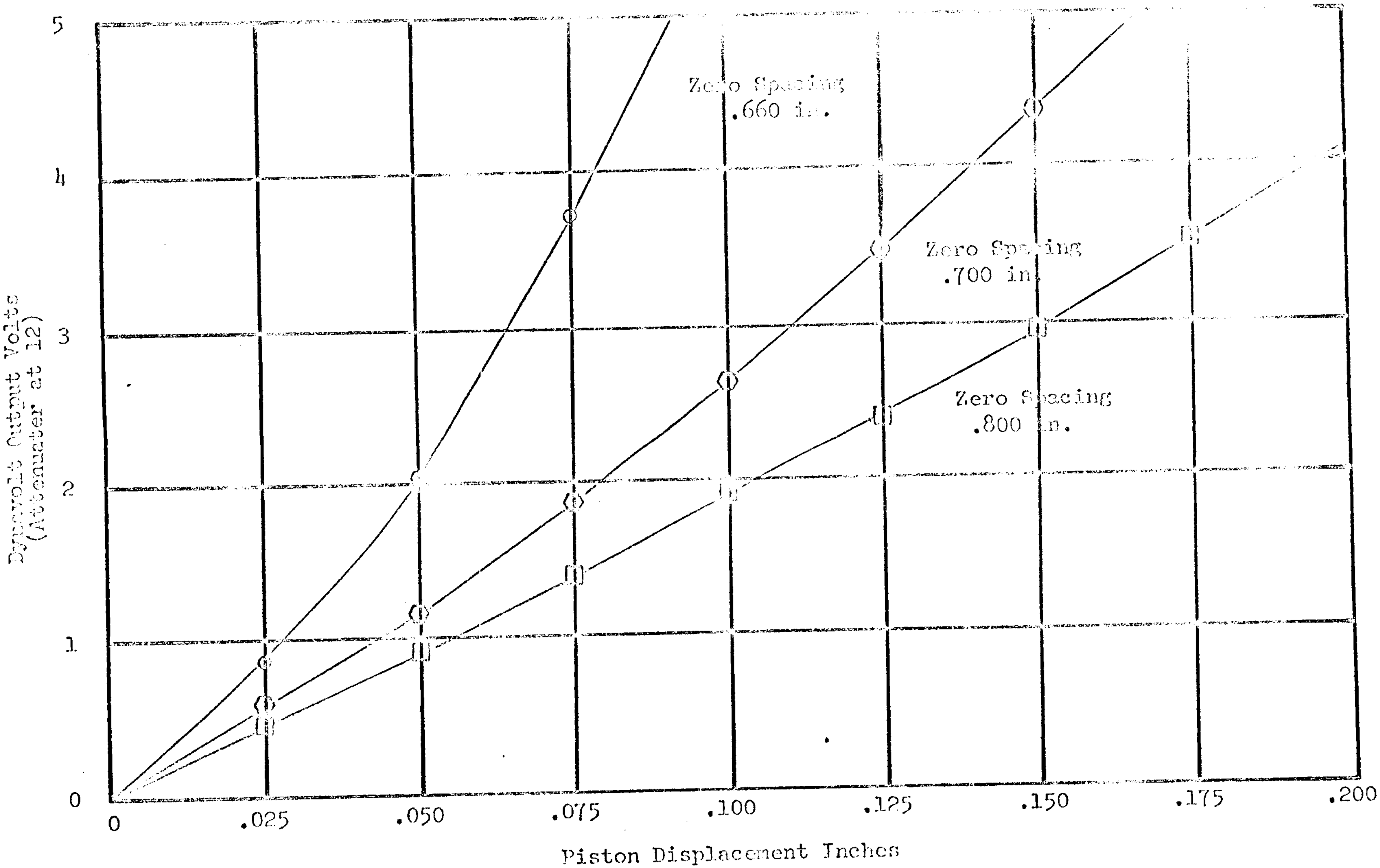

Fig 13. Calibration Curves for Capacitance Displacement Meter Plate Size 3" Dia.

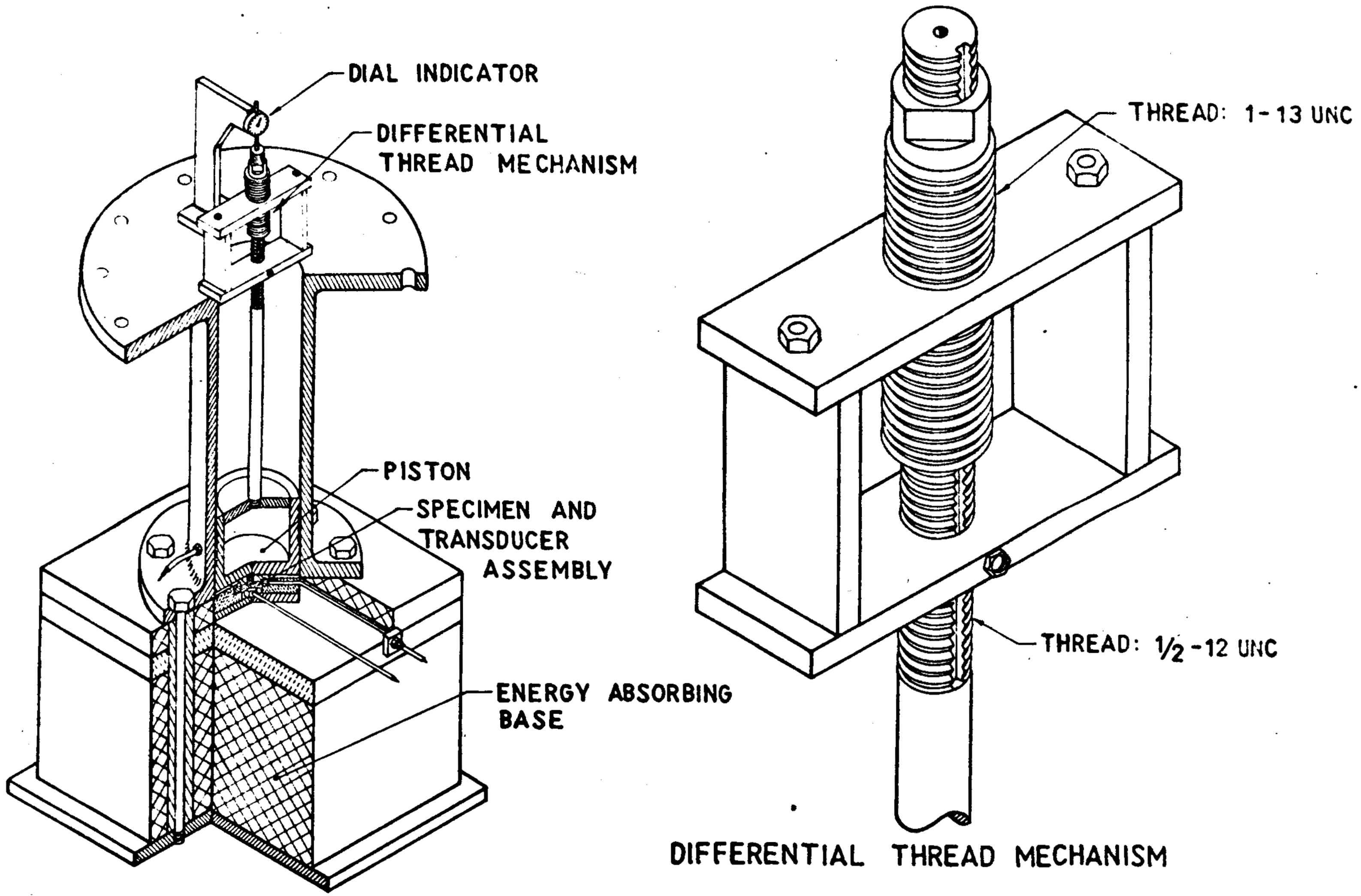

FIG. 14

CAPACITANCE STRAINMETER
CALIBRATOR

VI. SPECIMEN PREPARATION AND SELECTION

A) Human Bone

The human bone specimens were all obtained from the right femur of a 24-year old white male who died of an acute cardiac failure. The specimens were made from the middle third of the shaft. No attempt was made to study the variation of properties with location, and it was assumed that the specimen properties were approximately the same. The sample had been embalmed with a mixture of formilin, phenol, alcohol and glycerin, and was typical "dissecting room material." The middle third of the shaft was first sawed lengthwise into sixths, and these sextants then wet sanded into rectangular strips approximately 0.180 x 0.200 x 3 inches. Care was taken to maintain the axis of these strips parallel with the axis of the shaft, thus maintaining an approximate uniformity in the arrangement of the trabeculae of the various specimens. This wet sanding produces a surface finish that is smooth and free from defects with no heating of the material or moisture loss. Since drying causes significant changes in the mechanical properties of bone, the samples were kept either wet or submerged in water at all times, except for the Poisson's ratio test specimens. A small bench miller was employed for the final machining operation, (Figure 15). The final specimen size was 0.175 x 0.175 x 0.250 inches.

B) Bovine Bone

The samples tested were all machined from one bovine femur. Less than five days elapsed from the time the animal was sacrificed and the completion of all the tests except the highest strain rate test. The highest strain rate test was performed approximately thirty days later. During this time, the material was kept submerged in water and refrigerated. Other handling and machining was identical to that employed with human bone specimens.

C) Bovine Musculo Tissue

These samples came from the muscle tissue surrounding the bovine femur. All samples came from the same animal and testing was completed within three days after obtaining the material. The material was conditioned prior to this by aging under refrigeration until the mechanical stabilized state was attained. It is not known how closely this state approximates the *in vivo* state. The material was first sliced perpendicular to the long axis of the bone in sheets 3/8 inch thick. Then, using a cork boring tool, 0.875 inch dia. round, specimens were punched from the sheets, (Figure 16). Specimens composed primarily of muscle tissue with little or no fat were selected for testing.

D) Aluminum

Alcoa Aluminum Alloy QQ 1100, which is 99 percent pure aluminum, was selected for testing. The material was supplied in 1/4 inch square extruded bar stock. The specimens were machined so that the specimen axis was perpendicular to the extruding axis. After machining, the specimens were annealed at 700° F. for one hour and cooled in air. The specimen size was the same as for bone.

E) Nylon

Nylon is the generic name for the polymerization product formed in the reaction of an organic acid with an amine. The nylon used in this study was a diacid-diamine type manufactured by the condensation of adipic acid with hexamethylenediamine.

$$HO - \overset{\overset{O}{\|}}{C} - CH_2CH_2CH_2CH_2 - \overset{\overset{O}{\|}}{C} - OH \quad \text{(Adipic acid)}$$

$$+ \begin{matrix} H \\ H \end{matrix}\!\!>\!N - CH_2CH_2CH_2CH_2CH_2CH_2 - N\!<\!\!\begin{matrix} H \\ H \end{matrix} \quad \text{(Hexamethylenediamine)}$$

$$CH_2CH_2 - \underset{\underset{O}{\|}}{C} - \underset{\underset{O}{\|}}{N} - (CH_2)_6 - \underset{\underset{H}{|}}{N} - \underset{\underset{O}{\|}}{C} - CH_2 - CH_2 \quad \text{(Nylon 6,6)}$$

The chain length can be controlled by adding a slight excess of either acid or amine to the polymerizing mixture. In the commercial nylon used here, the chain length corresponded to a mass formula of about 12,000. The density for this material was 0.042 lbs/in^3.

The material was supplied in 1/4 inch square extruded bar stock and specimens machined in an identical fashion to the aluminum.

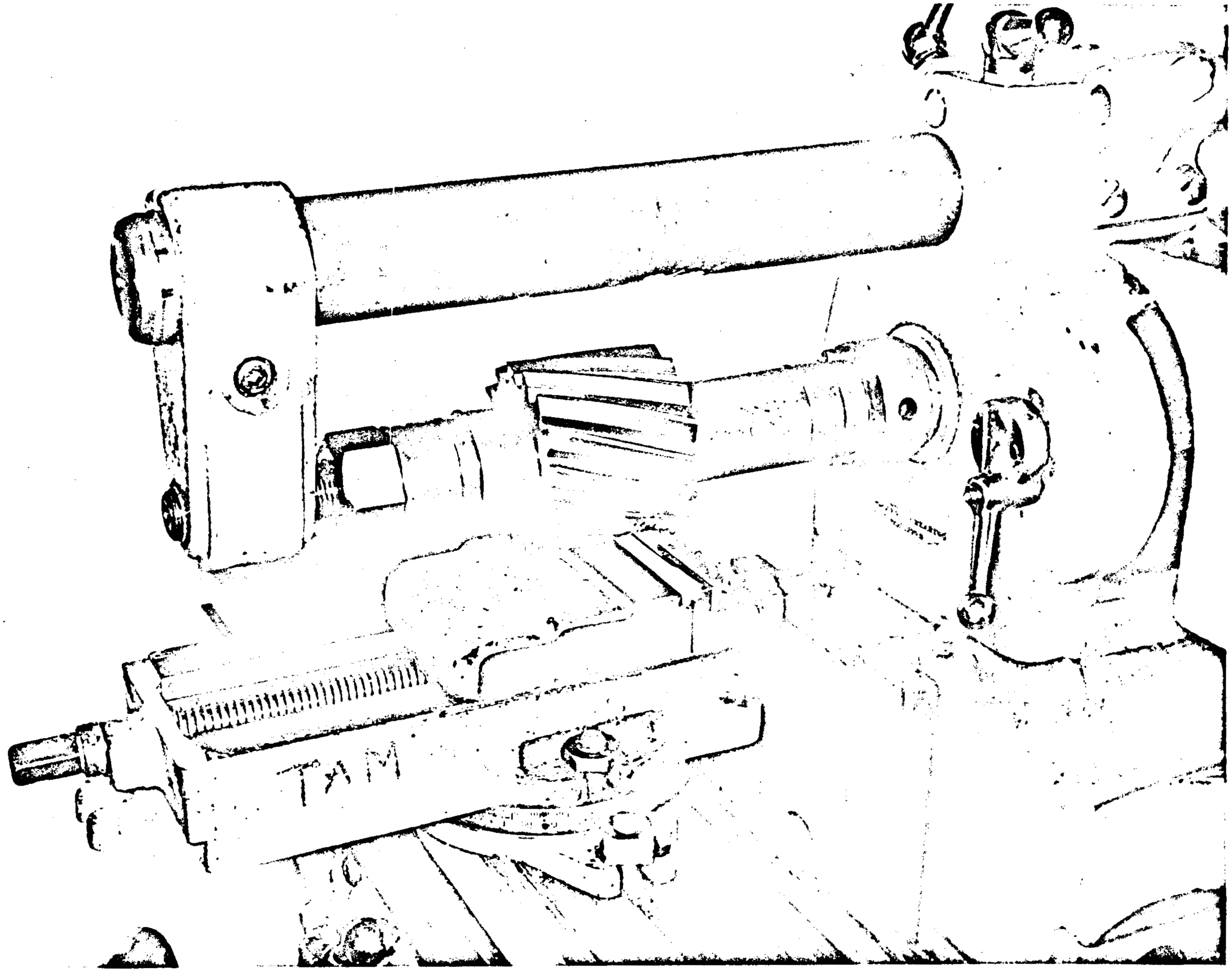

Fig.15 MILLING MACHINE SETUP FOR BONE

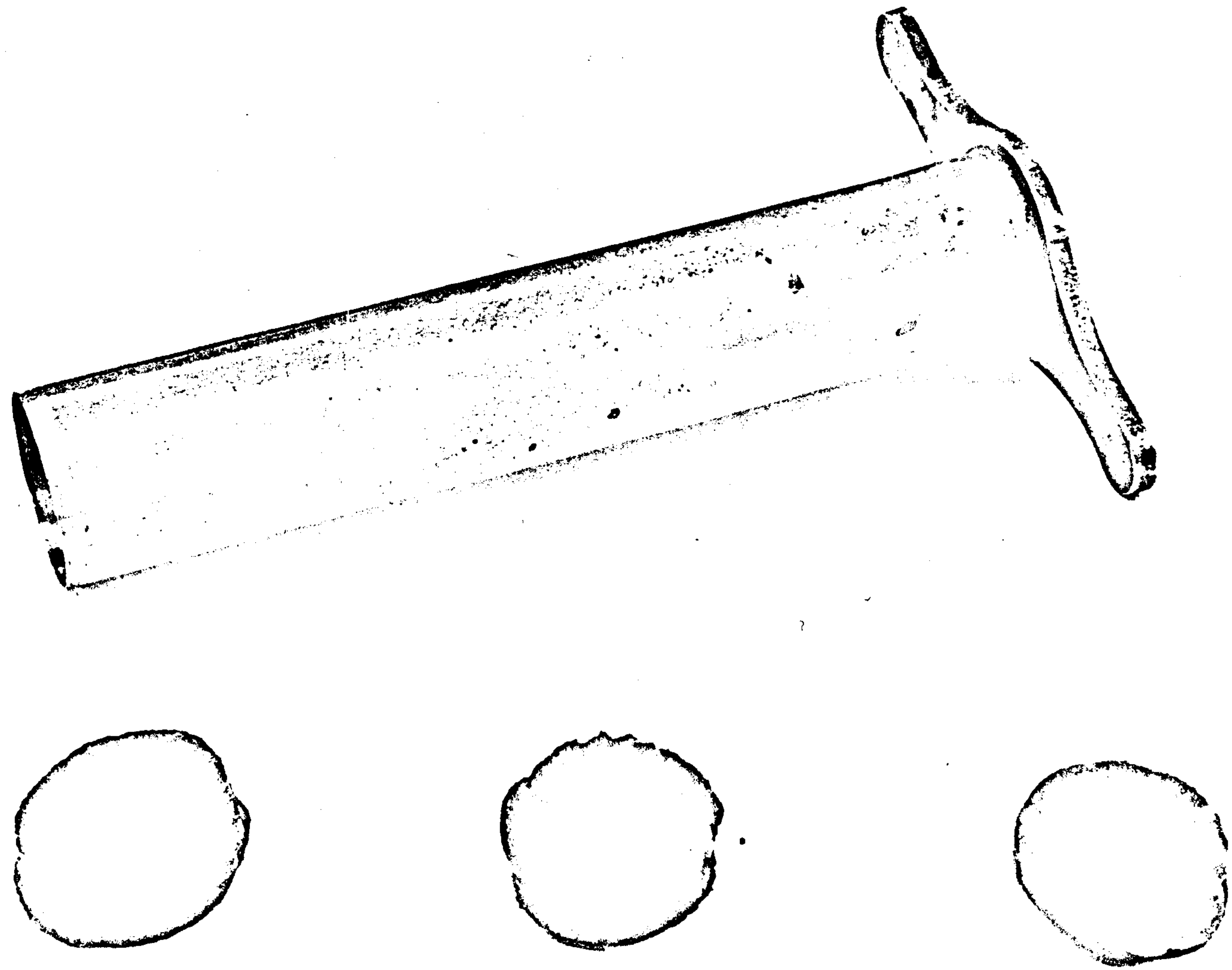

Fig. 16 BOVINE TISSUE SPECIMENS

VII. PROCEDURE

A) Data Collection

Once the specimen preparation and measuring systems calibration was accomplished, the actual test procedure becomes quite simple. The specimen was placed on the load transducer cap. A slight indentation provided for precise centering. The Electromatic testing machine was set for the proper head velocity and started; or, if the air gun were used, the reservoir was filled with the proper air pressure and the quick release handle turned. When the piston came to rest or the load indicator of the Electromatic indicated the head had bottomed and was compressing the rubber, the test was over. The film was then developed and, if the triggering had been precise, the load and displacement transducers properly adjusted and amplified, the scope intensity and camera aperature correct, and the film handled properly, a valid representation of the load-displacement history of the specimen was obtained. The piston was then returned to the top of the cylinder to engage the release mechanism by evacuating the reservoir through the air-operated asperator. The final size of the specimen was measured with a micrometer, provided it had not shattered as in the case of bone.

One difficulty in the study of rapidly occurring transient phenomena of this sort is that of setting precisely the load and displacement amplifiers and sweep time so that optimun use is made of the limited area of the oscilloscope. Each observation of the effect of an adjustment requires the expenditure of a specimen and a sheet of film. This situation also complicates trouble shooting or diagnosis of system malfunctions.

B) Data Processing

The oscillophotograph obtained from a strain rate test displays curves representing the force and displacement history of the specimen. The specific values of the force and displacement are obtained from the appropriate calibration curves. The engineering stress is by definition the force on the test piece divided by the initial cross-sectional area. The true stress is this force divided by the instantaneous area. If Poisson's ratio is 0.5 for the material, then the true stress equals the engineering stress multiplied by $(1 + e)$, where e is the strain based on the initial length. In the tests of bone, the maximum strain is very small so that there is no significant difference between the true stress and the engineering stress. In the tests of aluminum and nylon, however, there is a difference; therefore, the values given in this paper are all true stress values, (Figure 37, page 91).

True stress-strain curves were plotted from the oscillophotographs for each test. Figure 36 (page 90) shows the typical scattering of 10 tests of bovine femur bone. The modulus of elasticity, ultimate strength, and maximum strain were averaged and a stress-strain curve constructed, (Table 1). This curve represents the average material behavior at the strain rate under consideration.

The velocity of the piston or testing machine head is determined from the slope of the displacement time diagram. The strain rate is then approximated by dividing this velocity by the initial specimen length. Since the specimen length changes throughout the test, this series of experiments are better described as constant velocity rather than constant strain rate tests.

VIII. RESULTS

A) Introduction

The results of this experiment are presented in the form of stress-strain diagrams, (Figures 24-28); the significant features of which are summarized in Table 2. It has been tacitly assumed that the stress and strains were uniformly distributed throughout the specimen. The inhomogeneity of some of the materials tested invalidates this assumption to some extent. However, the data are still significant in that they represent average values; and it is the only information of its kind available. Also, homogeneity of stress and strain cannot exist so long as the time required for transmission is significant when compared to the test time. Therefore, tests at very high rates can only be interpreted by applying appropriate wave theory. Unfortunately, wave theories depend on information obtained from tests of this sort. This situation may be visualized as a circle of ever decreasing radius with theory and experiment gradually approaching an accurate description of the phenomena. It is hoped that the thinness of the specimens used here and the care with which they were selected and machined have minimized the errors due to this assumption.

B) Typical Test Records

Figures 17 through 21 show typical oscillophotographs of high and low rate tests for fresh bovine bone, embalmed human bone, bovine muscle tissue, nylon and aluminum. The displacement scale is approximate because of the nonlinearity of the capacitance vs. displacement curves. By using different sweep times, either the complete record of the test from impact with the specimen to contact with the stop or expanded portions of this record could be obtained. A rapid fall off of load and increase in deflection occurs in bone (Figures 17 and 18) for the low rate tests at failure. This is due to the rubber pad springing back when the bone suddenly fractures. A slight oscillation is visible in the high rate tests of aluminum and nylon, but not in the bone and tissue tests. This is probably due to wave reflections either in the load cell or specimen.

C) <u>Oscillations In Testing</u>

At the highest rate the air gun was capable of attaining, using the laboratory air supply, severe oscillations occurred in the force transducer output, (Figure 22). This corresponds with a strain rate of approximately 4,000 per second. This rate is outside the usable range of the force measuring system and no data are presented.

A number of other investigations[29,35,39] have shown force-time diagrams showing oscillations with various interpretations. However, it should be recognized that outside of its frequency response range a transducer can only be used as a frequency measuring device. It is true that inputs of higher frequency still cause outputs, but these generally cannot be interpreted[43].

Figure 22 also shows a force-time record that is typical of the Portevin-LeChatelier effect[34]. This phenomena is associated with two distinct factors. The first is rapid work hardening and the appearance of slip-bands causing discontinuous yielding. In most test situations, sudden and discontinuous yielding causes large oscillations in the force applied to the specimen. Many static load measuring systems are incapable of following these force surges; hence, they often go unnoticed. The second factor is oscillations induced by an unstable load-velocity condition due to the presence of a load-velocity relation with a negative slope. Such a mechanical system with elastic components and masses is subject to auto-oscillation.

The load for Figure 22 was applied using a modified hammer impact tester of the type used for Charpy and Izod tests. It is felt that the elasticity of the hammer plate contributed to auto-oscillation and was sustained through the discontinuous yielding phenomena described above. No oscillations of this type were observed when using the Electromatic testing machine or the Air Gun.

D) Poisson's Ratio

Figure 23 shows typical records of the Poisson's ratio tests using three channels of a Type M Tektronix four channel preamplifier. Figure 35 is a plot of the results of such tests for several strain rates. No significant variations of Poisson's ratio with strain rate were observed, since its value fell within the bounds given for each material. The curve for nylon is particularly interesting in that Poisson's ratio, even for large strains, stays considerably less than 0.5, the value required for constant volume flow.

It should be pointed out that this phase of the work represents only a preliminary study in regard to the effect of strain-rate on Poisson's ratio. There is a large spread in the data which would overshadow any small effect. The reason for this apparent lack of precision is twofold. First, the small specimen size (chosen as the largest stable compression sample possible from bone) requires the use of very small strain gages with resulting inaccuracies. Second, and most important, is the non-isotropic flow that occurred during the tests of nylon and aluminum. Specimens that were square in cross section prior to testing became decidedly rectangular during compression. This occurred in aluminum, even though it had been annealed. Thus, with the loads applied perpendicular to the direction of extruding, the dimension of the specimen in the direction of extruding increased as much as 30 percent more than the dimension perpendicular to both the extrusion axis and the load axis. In view of the foregoing, it is recommended that further studies be made on larger specimens using materials that are more nearly isotropic. Also, a different capicator plate with a smaller range, but better resolution, should be used.

E) Stress-Strain Curves

The average stress-strain curves obtained at various strain rates for fresh bovine bone, embalmed human bone, bovine musculo tissue, nylon and aluminum are displayed in Figures 24 through 28. Table 2 summarizes the various properties obtained from such diagrams. The ultimate compressive stress is the maximum stress that was attained during the test. Since the stress for the bovine tissue, nylon and aluminum increased continuously with strain, values are given at particular strains as noted. The energy absorbtion capacity is proportional to the area under the stress-strain curve. This represents the work done in straining the material to failure as in the case of the bone samples or to a particular strain level for the other materials noted in the table.

F) Types of Failures

Figures 39 and 40 show the general failure types. The final sizes are indicated also. No correlation of final size with any of the governing parameters was found. This was probably due to the difficulty of measuring small irregular shapes. The final configurations of the nylon and aluminum specimen were uninteresting, except for evidences of anisotrophy as mentioned previously. Also, slip planes or Leuder's lines were observed in both materials indicating that the basic flow mechanism was due to shear.

The bovine tissue specimen gave off sizeable amounts of fluid during compression. This caused considerable electrical difficulties in the transducers by shorting the capacitance plates and load cell. Piezoelectric devices are very sensitive to humidity infiltration, and the load cell had to be baked several times to restore the impedance values necessary for proper operation. A sealed system was finally used for the tissue tests.

Both the beef and human bone specimens indicated two regions of failure. For the low rates, shear failures similar to the cone failures of concrete compression tests were observed. This type of failure persisted up to strain rates of approximately 1/sec. Above this rate, bone failures were typified by vertical splitting with many small pieces being formed, (Figure 39, Page 93)

Table 1. Typical Data Sheet

Strain Rate 0.001

Specimen Type Bovine Femur

Specimen Number	Ultimate Strength psi	Maximum Strain in/in	Modulus psi
B1-.001	22,890	18,975	3.27×10^6
B2-.001	28,050	14,750	2.76×10^6
B3-.001	28,500	14,540	2.88×10^6
B4-.001	19,260	16,500	2.91×10^6
B5-.001	22,540	15,950	2.79×10^6
B6-.001	24,360	13,700	3.22×10^6
B7-.001	26,700	20,800	1.85×10^6
B8-.001	25,060	22,300	2.00×10^6
B9-.001	19,800	21,000	1.82×10^6
B10-.001	28,440	28,900	2.01×10^6
AVERAGE	25,460	18,742	2.73×10^6

Table 2

SUMMARY DATA

Material	Strain Rate 1/sec	Ultimate Compressive Strength psi	Energy Absorbtion Capacity in#/in^3	Elastic Modulus psi	Maximum Strain to Failure Percent	Poisson's Ratio Elastic Dried	Number of Tests
Fresh Bovine Femur Bone	0.001	25,500 (19,300-28,500)	350	2.7×10^6 (1.8-3.2)	1.88 (1.37-2.89)	.30	10
	0.01	30,000 (24,500-36,300)	416	2.9×10^6 (2.2-3.8)	1.82 (1.40-2.05)		10
	0.1	33,500 (24,600-37,000)	420	3.5×10^6 (2.7-4.7)	1.75 (1.41-2.15)	.28	10
	1	36,500 (32,000-38,000)	260	4.0×10^6 (3.3 - 5)	1.25 (.90-1.50)		5
	300	41,000 (38,000-46,000)	230	4.8×10^6 (4.6-5.1)	1.00 (.8 - 1.50)	.26	5
	1500	53,000 (47,000-58,000)	220	6.1×10^6 (5.0-7.0)	0.90 (.65 - 1.3)		5
Embalmed Human Femur Bone	0.001	21,800 (18,000-23,000)	270	2.2×10^6 (1.6-2.7)	1.65 (1.10-2.65)	Not Measured	5
	0.01	26,000 (21,000-28,000)	310	2.5×10^6 (1.9-3.2)	1.75 (1.30-2.91)	Not Measured	3

Table 2 (cont.)

Material	Strain Rate 1/sec	Ultimate Compressive Strength psi	Energy Absorbtion Capacity in#/in^3	Elastic Modulus psi	Maximum Strain to Failure Percent	Poisson's Ratio Elastic	Number of Tests
Embalmed Human Femur Bone	0.1	29,000 (24,000-32,000)	340	2.6×10^6 (2.0-3.5)	1.8 (1.42-3.2)	Not Measured	5
	1	32,000 (27,000-36,000)	350	3.2×10^6 (2.7-3.9)	1.78 (1.60-3.2)	Not Measured	3
	300	40,500 (36,000-42,000)	300	4.3×10^6 (3.3-4.8)	1.10 (.96-1.30)	Not Measured	3
	1500	46,000 (39,000-58,000)	260	5.9×10^6 (4.8-7.0)	0.95 (.91-1.16)	Not Measured	5
Bovine Musculo Tissue	0.001	75% Strain 110 (75-146)	75% Strain 12	Not Applicable	No Failure	Not Measured	5
	0.1	125 (95-162)	15	Not Applicable	No Failure	Not Measured	5
	1	160 (125-180)	20	Not Applicable	No Failure	Not Measured	5
	100	200 (175-220)	27	Not Applicable	No Failure	Not Measured	5
	1000	285 (238-320)	38	Not Applicable	No Failure	Not Measured	5

Table 2 (cont.)

Material	Strain Rate 1/sec	Ultimate Compressive Strength psi	Stress at 2% Strain psi	Energy Absorbtion Capacity in#/in3	Elastic Modulus psi	Poisson's Ratio Elastic	Number of Tests
		10% Strain		1.5% Strain			
Aluminum QQ1100-0	0.001	18,000 (17,200-18,600)	13,000	120	10×10^6 (9.4-11)	.32	3
	0.1	22,000 (21,000-22,800)	17,600	175	10×10^6 (9.7-10.5)	.32	3
	1	25,000 (24,200-25,600)	21,000	210	10×10^6 (9.3-10.8)		3
	300	29,000 (28,500-29,500)	25,200	255	10×10^6 (9.6-10.8)	.30	3
	1500	31,000 (27,500-33,000)	27,300	260	10×10^6 (9.6-10.5)		3
		15% Strain		1.5% Strain			
Nylon	0.001	10,600 (9,800-11,200)	4,000	22	1.9×10^5 (1.7-2.1)	.25	3
	0.1	14,200 (13,600-15,000)	6,000	35	3.1×10^5 (3.0-3.2)	.25	3
	1	16,600 (16,000-17,000)	8,000	45	4.0×10^5 (3.7-4.2)		3
	300	20,200 (18,500-20,900)	11,000	65	5.6×10^5 (5.4-5.7)	.22	3
	1500	21,000 (19,500-22,000)	13,500	85	7.5×10^5 (7.3-7.6)		3

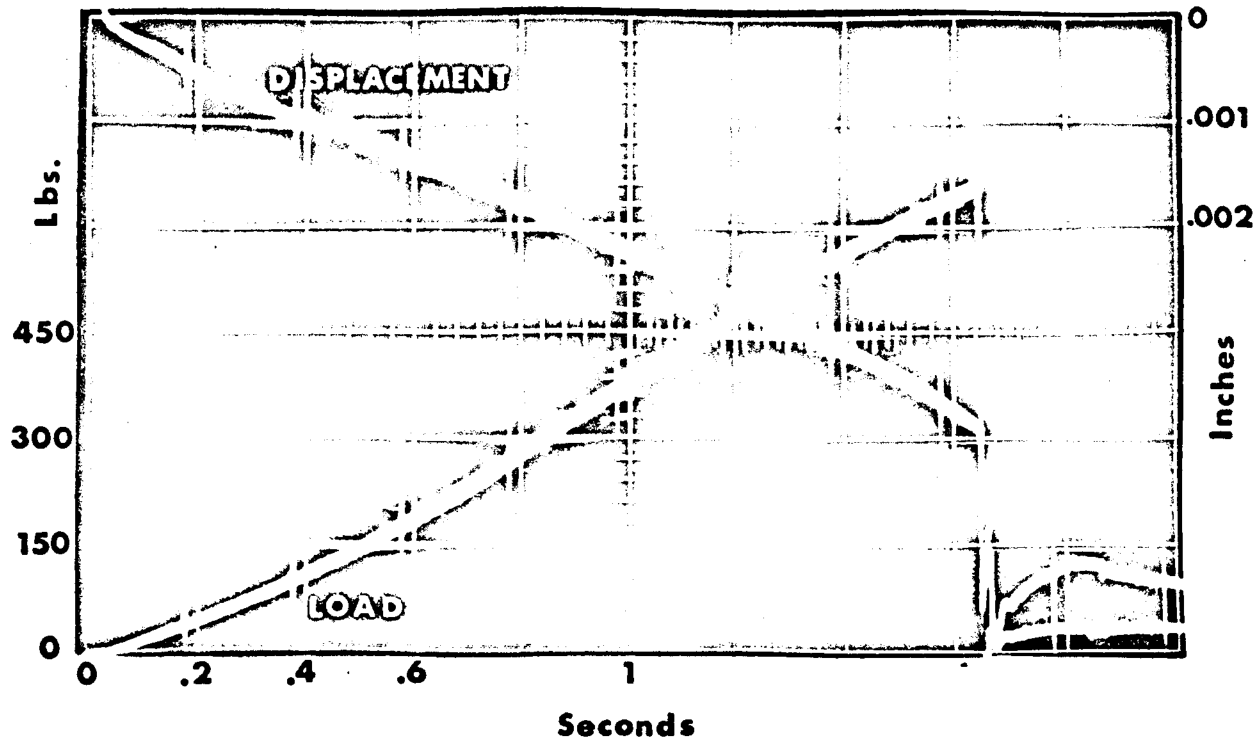

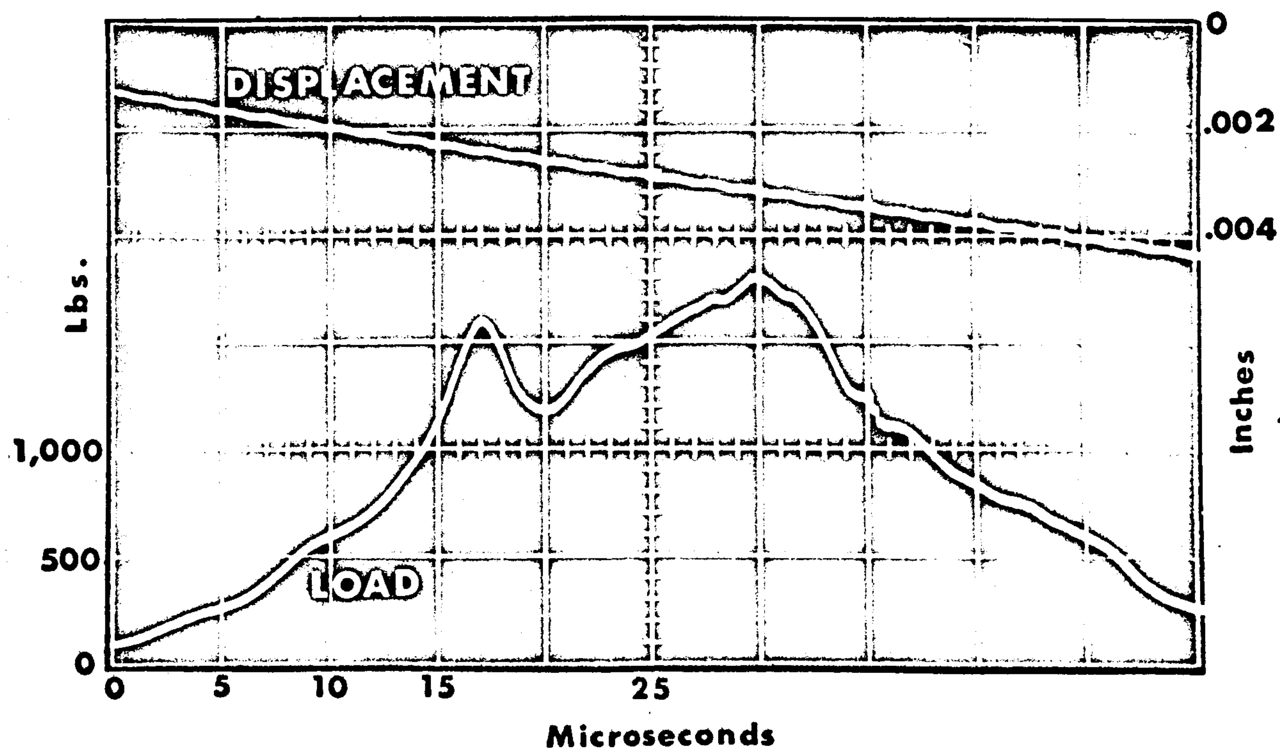

Fig.17 BOVINE FEMUR BONE

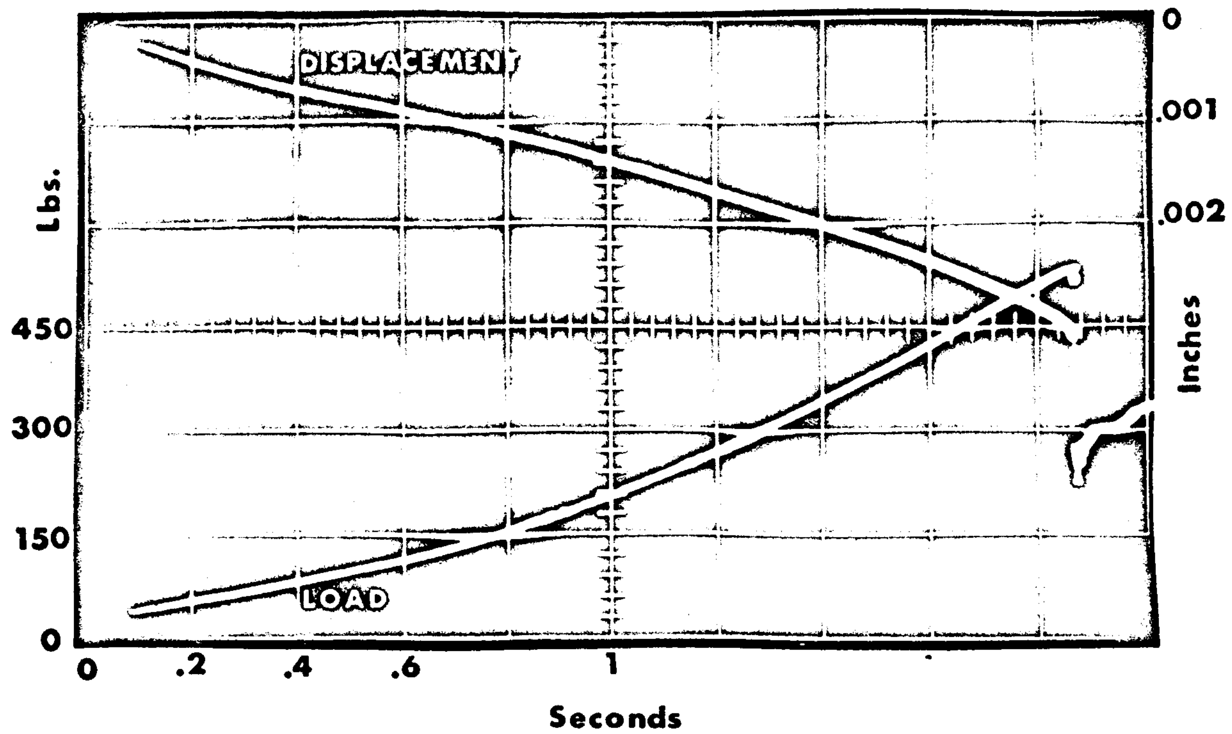

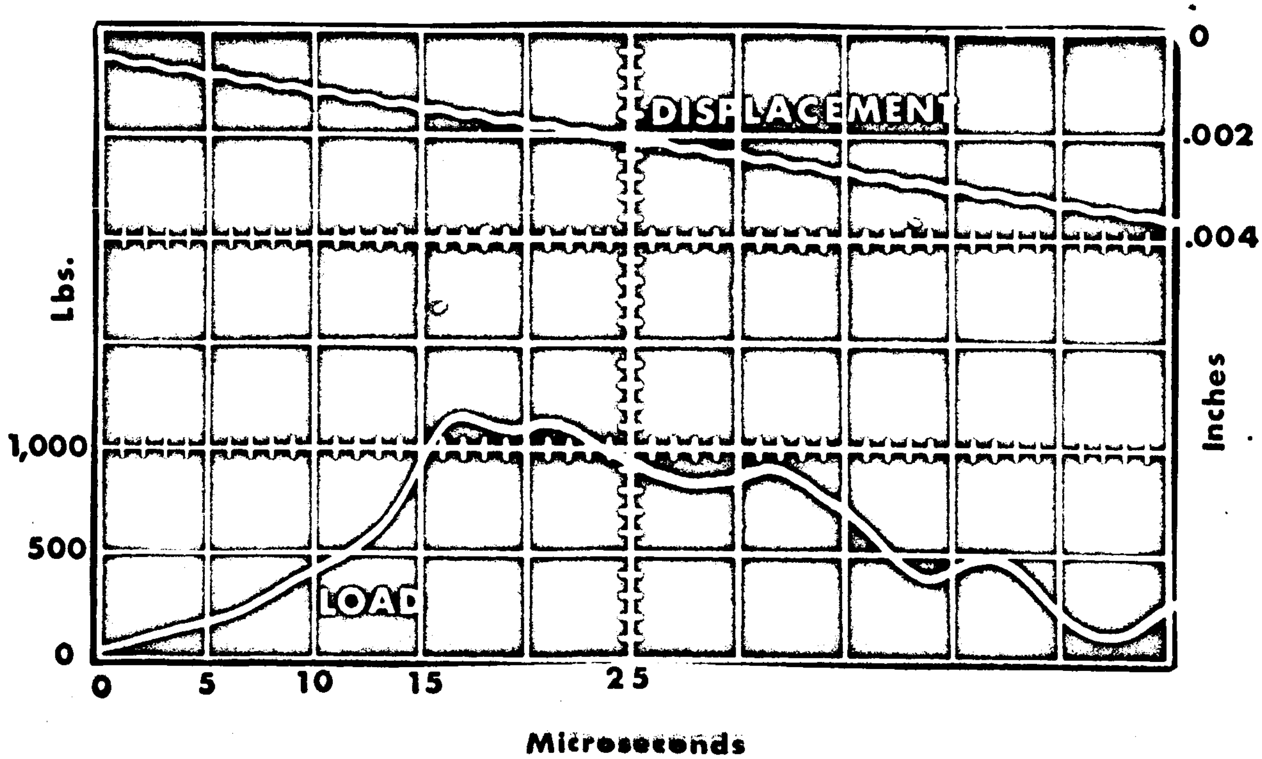

Fig. 18 HUMAN FEMUR BONE

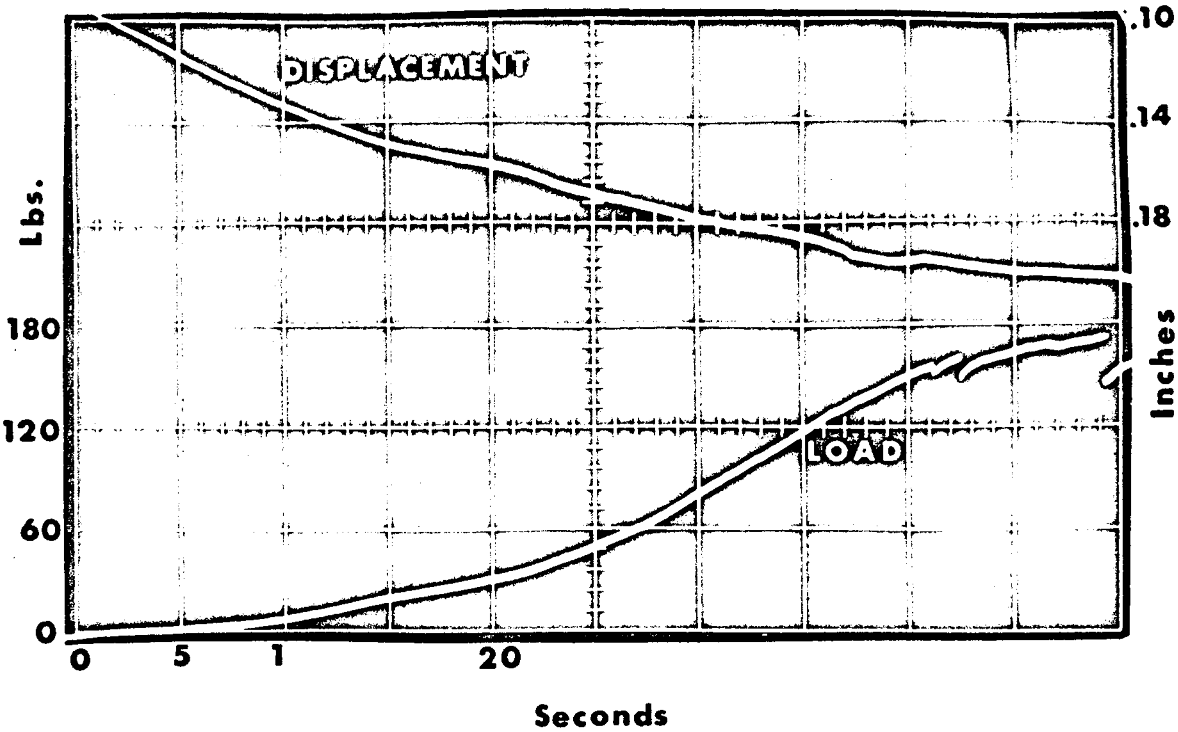

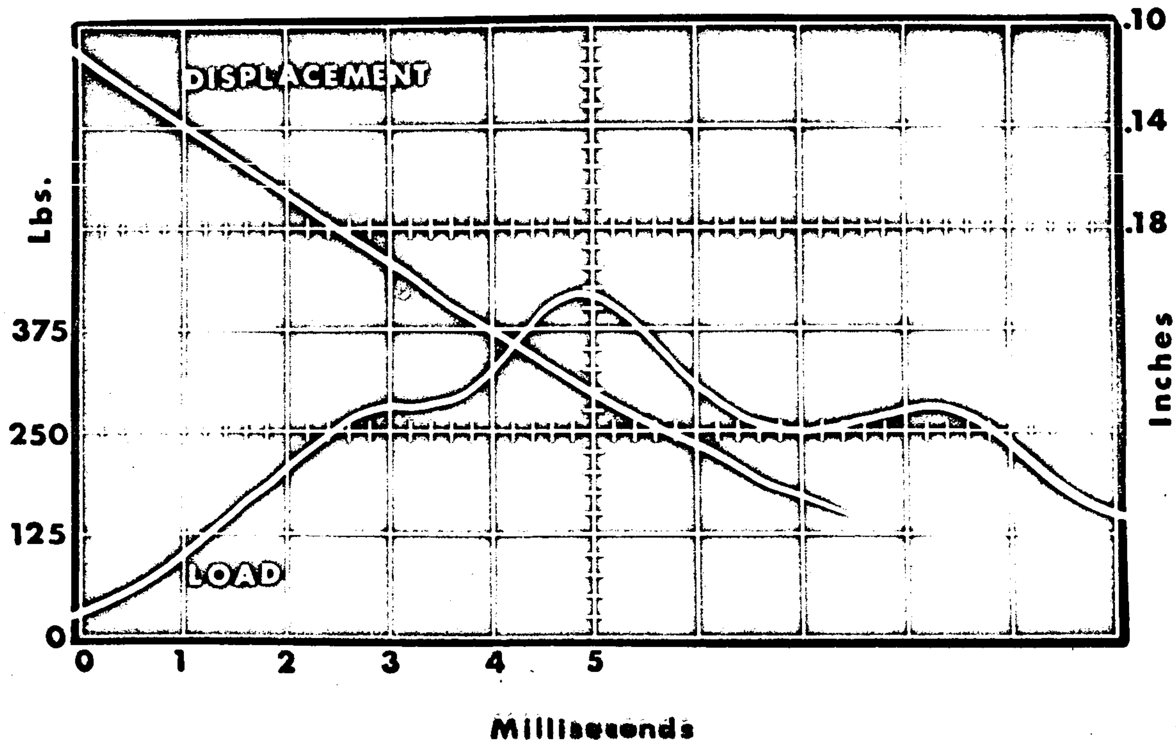

Fig. 19 BOVINE TISSUE

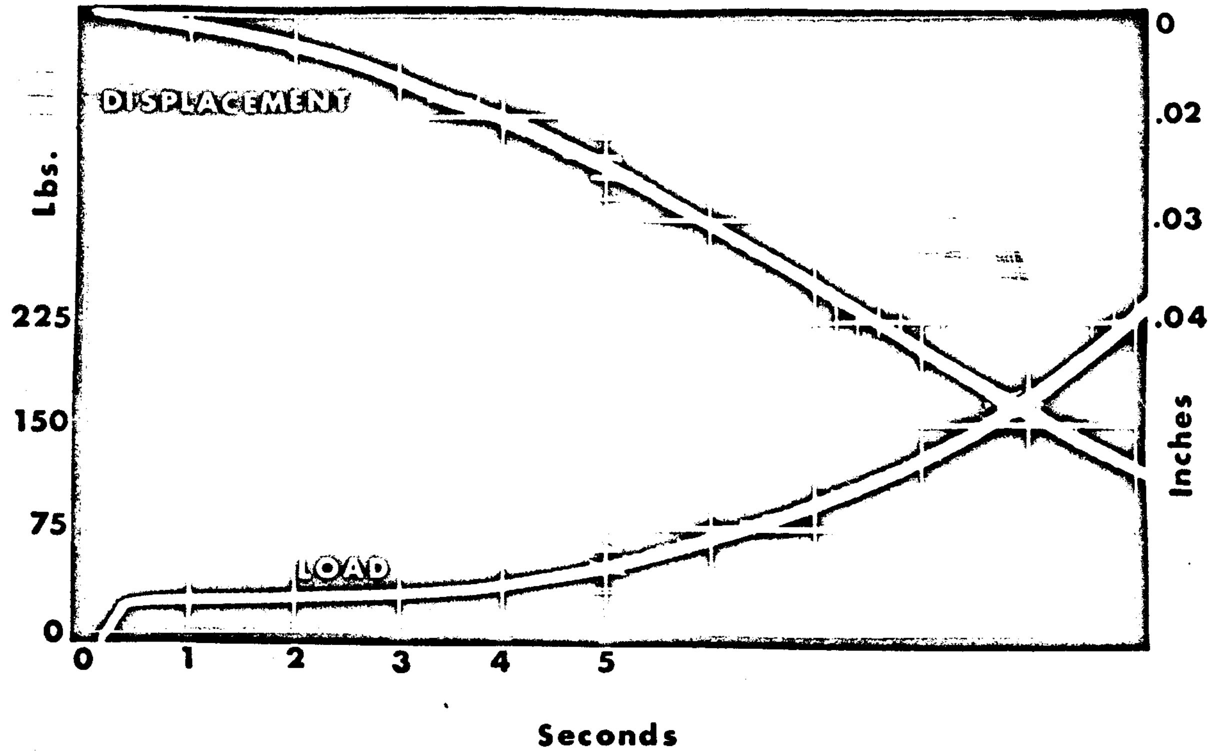
DISPLACEMENT
LOAD
Lbs.
225
150
75
0
0
1
2
3
4
5
Seconds
0
.02
.03
.04
Inches

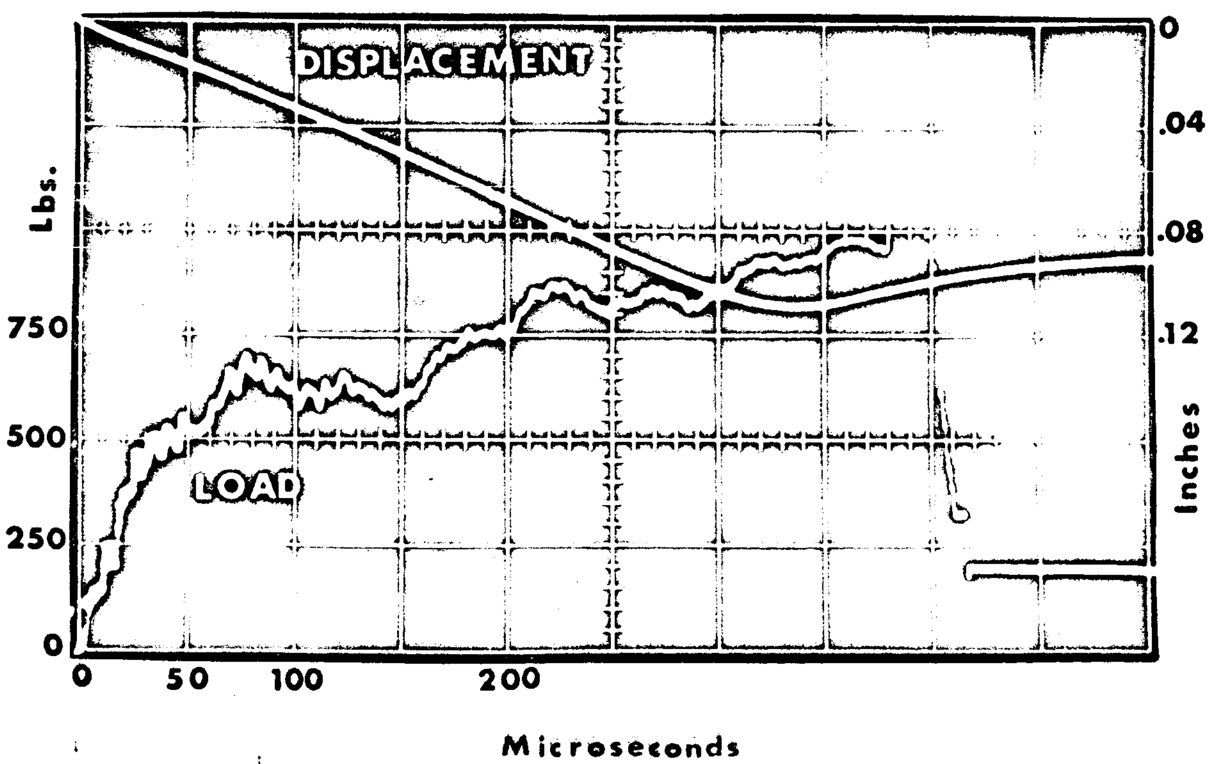
DISPLACEMENT
LOAD
Lbs.
750
500
250
0
0
50
100
200
Microseconds
0
.04
.08
.12
Inches

Fig. 20 NYLON

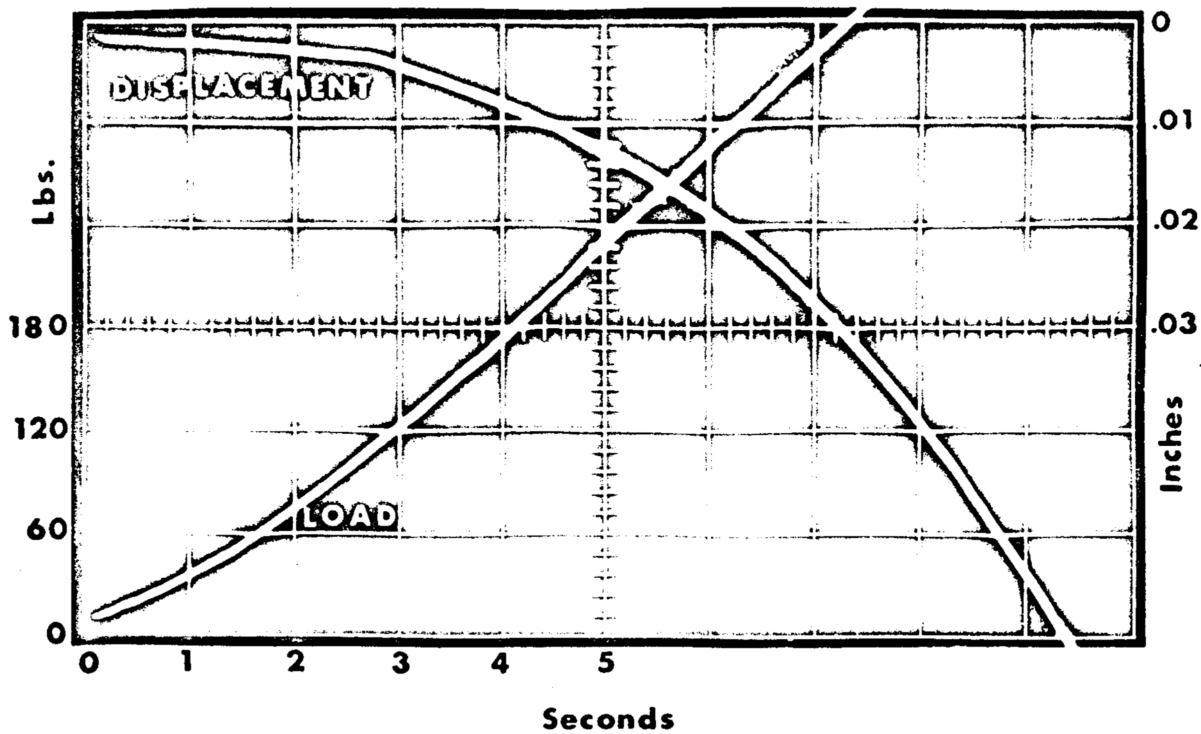

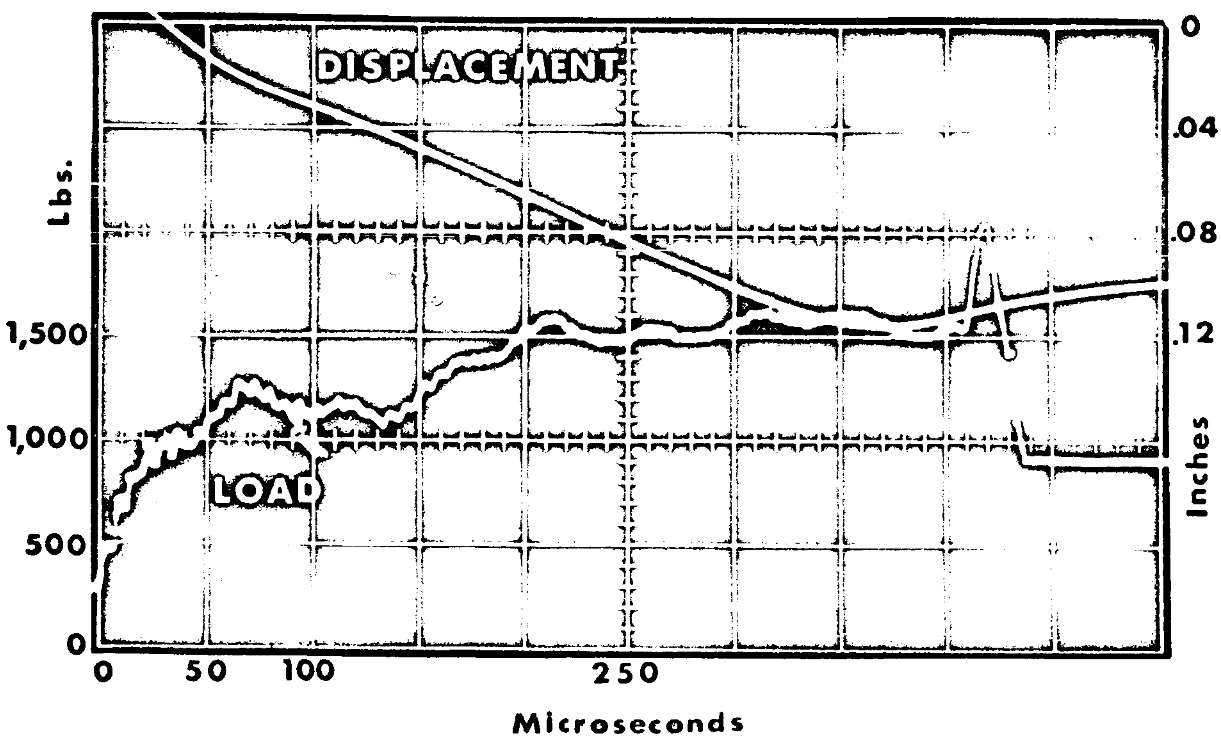

Fig. 21 ALUMINUM

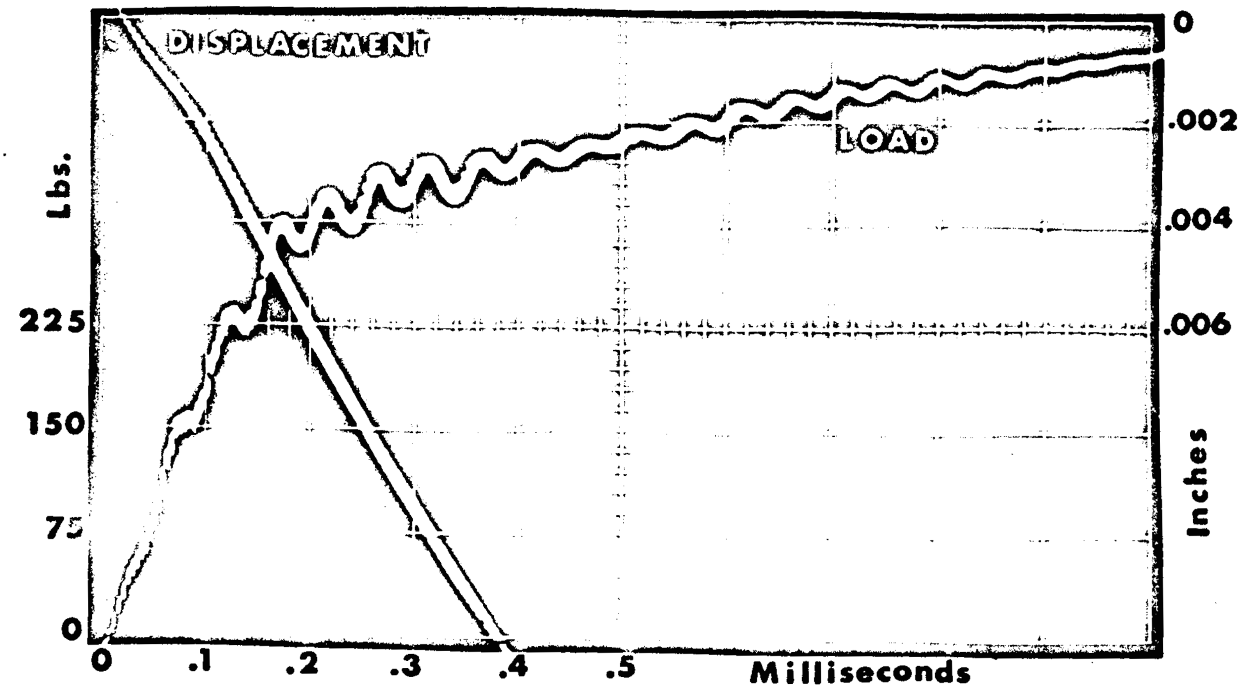

Portevin–LeChatelier Effect in Nylon

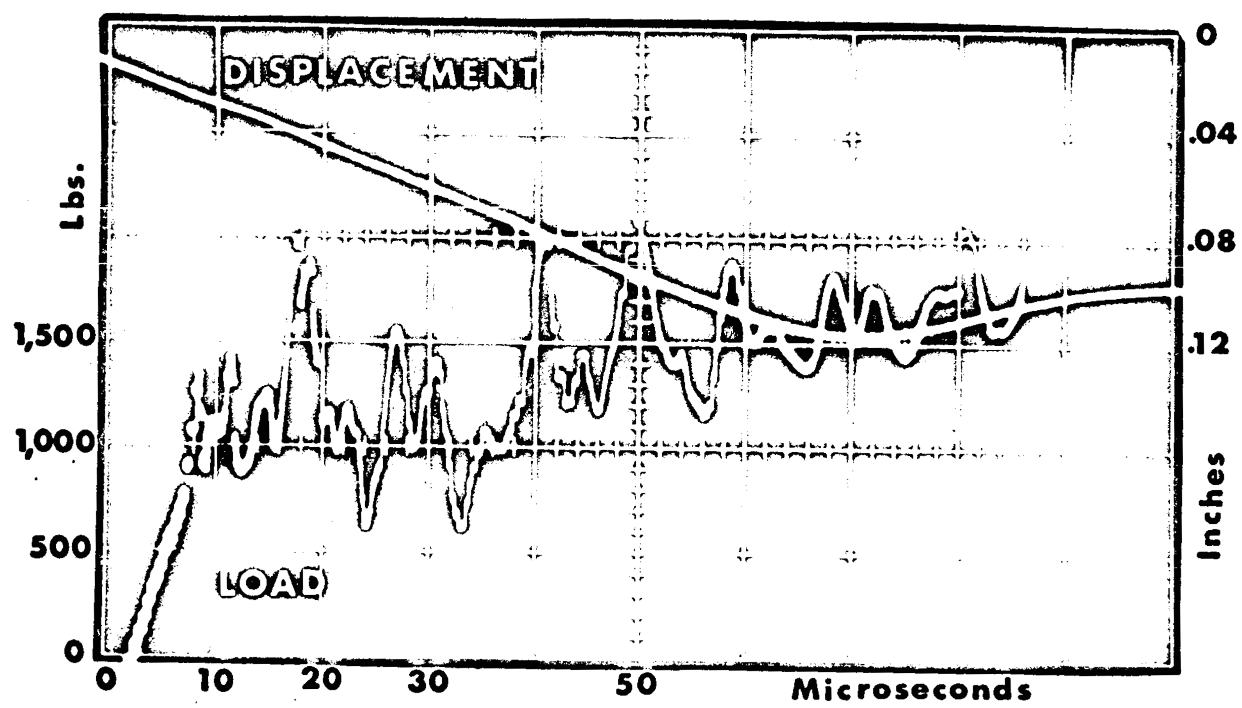

ALUMINUM

Load Rate too fast for Force Transducer

Fig. 22

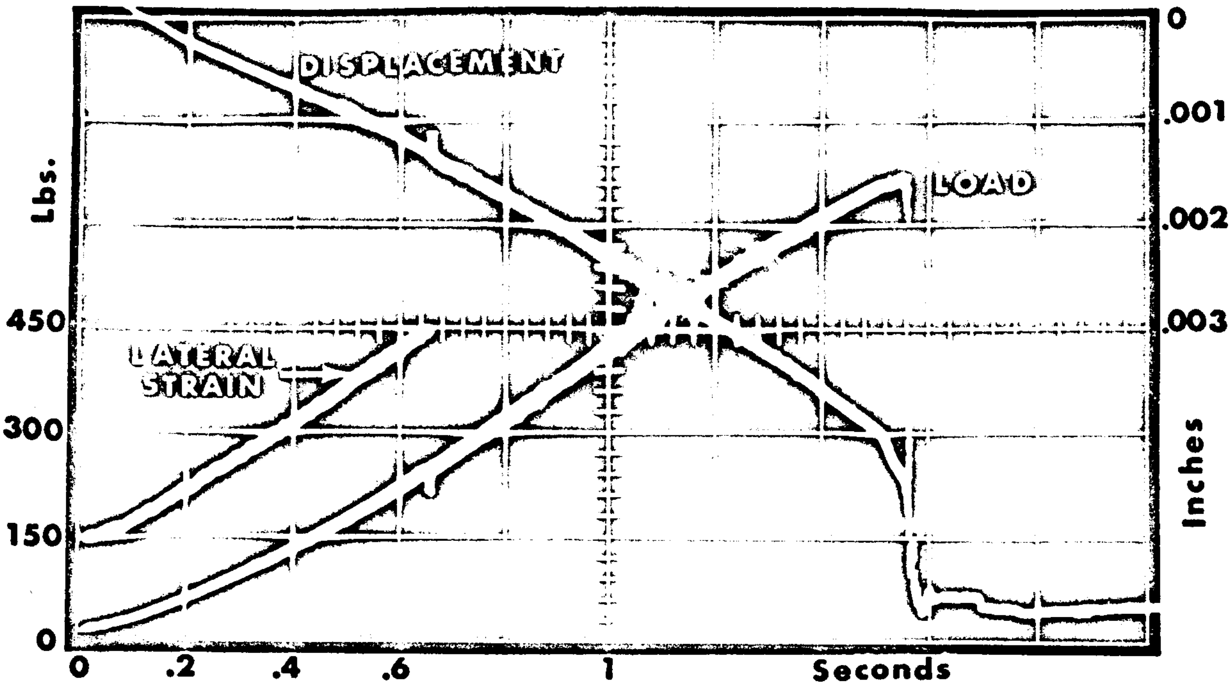

DRY BOVINE BONE

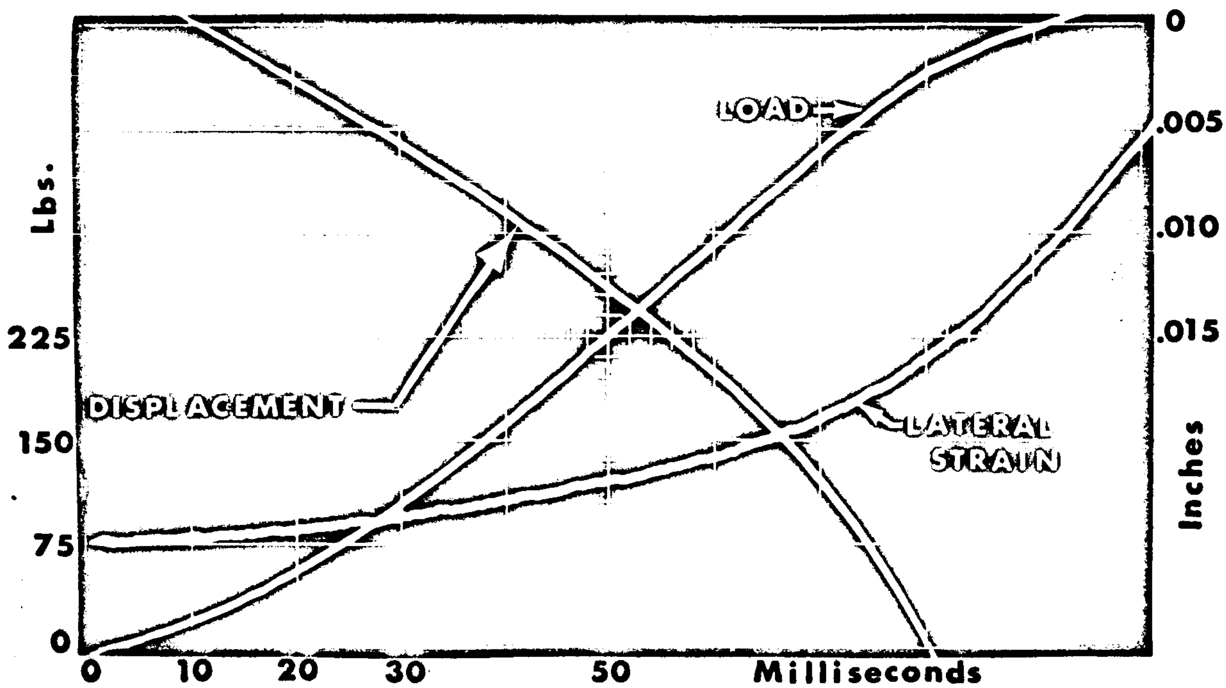

NYLON

Fig. 23

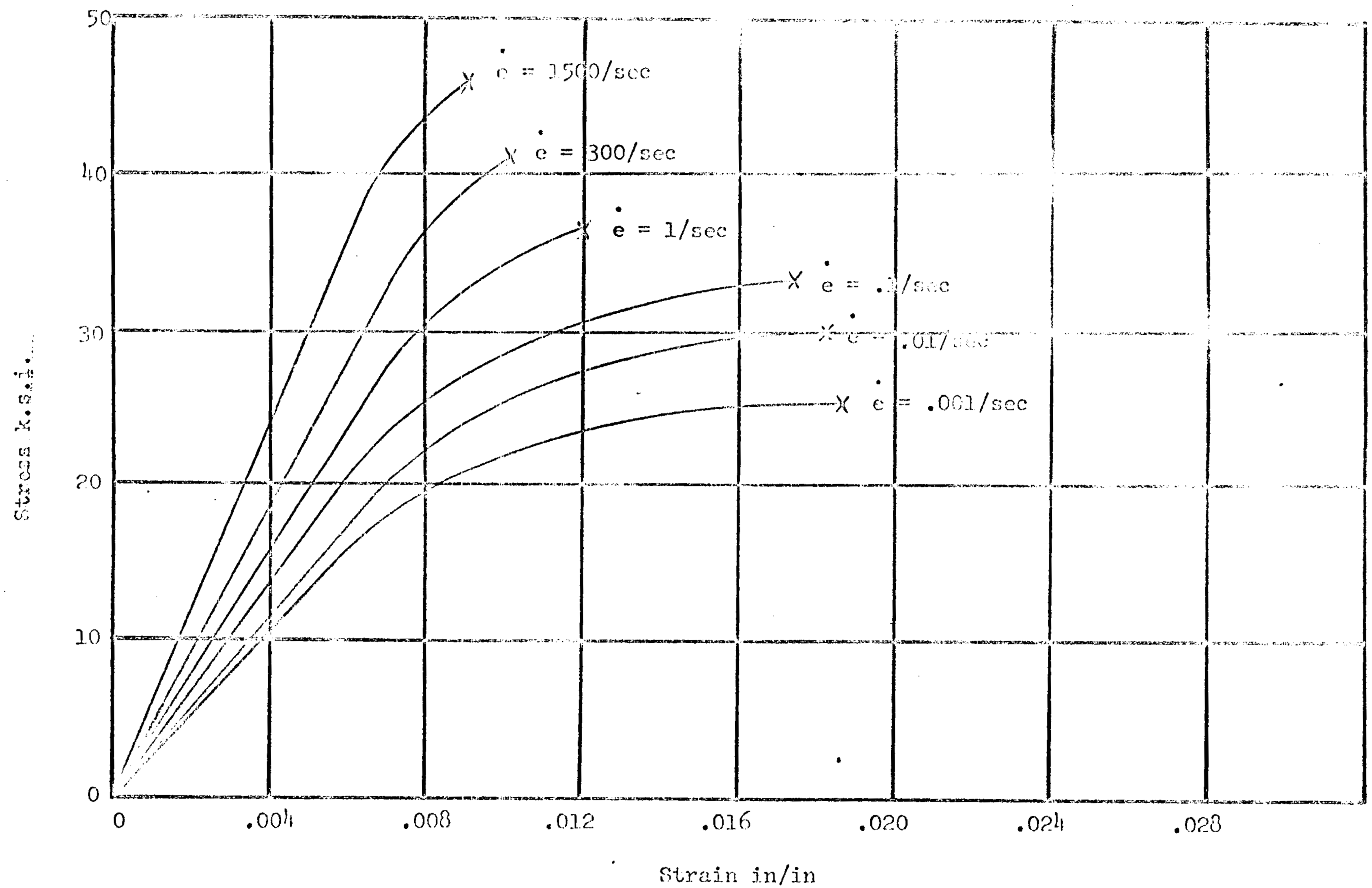

Fig. 24. Stress-Strain Curves for a Bovine Femur Bone.

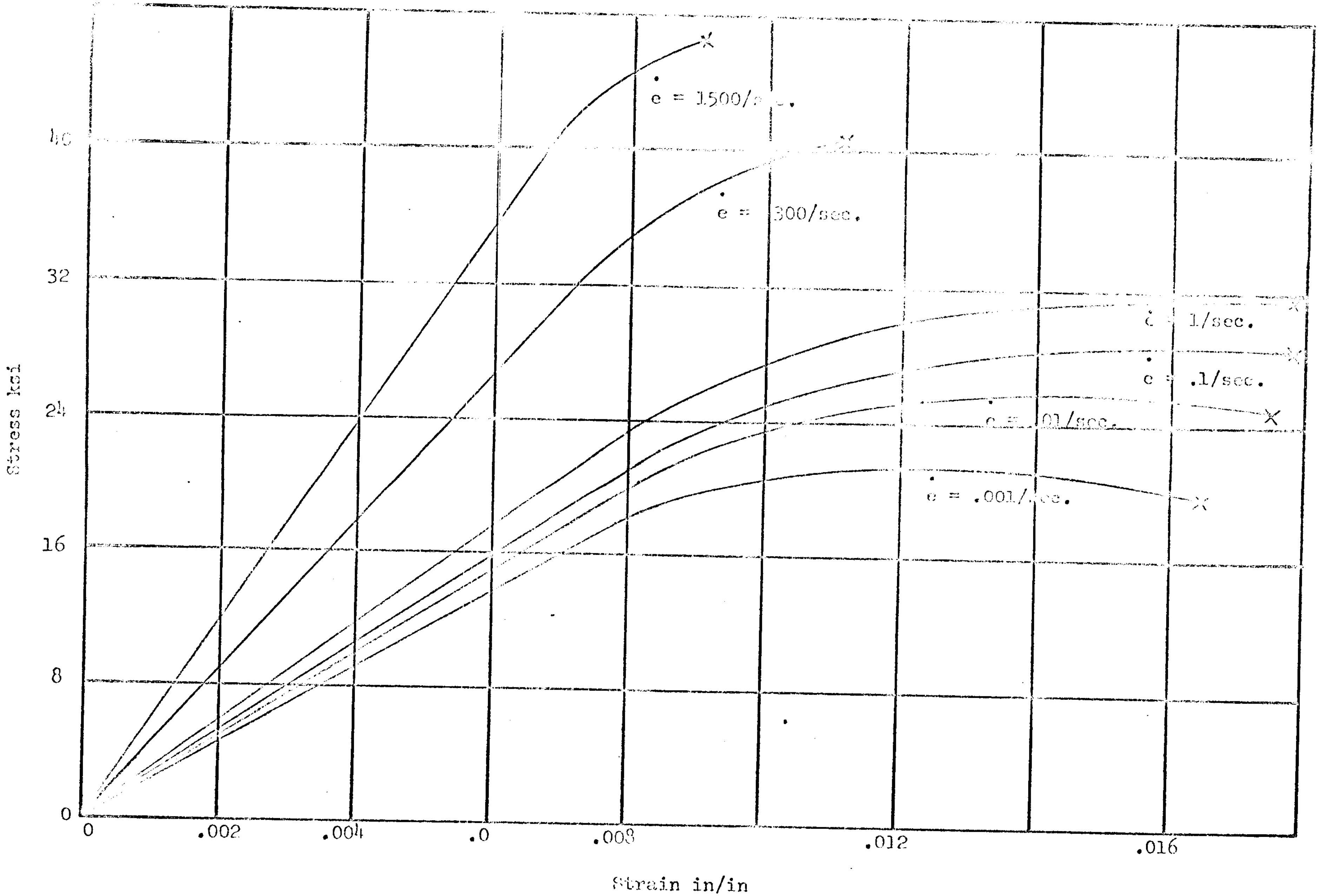

Fig. 25 . Stress-Strain Curves for Embalmed Human Femur Bone

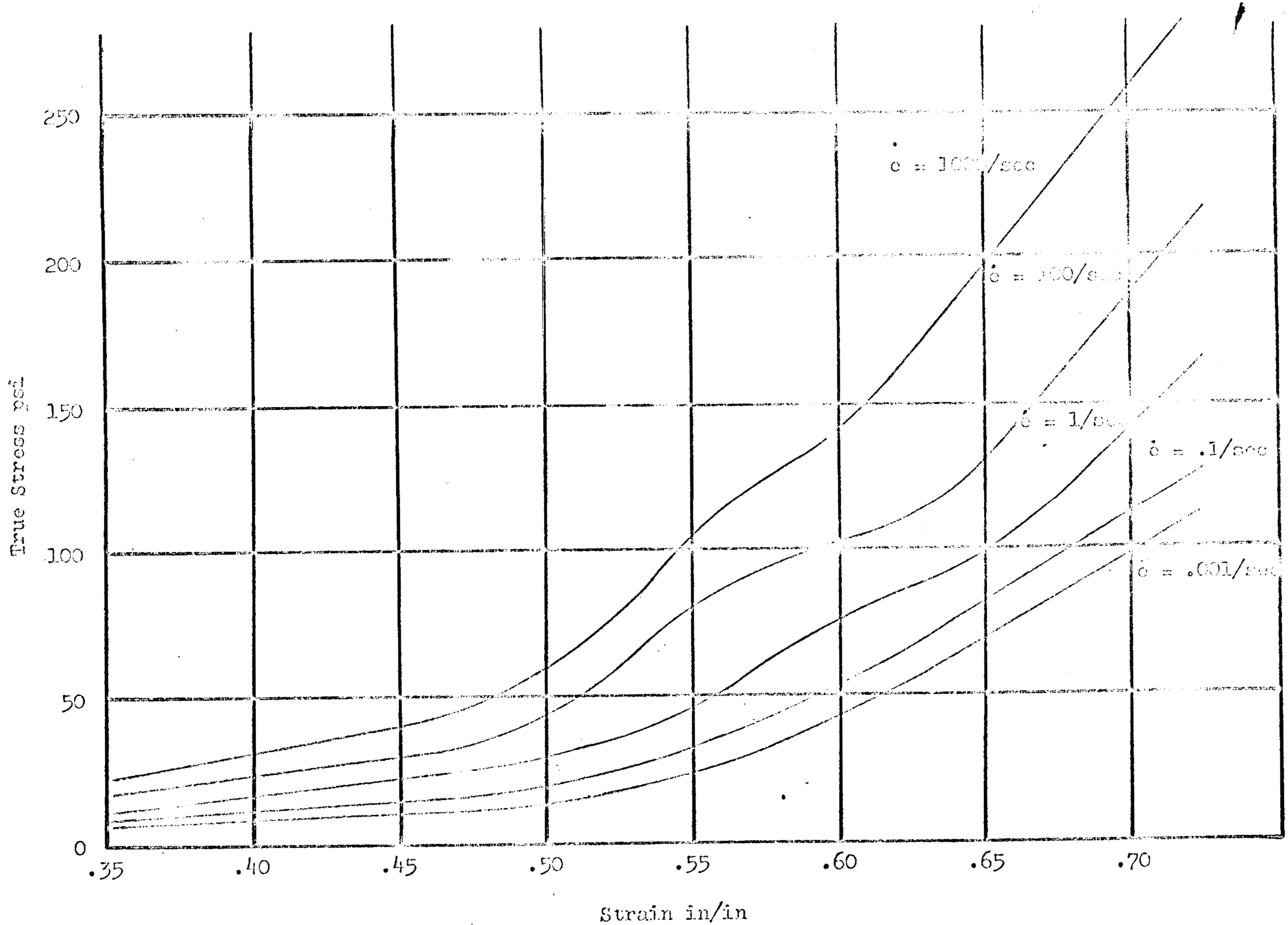

Fig 26. Stress-Strain Curves for Bovine Muscle Tissue

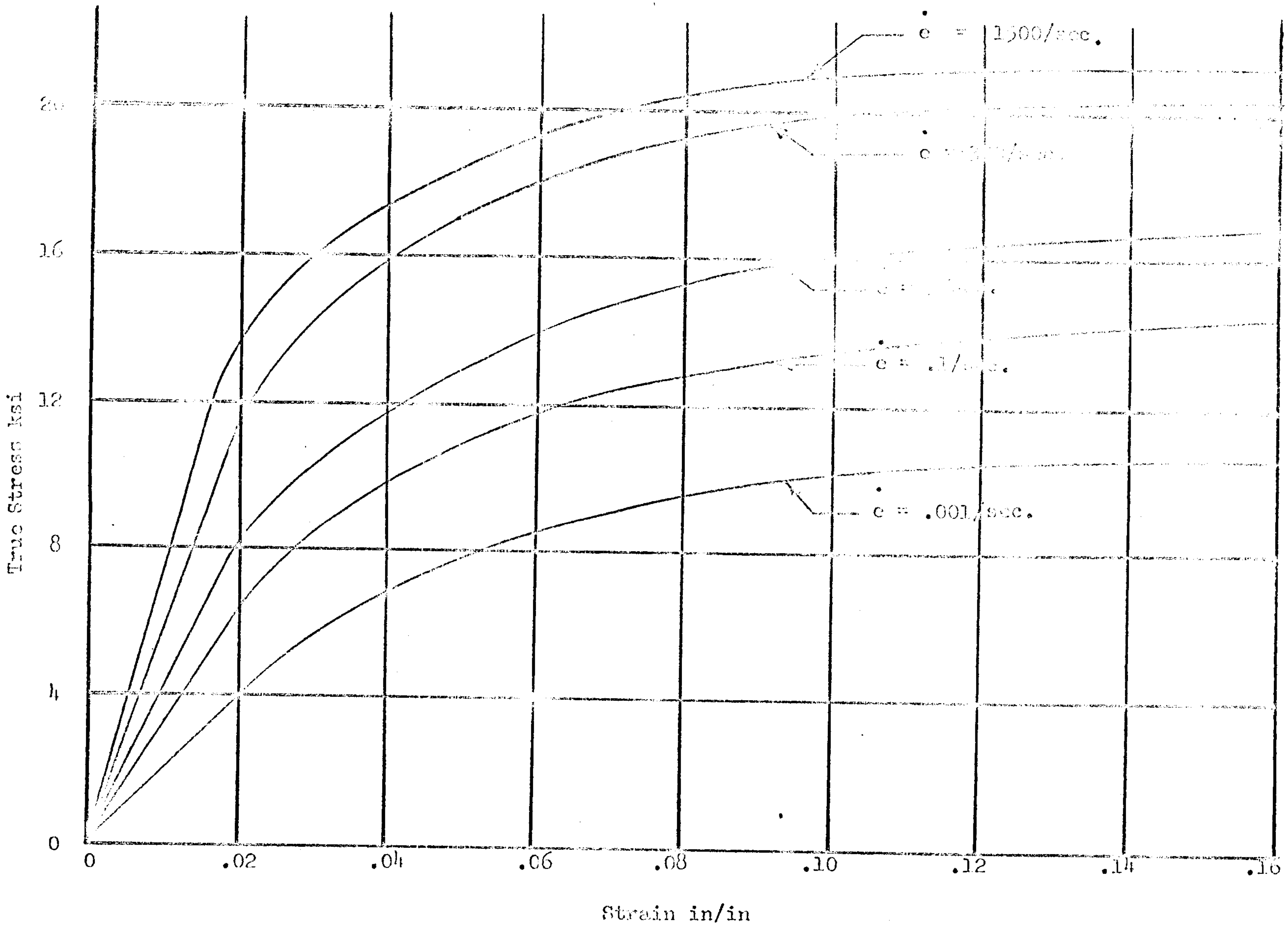

Fig. 27. Stress Strain Curves for Nylon.

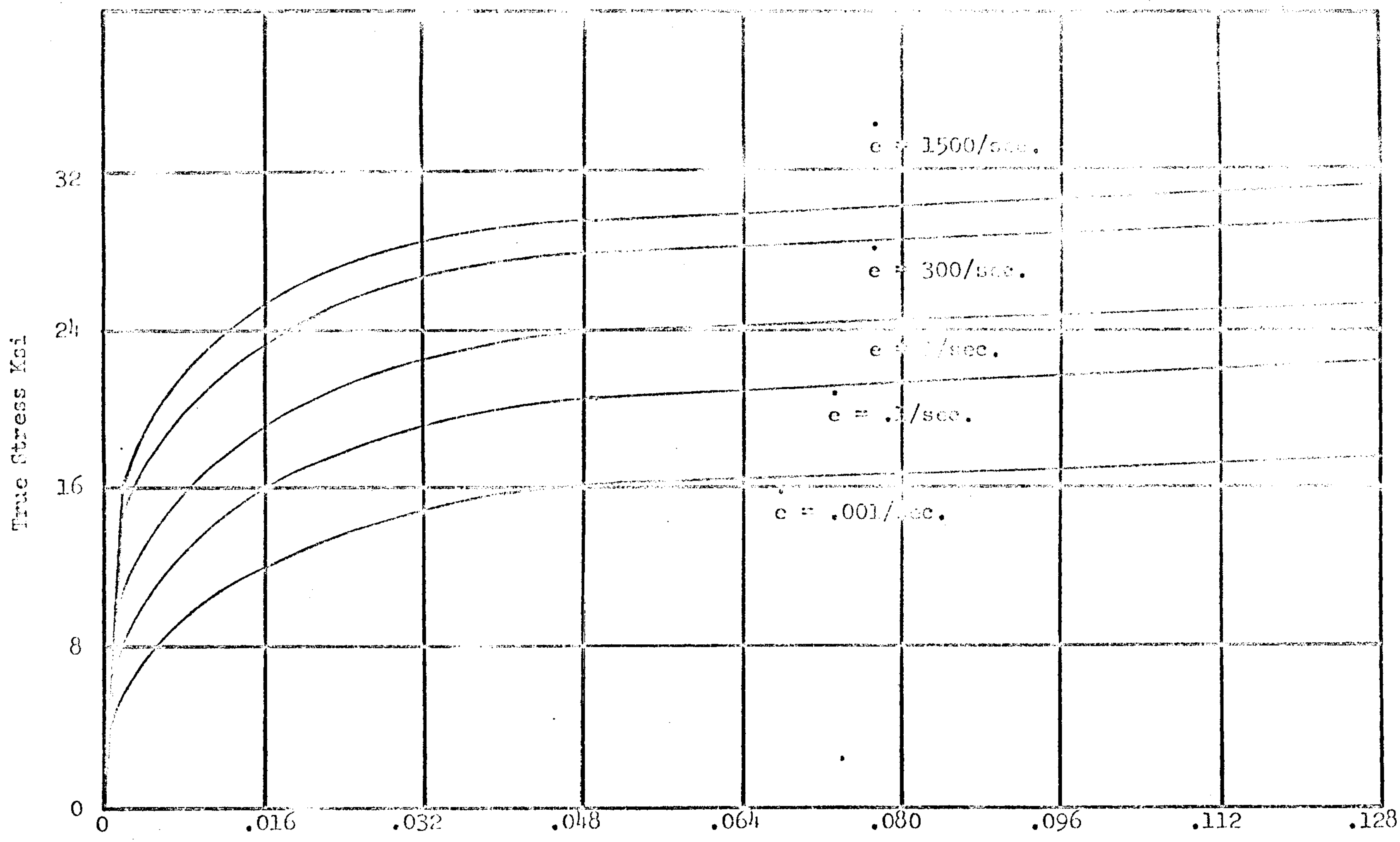

Fig. 28. Stress-Strain Curves for Aluminum.

IX. COMMENTS AND CONCLUSIONS

A) General Remarks

Figures 29 through 34 show the variation of various properties with strain rate. Other investigations[29,39] have indicated that certain properties of metals, notably ultimate tensile strength, vary exponentially with strain rate. Therefore, these curves are all plotted with a logarithmic scale for the strain rate. Of remarkable interest are Figures 29 and 32, where the stress vs. strain rate for a constant strain are plotted. The points fall very nearly on a straight line, indicating a functional relationship of the form

$$\sigma_{e\,=\,\mathrm{const}} = A\ \ln \dot{e} + B$$

applies.

In this equation, σ represents the stress, $\dot{e}$ the strain rate, and A and B are constants equal to the slope and stress intercept at a strain rate of 1/sec. of the straight line, respectively. Values of A and B are found in Table 3, along with other material and test parameters. It would appear that, since the slopes of these lines are approximately the same for the same material, that A represents a true material property, while B is a function of the strain rate.

A general functional relationship connecting stress, strain, and strain rate may be thought of as being represented by a surface,

Table 3

Material Properties

Property	Aluminum QQ1100-O	Nylon	Fresh Bovine Femur Bone	Embalmed Human Femur Bone
Weight #/in^3	0.098	0.042	0.070	0.068
Static Elastic Modulus psi	10×10^6	0.19×10^6	2.7×10^6	2.2×10^6
Elastic Wave Velocity 10^5 in/sec. $\sqrt{E/\delta}$	1.90	0.42	1.21	1.05
Elastic Wave Specimen Transit Time 10^{-6} sec.	1.3	6.0	2.06	2.4
Maximum Elastic Test Time 10^{-6} sec.	10	20	15	15
Impedance $z = \delta c$ Slug/ft^2 sec.	87,000	77,000	37,000	32,000
Density (δ) Slug/#^{3}	5.2	2.2	3.7	3.6
*Rate Sensitivity	1.7**	2.0**	2.1	2.1
A. Psi Sec.	2,000+	1,600+	4,300	4,200
B. Psi	20,000+	13,000+	39,000	33,000
A. Psi Sec.	2,050**	1,650**	--	--
B. Psi	24,000**	15,000**	--	--

*Rate Sensitivity, the ratio of the static strength to the strength at a strain rate of 1,500/sec.

**Measured at 10 percent strain

+Measured at 2 percent strain

(Figure 38). The projections on the stress-strain coordinate plane of the intersections of planes parallel to this coordinate plane and the surface would be similar to the family of stress-strain curves of Figures 24 through 28. Likewise, the projections of the stress-strain rate coordinate plane of the intersections of planes parallel to this coordinate plane and the surface may be likened to the family of exponentials of Figures 29 and 34. Thus, this surface may be constructed from the data of this experiment. Furthermore, since these projections represent derivatives of the stress function with respect to a coordinate, if the equations of these families could be deduced, then the equation of the surface could be obtained.

Thus for

$$\sigma = f(e, \dot{e})$$

$$\frac{\partial \sigma}{\partial e} = A \ell n \, \dot{e} + G(e)$$

Integrating yields

$$\sigma = A(\dot{e} \, \ell n \, \dot{e} - \dot{e}) + \dot{e} \, G(e) + G'(e)$$

This is an interesting formulation and worthy of more consideration than it is our purpose to give here. However, it has been shown that a family of stress-strain curves obtained at constant strain rates is sufficient to construct a surface $\sigma = f(e, \dot{e})$. It would be worthwhile to determine if a variable rate test yields curves that stay on this surface.

It is recommended that other materials be evaluated to establish the feasibility of using the constant A (slope of the $\sigma - \mathring{e}$ curves) as a material property indicative of the strain rate sensitivity of the strength characteristics of materials. The results of this experiment indicate that three quite different solids, bone, nylon, and aluminum, follow this relation to a good approximation.

B) Bone

The results, particularly as displayed in Figures 30 and 34, indicate the existence of a critical velocity for bone. A critical velocity occurs when the properties of a material exhibit large variation over a small range of strain rates. For these bone tests, a large change in the energy absorbtion capacity and the maximum strain to failure occurs at strain rates between 0.1 and 1 per second. Similar critical velocities for certain plastics have been reported by another investigation[47]. The difference in the fractures that occur as the strain rate is increased also verifies the existence of a critical velocity. Associated with this is the occurance of a maximum in the energy absorption curves, (Figure 30). These data indicate that, in designs where energy absorption is a criteria, the velocity of impact should be kept as low as possible.

Bone, as a material, is a specialized type of connective tissue, characterized by the presence of cells with long branching processes (osteocytes) which occupy cavities (lacunae) and fine canals (canaliculi) in a hard dense matrix consisting of bundles of collagenous fibers in an amorphous ground substance (cement) impregnated with calcium phosphate complexes. The bone structure is, therefore, typified by a highly oriented fiber matrix with calcium salts cemented in place to provide rigidity. Bone tissue shows many levels of organization, the most prominent of which, in the type used here, is the lamellar structure resembling a laminated plywood type matrix. In these tests, the loads were applied in the direction of the axis of the bone. This corresponds to the direction of the fiber bundles which are arranged in parallel or concentric sheets. Successive sheets differ in this predominant fiber direction, so that an area of lamellae has a stratified appearance. The frontispiece shows a cross-section of a typical human bone specimen. The magnification is approximately 100x. The section was dried, ground, and polished. Illumination is by polarized light. It is suggested that the low rate shear failures result from a distortion of the lamellar substructure resulting in final separation and fracture along several weaker planes. The high rate failures, however, appear to follow the cementing lines marking the extreme boundaries of each Haversian system, which are, in reality, integral cylinders extending from considerable distances in the long axis of the bone.

Other investigators,[42] including this author, have made studies that indicate embalming does not significantly alter the static properties of fresh bone. This allows extrapolation of tests on embalmed bone to "in vivo" properties. The principal effect of embalming on compact bone is the fixation of the collagenous fibers. If, as hypothesized, the low rate failures occur through the collagen matrix, then the differences between the curves (Figures 30 and 34) for fresh bovine bone and embalmed human bone may be due to embalming. A series of tests is being planned to test this theory.

C) <u>Bovine Musculo Tissue</u>

The dynamic response of this material is perhaps best understood by considering that, in essence, it has a cellular structure where the individual cells are membranes surrounding a fluid. There is also fluid in the interstitial spaces between the cells. The shape of the curves (Figure 26) suggests that, at the low rates, this fluid has time to squeeze out both through the membrance of the individual cells and around them. This gives a smooth stress-strain diagram. As the rate is increased, there is less and less time for this to occur, and the cells tend to rupture causing the characteristic hump in the curves. That this humping feature starts to disappear at the higher rates may imply that the viscoelastic properties of the collagen are approaching those of the fluid as to dynamic response. Some credence is given to this explanation by the fluid configuration after the tests. In the low rate tests, the fluid and material were interspersed; while in the higher rate tests, the fluid was spread out in a much wider area and the material remaining was dryer.

D) Nylon and Aluminum

In this series of experiments, nylon and aluminum were tested so that their dynamic properties could be compared with the biological materials. As the various cross plots indicate, embalmed human bone, fresh beef bone, and nylon respond in a similar manner to variable rate tests, except where the maximum strain is concerned. Since bone fractures, while nylon and aluminum do not actually fail under compressive loading, no comparison can be made on this basis. If, however, the bone tests are not taken to failure, then the general shape of the curves will be the same for all three materials. This implies that a surface representation of the results of these tests, on bone, nylon, and aluminum, as suggested earlier, would possess remarkable similarities.

E) Recommendations for Future Studies

There are several plastic wave theories in existence. Generally, in these theories, assumptions are made about the form of the constitutive equation with emphasis on the static stress-strain curve. Needless to say, these theories explain the various experimental data available with only limited accuracy. It would, therefore, be worthwhile to perform an analysis based on the general wave equation, but using the results of this paper in place of the constitutive equation. In this connection, a numerical solution could be obtained using the digital computer. In which case, the information contained in the stress-strain curves could be programmed directly and an empirical functional representation would not be required. Such important parameters as pulse shape, speed, and dispersion characteristics might be obtained in this way.

The author eventually expects to fit the data on biological materials into a mechanical impedance model of the human body.

Further testing should be done to establish the effect of specimen size on the rate sensitivity, also to determine with more accuracy the effect on Poisson's ratio and the modulus of elasticity of aluminum and other materials. No major modifications of the equipment would be required for these investigations.

The real value of this work lies in the development of a variable strain rate compression test which is capable of producing dynamic physical property measurements with better accuracy than other methods have been able to attain. It, therefore, provides a useful experimental tool for purposes of verifying future theoretical considerations of the mechanics of dynamic plastic deformation.

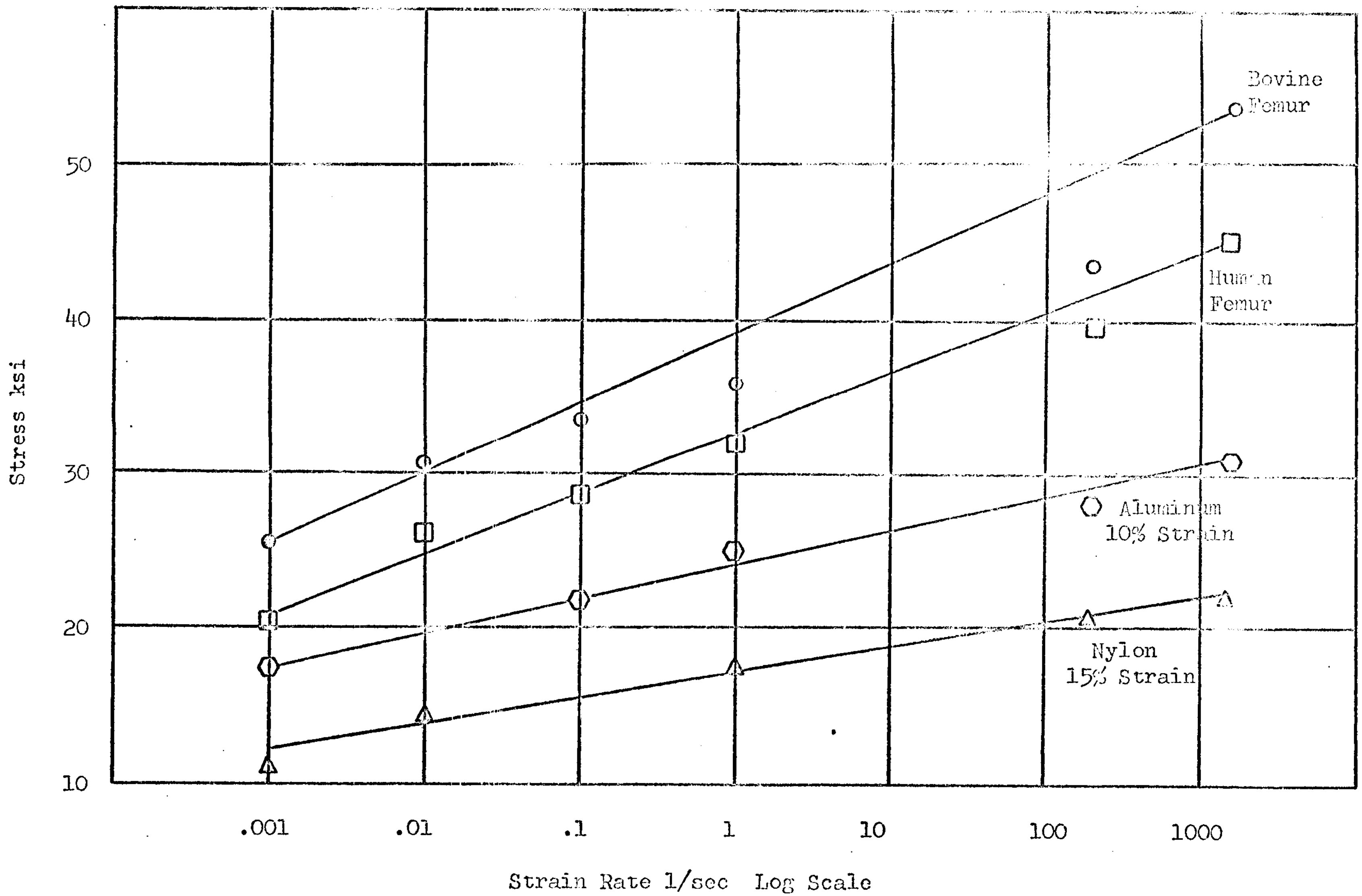

Fig 29. Ultimate Compressive Strength vs Strain Rate

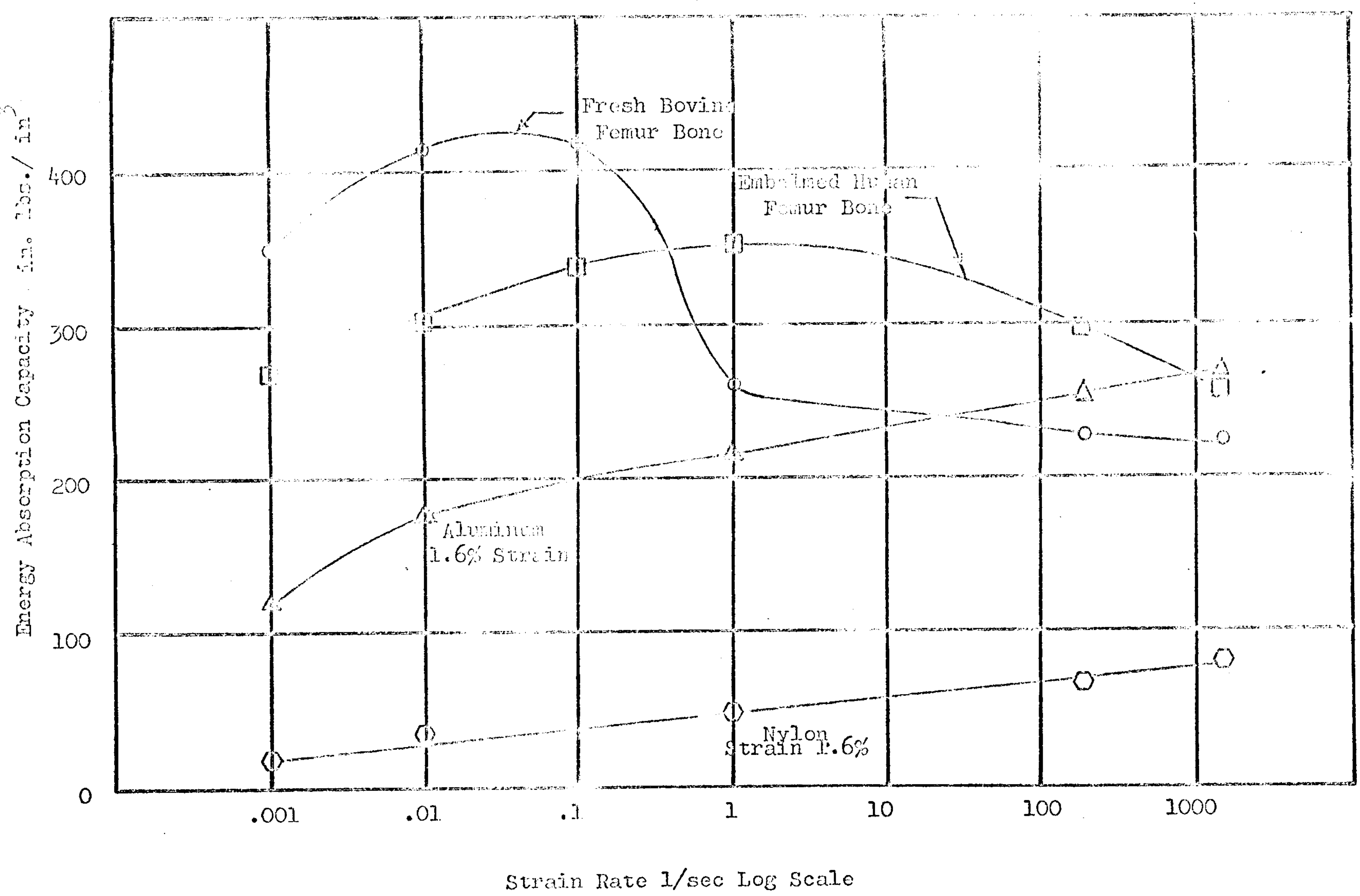

Fig 30. Energy Absorption Capacity vs Strain Rate For Bone, Aluminum, and Nylon

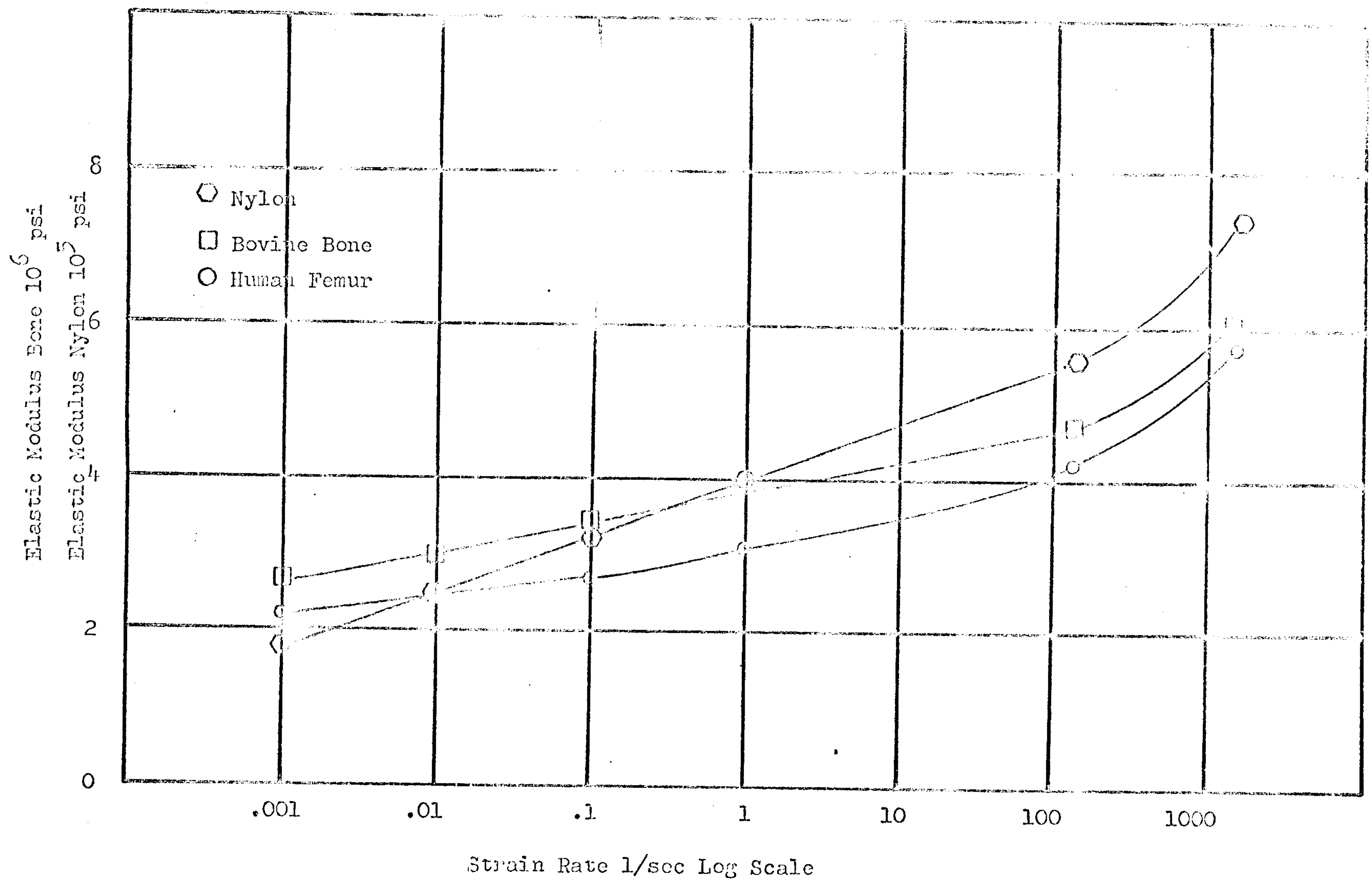

Fig 31. Modulus of Elasticity vs Strain Rate for Bone and Nylon

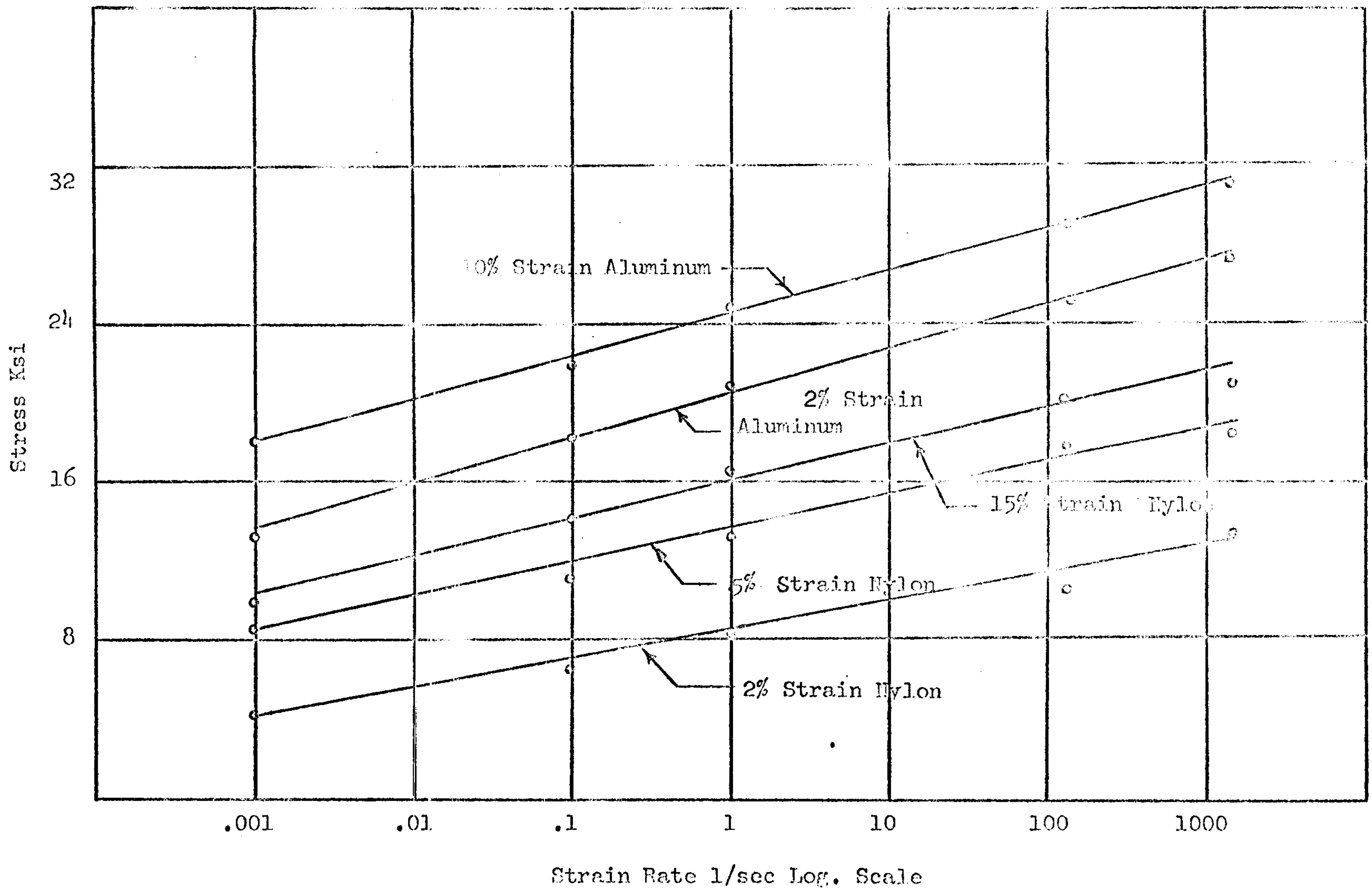

Fig. 32. Yield and Ultimate Strengths vs Strain Rate for Nylon and Aluminum

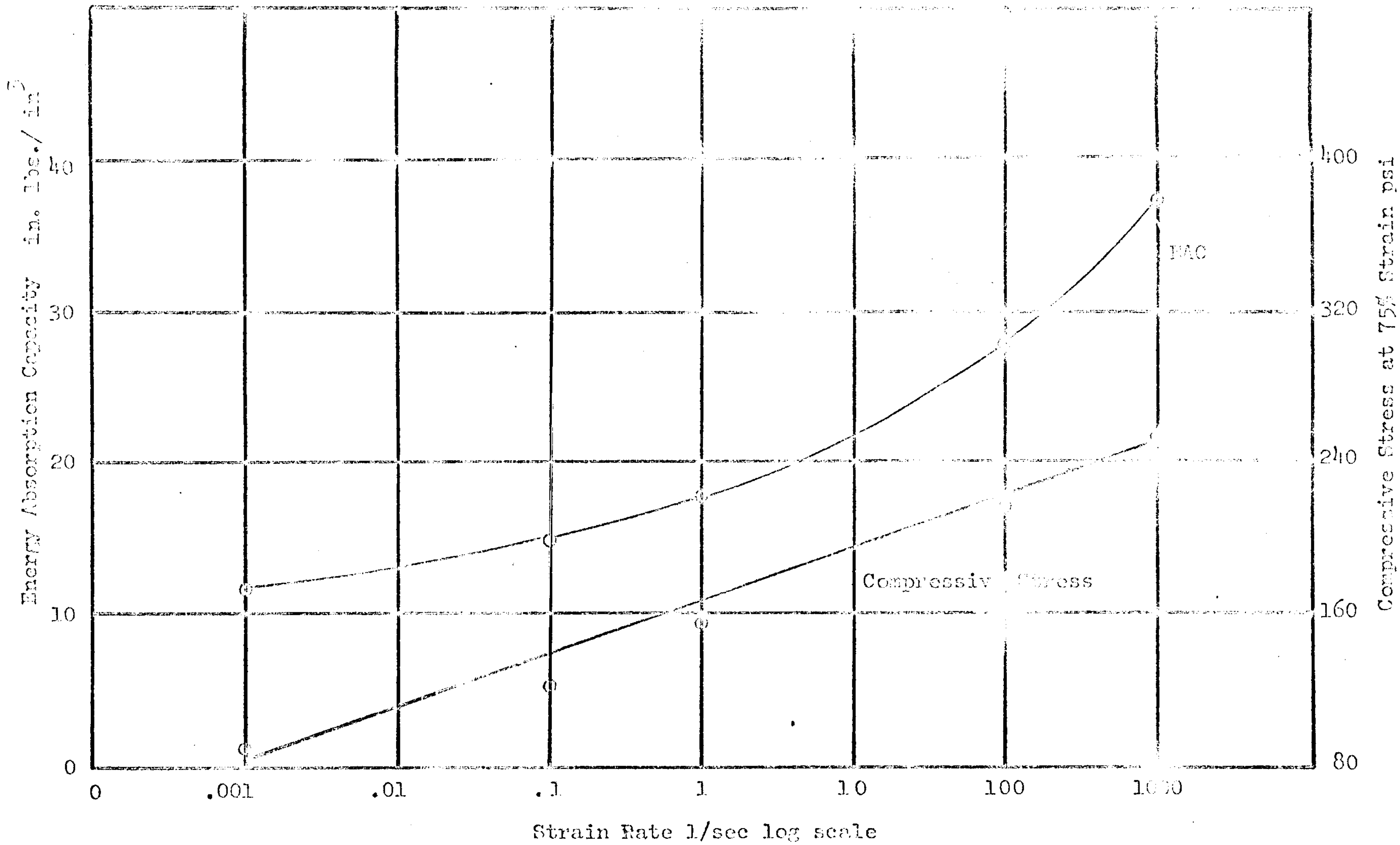

Fig 33. Energy Absorption Capacity and Compressive Stress vs Strain Rate for Bovine Muscle Tissue. 75% Strain.

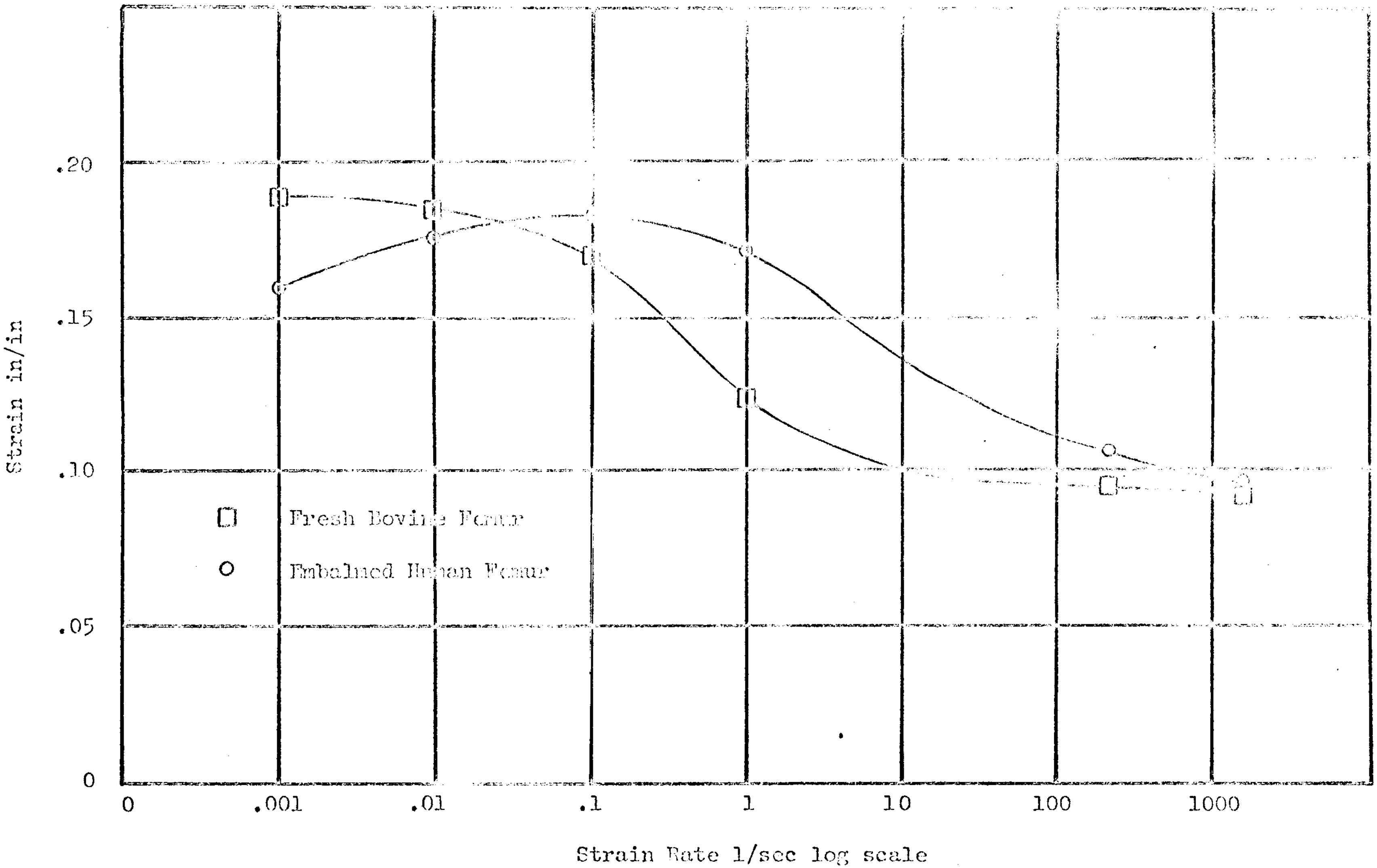

Fig 34 Maximum Strain vs Strain Rate for Bone.

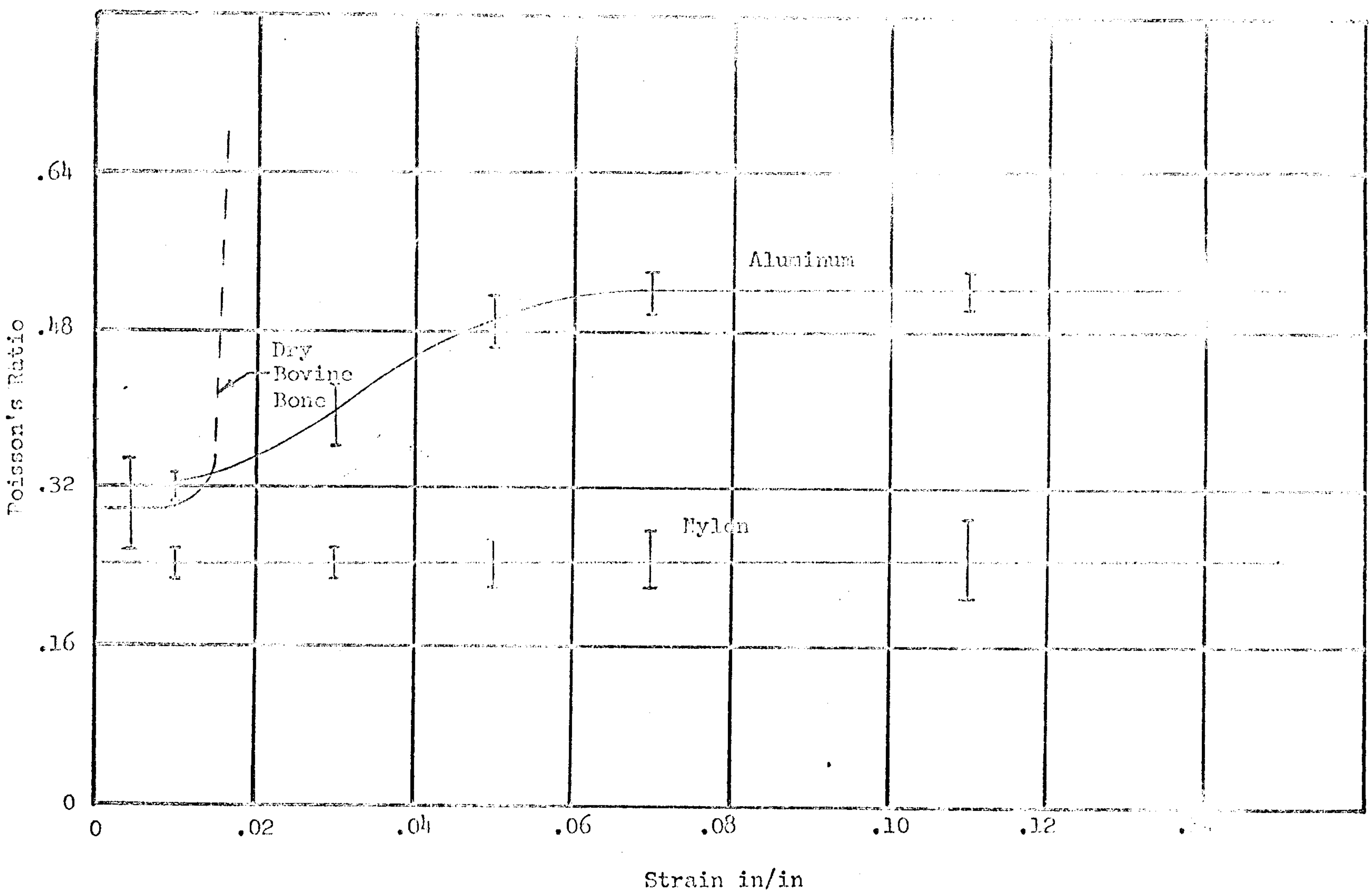

Fig. 35. Poisson's Ratio vs. Strain for Bone, Nylon and Aluminum

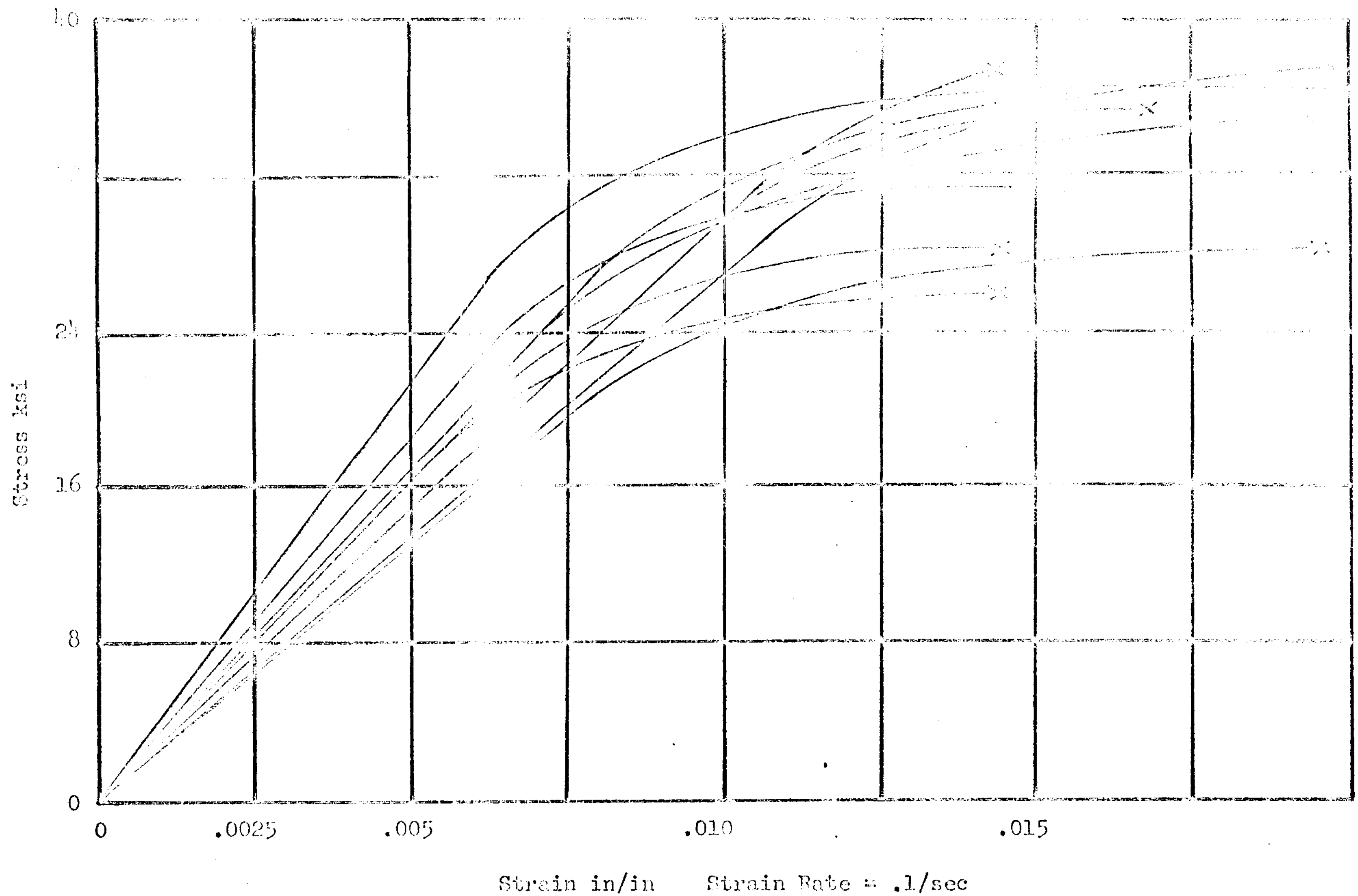

Fig. 36. Typical Scatter of 10 Tests of Bovine Femur Bone.

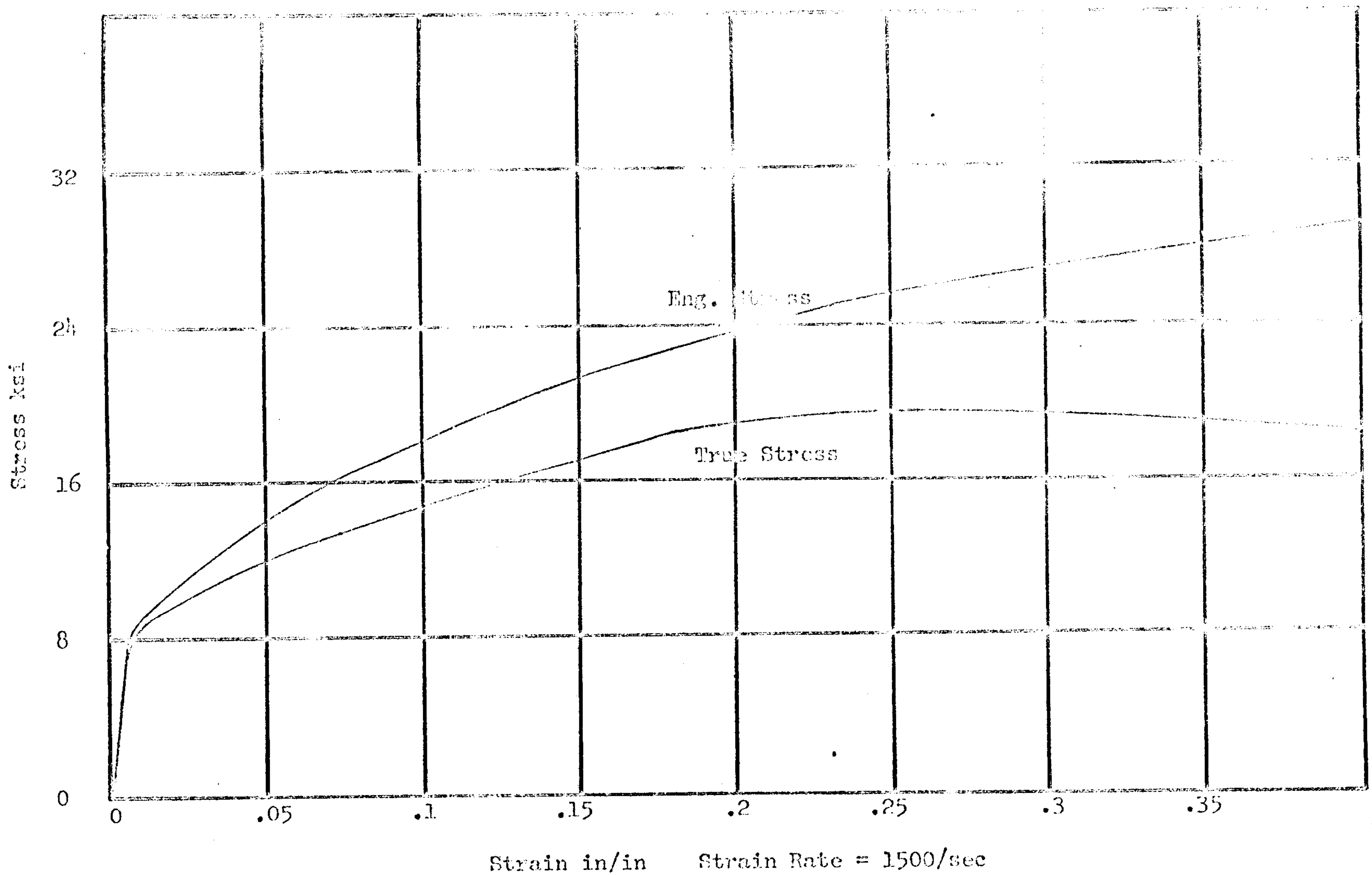

Fig. 37. Eng. and True Stress-Strain Diagrams for Nylon

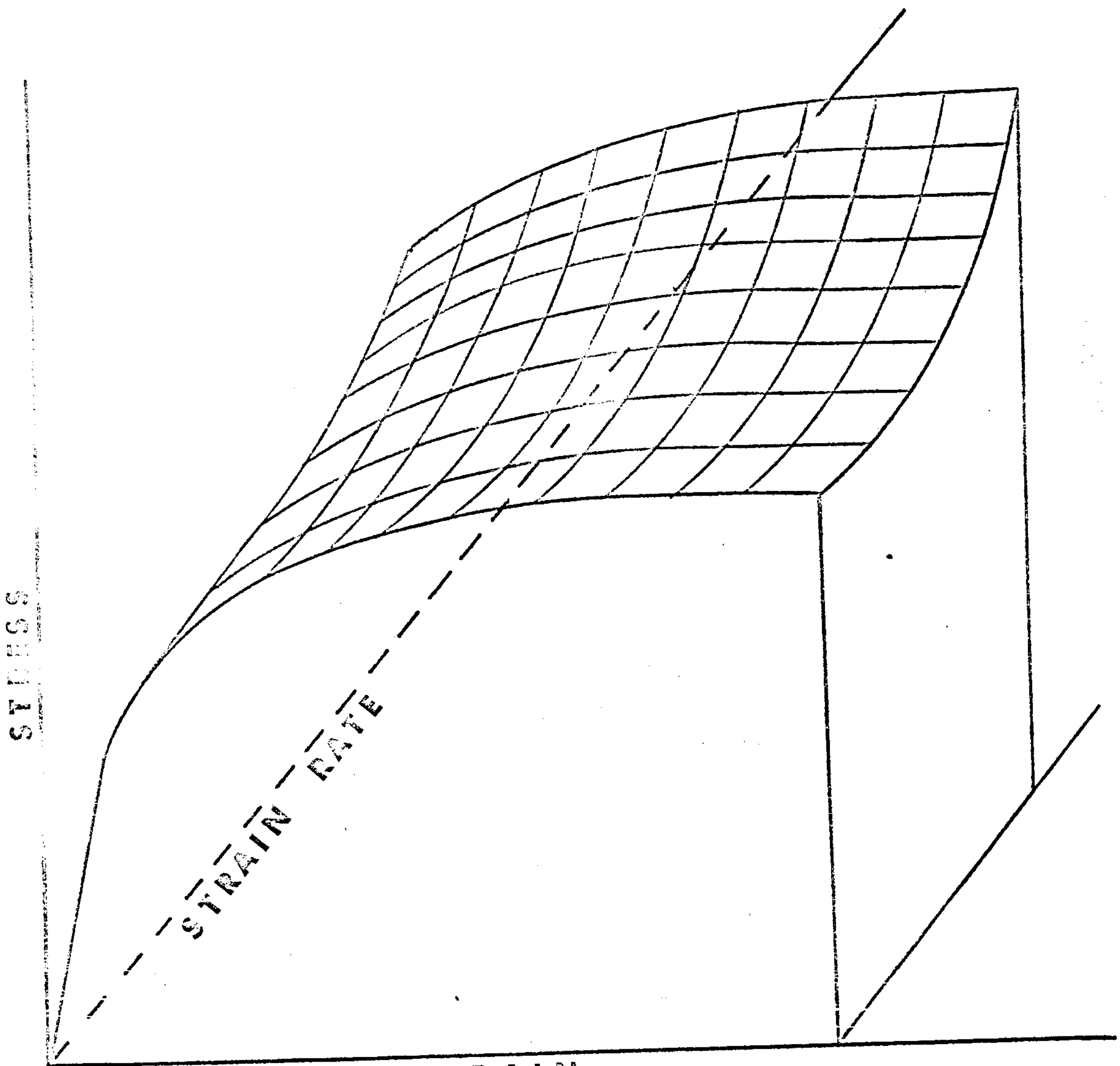

Fig.38
STRESS-STRAIN-STRAIN RATE
SURFACE

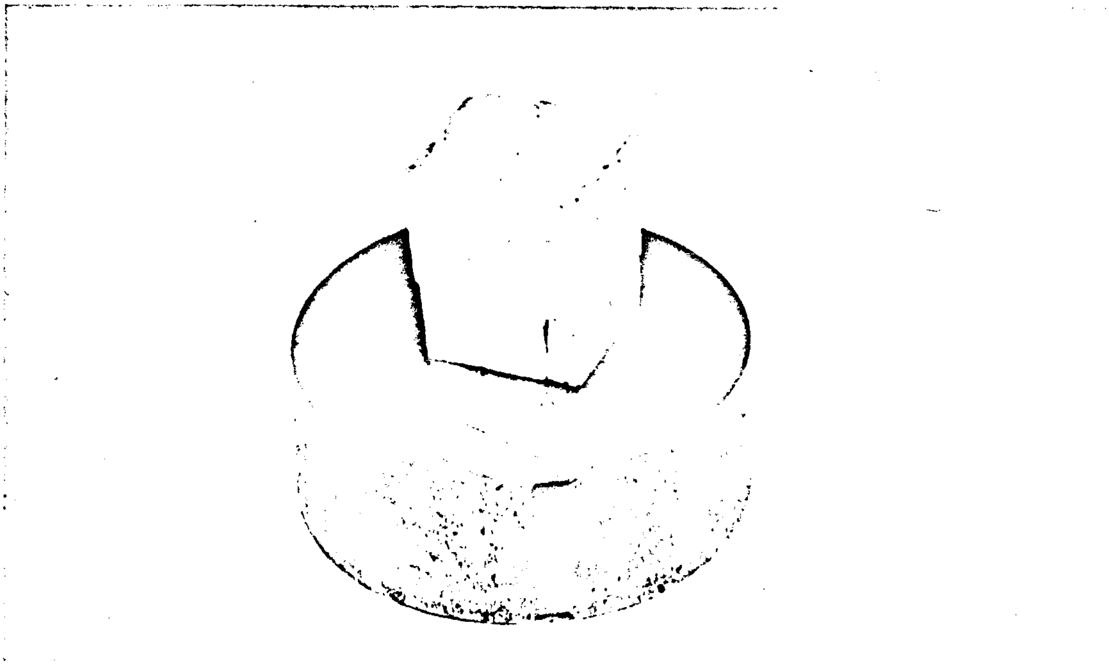

LOW RATE FAILURE OF BONE

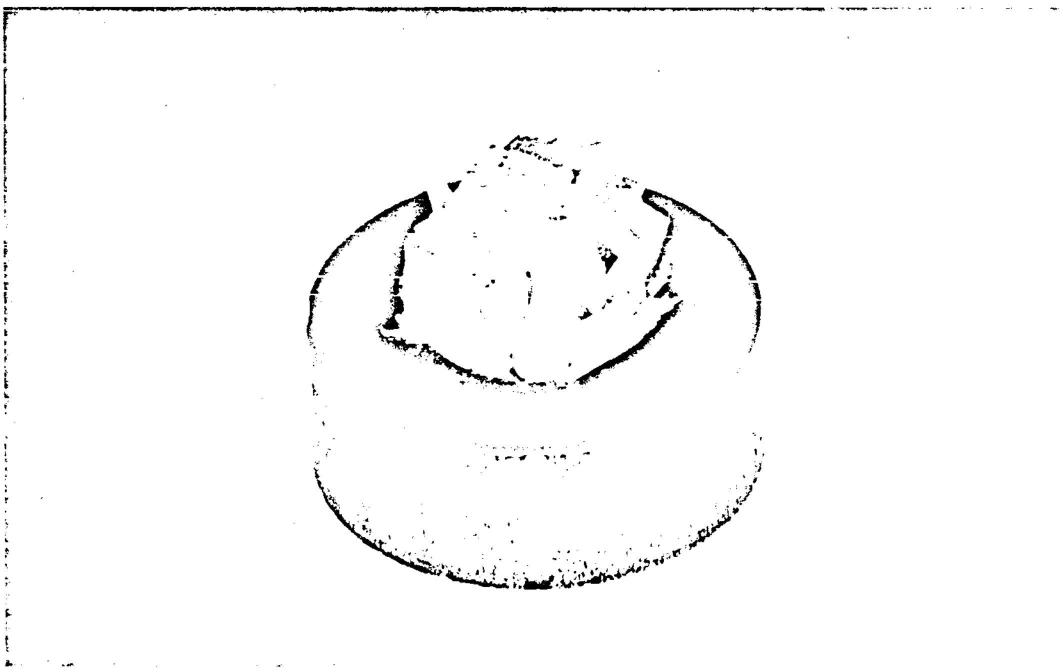

HIGH RATE FAILURE OF BONE

Fig. 39

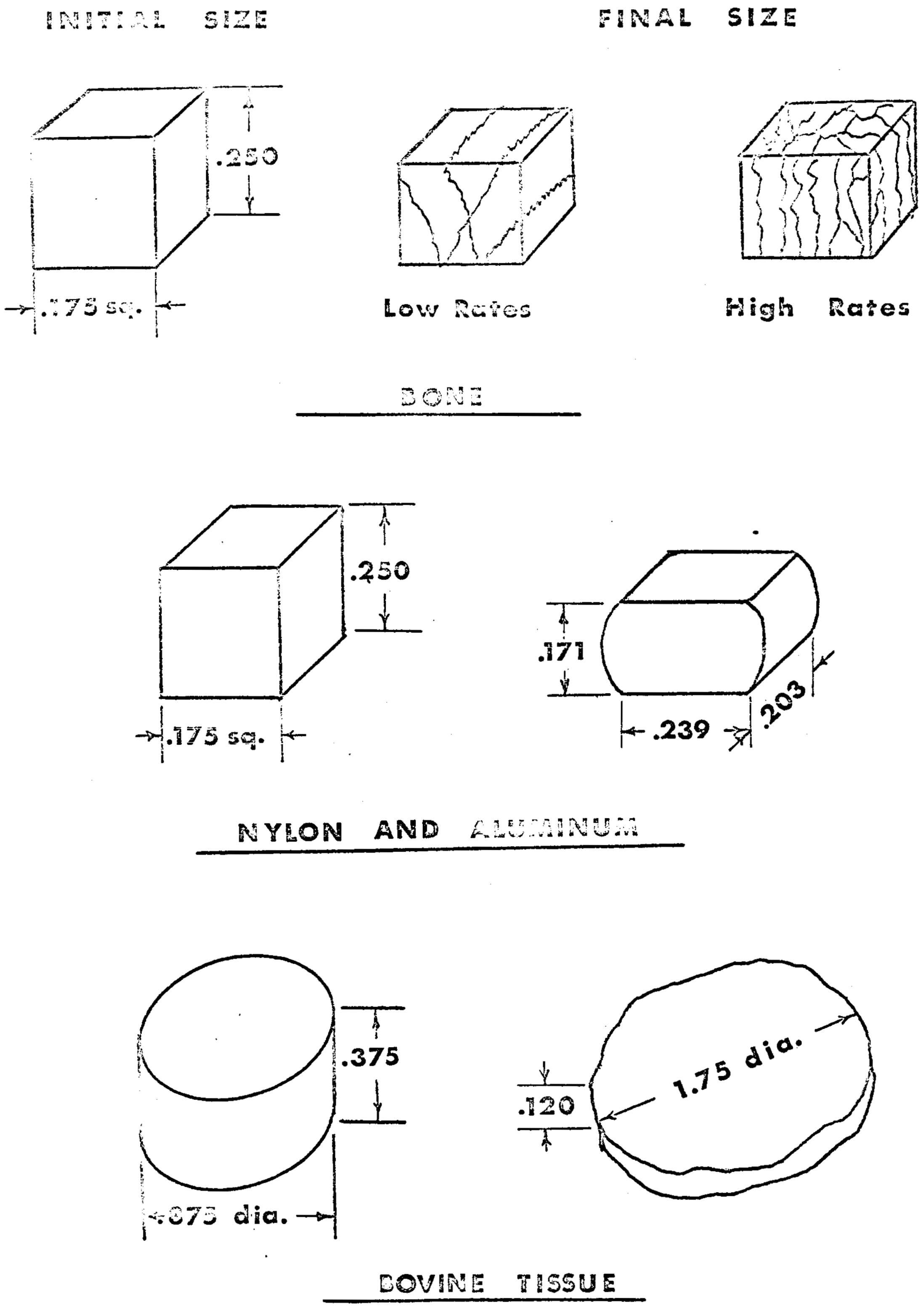

Fig. 40 TYPICAL FAILURES

SELECTED BIBLIOGRAPHY

1. Alter, B. E. and Curtis, C. W., "Effect of Strain Rate on the Propagation of a Plastic Strain Pulse Along a Lead Bar," Journal of Applied Physics, Vol. 27, No. 9, (1956) 1079.

2. Austin, A. L. and Steidel, R. F., "A Method for Determining the Tensile Properties of Metals at High Strain Rates," Proceedings, Journal of the Society for Experimental Stress Analysis, Vol. 17, No. 1, (1959) 99.

3. Beckwith, T. G., et al, "Standardization of Methods for Measuring the Mechanical Properties of Wounds," ASME No. 63WA-276, (1963).

4. Bell, J. F., "Propagation of Large Amplitude Waves in Annealed Aluminum," J. Applied Physics, 31 (1960) 277.

5. Brown, A. F. and Vincent, N. D., "The Relationship between Stress and Strain in the Tensile Impact Test," Proceedings of the Institute of Mechanical Engineers, Vol. 145, (1945) 126.

6. Chiddister, J. L., "Compression Impact Testing of Aluminum at Elevated Temperatures," Ph.D. Thesis, Michigan State University (1962).

7. Clark, D. S., "The Behavior of Metals under Dynamic Loading," Transactions, Americal Society of Metals, Vol. 46, (1954) 34.

8. Clark, D. S. and Duwez, P. E., "Discussion of the Forces Acting in Tension Impact Tests of Metals," J. of Applied Mech. 15 (1948) 243.

9. Costello, E. deL., "Yield Strength of Steel at an Extremely High Rate of Strain," Proceedings of the Conference on the Properties of Materials at High Rates of Strain, Institute of Mechanical Engineers, London (1957) 13.

10. Davies, E. D. and Hunter, S. C., "The Dynamic Compression Testing of Solids by the Method of the Split Hopkinson Pressure Bar," Journal of Mech., Physics, Solids, Vol. 11, (1963) 155.

11. Davis, C. D. and Hunter, S. C., "Assessment of the Strain Rate Sensitivity of Metals by Indentation with Conical Indenters," J. Mech., Physics, Solids, Vol. 8, (1960) 235.

12. Davies, R. M., "A Critical Study of the Hopkinson Pressure Bar," Phil. Trans. Soc. London, 240, (1948) 375.

13. deForest, A. V., et al, "Rapid Tension Tests Using the Two Load Method," AIME, Tech. Pub. No. 1393, (1941).

14. Dempster, W. T. and Liddicoat, R. T., "Compact Bone As A Non-Isotropic Material," Am. J. Anatomy, Vol. 91, (1952) 331.

15. Duwez, P. E., Clark, D. S. and Wood, D. S., "Discussion of Energy Measurements in Tension Impact," NDRC Report A-217, OSRD No. 1829.

16. Duwez, P. E. and Clark, D. S., "An Experimental Study of the Propagation of Plastic Deformation under Condition of Longitudinal Impact," Proceedings, ASTM, Vol. 47, (1947) 502.

17. Evans, F. G., "Stress and Strain in Bones," Americal Lecture Series, No. 296, CC Thomas Publication.

18. Evans, F. G. and Lebow, M., "The Strength of Human Compact Bone," Am. J. of Surgery, Vol. 83, (1952) 326.

19. Fitzgerald, E. R., "Dynamic Mechanical Properties of Polyvinyl Stearate at Audio-Frequencies," Journal of Applied Physics, Vol. 29, No. 10 (1959) 1442.

20. Goldsmith, W., "Impact," E. Arnold, London, (1960).

21. Gurdjian, E. S., Webster, J. E. and Listner, H. R., "The Mechanism of Skull Fracture," J. Neurosurg., 7 (1950) 106.

22. Habib, E. T., "A Method of Making High Speed Compression Tests on Small Copper Cylinders," Journal of Applied Mechanics, Vol. 70, (1948) 248.

23. Hagen, R. S., et al, "Impact Testing of High Impact Thermoplastic Sheet," 17th ANTEC Preprint, No. 28-55 PE VII, (1961).

24. Harding, R. S., et al, "Tensile Testing of Materials at Impact Rates of Strain," J. Mech. Eng. Science, 2 (1960) 88.

25. Hopkins, H. G. "Dynamic Anelastic Deformations of Metals," Applied Mechanics Reviews, Vol. 14, No. 6 (1961) 417.

26. Hopkinson, J., "Experiments on the Rupture of Iron Wires," Proceedings, Manchester Literary and Philosophical Society, Vol. 11, 1872, 119.

27. Harth, J. H., et al, "Some New Data on High Speed Impact Phenomena," J. Applied Mechanics, 24 (1957) 65.

28. Karnes, C. H., "Stress-Strain Characteristics of Materials at High Strain Rates," Part IV - Experimental and Theoretical Analysis of Plastic Impaction Short Cylinders, Report issued by Structural Mechanics Research Lab, University of Texas, Austin, (1960).

29. Kelly, P. P. and Dunn, T. J., "Instrumented Tensile Impact Testing of Thermoplastics," Materials Research and Standards, Vol. 3 No. 7, (1963) 545.

30. Kolsky, H., "Experimental Wave Propagation in Solids," Pergamon Press, Oxford (1960).

31. Kolsky, H., "Stress Waves in Solids," Clarendon Press, Oxford, (1953).

32. Kolsky, H., "An Investigation of the Mechanical Properties of Materials at Very High Rates of Loading," Proc. Phys. Soc., 62 (1949) 676.

33. Lee, E. H. and Wolf, H., "Plastic-Wave Propagation Effects in High Speed Testing," J. Applied Mechanics, 18 (1951) 379.

34. Lempriere, B. M., "Oscillations in Tensile Testing," International Journal of Mechanical Sciences, Vol. 4 (1962).

35. Lindholm, U. S., "An Experimental Determination of the Stress-Strain Rate Relations of Several Metals," Ph.D. Thesis, Michigan State University (1961).

36. Malvern, L. E., "Plastic Wave Propagation in a Bar of Material Exhibiting a Strain-Rate Effect," Quart. Applied Math, 8 (1950) 405.

37. Malvern, L. E., "The Propagation of Longitudinal Waves of Plastic Deformation in a Bar of Material Exhibiting a Strain-Rate Effect," J. Appl. Mech. 18 (1951) 203.

38. Manjoine, M. J., "Influence of Rate of Strain and Temperature on Yield Stresses in Mild Steel," Journal of Applied Mechanics, II (1944) 211.

39. Manjoine, M. J. and Nadai, A., "High Speed Tension Tests at Elevated Temperatures," Journal of Applied Mechanics, Vol. 63 (1941) 77.

40. Mann, H. S., "High Velocity Tension-Impact Tests," Proceedings, American Soc. Testing Materials, 36 (1935) 85.

41. McElhaney, J. H., "The Mechanical Properties of Bone," Second Annual Engineering in Medicine Conference, Andover, New Hampshire (1964).

42. McElhaney, J. H., et al, "The Effect of Embalming on the Mechanical Properties of Beef Bone," Journal of Applied Physiology, Vol. , No. (1964).

43. Murphy, G., et al, "Response of Resistance Strain Gages to Dynamic Strains," 9th Int. Congr. Appl. Mechanics, (1960) 448.

44. Nadai, A., "Theory of Flow and Fracture of Solids," McGraw-Hill Company Publishers, (1950) 17-30; 117-130.

45. Payne, A. R., "Sinusoidal-Strain Dynamic Testing of Rubber Products," Materials Research and Standards, Vol. 1, No. 12 (1961) 942.

46. Reiner, M., "Deformation, Strain and Flow," H. K. Lewis & Co. Publishers, (1960) 126-156.

47. Richard, K., "Determination of the Mechanical Properties of High Polymers at High Speeds of Testing," Journal of Polymer Science, Vol. 58, No. 166 (1962) 71.

48. Rinehart, J. S. and Pearson, J., "Behavior of Metals under Impulsive Loads," The American Society for Metals, (1954) 202.

49. Shepler, P. R., "Impact Research," Sc.D. Thesis, Massachusetts Institute of Technology, (1943).

50. Smith, J. E., "Tension Tests of Metals at Strain Rates up to 200/sec." Materials Research and Standards, Vol. 3, No. 9 (1963) 713.

51. Spunik, R. H., "Rate Sensitivity," Materials Research and Standards, Vol. 6 (1962) 498.

52. Stulen, F. B., "A Model for the Mechanical Properties of Metals," Materials Research and Standards, Vol. 2, No. 2 (1962) 102.

53. Symposium on Speed of Testing of Nonmetallic Materials," ASTM STP No. 185 (1955).

54. Taylor, G. I., "The Testing of Materials at High Rates of Loading," J. Instn. Civil Engineers, 26 (1946) 486.

55. Ting, T. C. and Symonds, P. S., "Impact of a Cantilever Beam with Strain Rate Sensitivity," Technical Report No. 73, Contact Nonr-562(10) of Brown University to Office to Naval Research (1962).

56. Turnbow, J. W., "Stress-Strain Characteristics of Materials at High Strain Rates," Ph.D. Dissertation, University of Texas (1959).

57. vonKarman, Th., "The Propagation of Plastic Waves in Tension Specimens of Finite Length," NDRC Report A-103 (OSRD 946), (1942).

58. vonKarman, Th., and Duwez, P., "The Propagation of Plastic Deformation in Solids," J. Applied Physics, 21 (1950), 987.

59. White, M. P., "On the Impact Behavior of a Material with a Yield Point," J. of Applied Mechanics, 16 (1949) 39.

60. White, M. P., and Griffis, L., "The Propagation of Plasticity in Uniaxial Compression, J. Applied Mechanics, 15 (1948) 256.

61. Wolstenholme, W. E., "Characterizing Impact Behavior of Thermoplastics," Journal of Applied Polymer Science, Vol. 6, No. 21, (1962) 332.